Universitetet i Stavanger

FACULTY OF SCIENCE AND TECHNOLOGY

MASTER'S THESIS

Study program/specialization: Master of Science in Biological Chemistry/ Molecular Biology	Spring semester, 2020 Not to be published by UiS until 2022
Author: Karina Kvia Varhaug	
Programme coordinator: Prof. Cathrine Lillo **Supervisors:** Estefanía Noriega Fernández Izumi Sone	
Title of master's thesis: Plasma Activated Water: The Next Generation Technology for Food and Agricultural Applications	
Credits: 60	
Keywords: Plasma activated water (PAW); plasma power; exposure time; PAW composition; storage stability; *Listeria monocytogenes;* Macroalgae; Ultrasound (US); Total bacterial counts	Number of pages: 132 + supplemental material/other: 9 Stavanger, 15.06/2020

Abstract

Plasma activated water (PAW) has recently gained increased attention as a next generation non-thermal food processing technology. It has promising potential as a eco-friendly alternative to traditional decontamination methods in the food industry, as well as promising applications in agriculture, such as plant growth enhancement.

In this MSc thesis, PAW composition and stability during four-week storage at different temperatures, relevant for industry settings, (10, 4 and -20 °C) were assessed as a function of PAW operating conditions (i.e. plasma power and activation time). Increasing plasma power (25 and 35 W) and activation time (10 and 30 min) resulted in a significant drop in pH (up to 2.5 ± 0.1) and significantly higher oxidation reduction potential (ORP) level (up to 284.1 ± 11.5 mV) and concentration of the monitored reactive oxygen and nitrogen species (RONS), i.e. nitrates, nitrites and hydrogen peroxide (up to 342.5 ± 13.6, 1.6 ± 0.1 and 1.1 ± 0.2 mg/L, respectively). Furthermore, the presence of carbonic compounds (carbonic acid, bicarbonate and carbonate ion) in PAW significantly increased with activation time, where the main specie was carbonic acid (maximum of 693.3 ± 131.9 μM), and estimation of the hydronium ion and hydroxide levels increased and decreased, respectively. The nitrous and nitric acid in PAW both increased with increasing plasma power and activation time. Regarding PAW storability, the pH, ORP and nitrates level remained stable during the four-week storage, independently of the temperature. However, nitrites levels were not detectable after 24 h for all operating conditions and storage temperatures, except for the most severe activation settings (36 W for 30 min), where a significant decrease was still detected only at 10 and 4 °C. Hydrogen peroxide levels were also non-detectable after 24 h for all operating conditions and storage temperatures, which was attributed to its instability in acidic environments.

The potential of PAW for microbial inactivation, alone or combined with ultrasonication (US), was assessed on planktonic cells of *Listeria monocytogenes*, with high prevalence in fresh produce, and also on wild harvested macroalgal biomass (*Laminaria hyperborea*), as a sustainable alternative to current preservation strategies. About 5 log reductions on *L. monocytogenes* suspensions were achieved after 5 min treatment with PAW, whilst there was no significant difference for the synergistic effect was observed when combined with US. For macroalgae decontamination, the combined effect of PAW and US resulted in about ≈ 2 log reductions of the total viable counts. Thus, the potential of PAW to extended product shelf-life

and reduce food waste generation was demonstrated. Assessment of PAW as a nitrogen rich fertilizer and growth enhancement was conducted on *Solanum lycopersicum* (tomato) cultivar Heinz plants, resulting in significantly longer and heavier plants irrigated with PAW, alone and with the synergistic effect with a nutritional solution. In conclusion, this MSc thesis has demonstrated the potential of PAW as a promising alternative to traditional sanitizers applied in the food industry, as well as to mineral fertilizers in agriculture applications.

Acknowledgments

I would like to express my deepest gratitude to my supervisors Estefanía Noriega Fernandez, Izumi Sone and Cathrine Lillo for all the advice and guidance I have received throughout my thesis. Especially, thanks to Estefanía for the support, patience and for all the time on evenings, weekends and non-working hours spent to help and guide me in your already thigh schedule. Furthermore, I want to show my appreciation for the help I have received from Mette Rise Vaka, Irina Orestovna Averkina and Stephane Florent Joel Simon for answering all of my questions and for the guidance in the lab. Additionally, a big thanks to everyone in Nofima for making me feel welcome and answering questions, helping me find equipment and giving me tips in the lab. I am also very grateful for all the fun memories made in the lab and in the office with fellow students and friends.

Finally, a special thanks to my family and all of my friends for being so supportive in this period of my life. Especially, a huge thanks to my mother, Mari Varhaug and my fiancé, Sven Jørgen Ledaal Undheim for showing immense patience and support during stressful and hectic periods.

Table of Contents

List of figures

List of tables

Abbreviations

Table 1. List of the abbreviations used in present work, and their full form

CP	Cold plasma
DBD	Dielectric barrier discharge
FAO	The united Nations Food and Agriculture Organization
NFSA	Norwegian Food Safety Authorities
ORP	Oxidation reduction potential
PAW	Plasma activated water
RNS	Reactive nitrogen species
ROS	Reactive oxygen species
RTE	Ready to eat
SDBD	Surface dielectric barrier discharge
US	Ultrasound

1. Introduction

1.1 Current challenges in the food industry

The world population reached 7.7 billion mid 2019 and the population continues to grow, expecting to reach 8.5 billion in 2030 and 9.7 billion in 2050, according to United Nations (UN) [1]. At the same time, according to the united Nations Food and Agriculture Organization (FAO) urbanization will continue at an accelerating pace, going from the 55% of today's population to 68% by 2050 [2]. Leading to an increase of 60% more food required by 2050 to feed a larger, more urbanized population [3]. Additionally, reducing food loss and waste, while improving food safety and nutritional value and contribute towards environmental sustainability are important to face the challenge of sustainably feeding a growing world population [4]. The Norwegian food industry is ranked amongst the safest in Europe, yet the Norwegian food safety authority (NFSA) registered regulatory violations in 46% of the inspected companies in 2018 [5]. In addition, around 5,000-7,000 cases of diseases originating from food or water are reported every year. The actual number is presumable larger considering many will not seek medical assistance for foodborne diseases [5]. Figure 1 illustrates the top 10 hazards and product categories in food products in 2017 [6] .

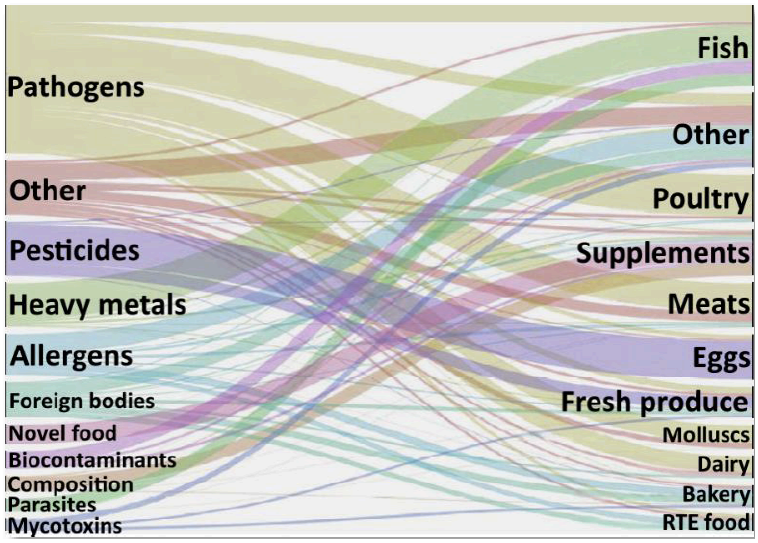

Figure 1. Major food safety risks (left) and their incidence in different types of food (right). (From ref [6])

The prevalence foodborne diseases are related to the consumers choice of food, which is further influenced by several aspects, e.g. the nutritional value, impact on consumers health, quality

and sensory properties being enhanced and the price tag [7, 8]. Convenience is also of importance for many; in a hectic everyday life, ready to eat (RTE) foods and fresh produce have gotten increasingly popular among present day consumers [9]. According to Regulation (EC) No. 2073/2005 RTE foods are defined as food intended by the producer or the manufacturer for direct human consumption without the need for cooking or other processing effective to eliminate or reduce to an acceptable level microorganisms of concern [10]. Healthy eating is also a critically important consumer drive, and as the population increases with demographic changes such as aging and a raising gross domestic product, it can be presumed that this trend will continue to gain importance until 2030 [11, 12]. Consumer of the future will have a better level of education worldwide with a better knowledge of health and healthy eating, reinforcing this trend [12]. Fresh produce is a major contributor of essential vitamins and minerals to a healthy diet for the global population [13]. Due to fresh produce and RTE foods being consumed directly it could be microbiologically contaminated via various routes, including agricultural practices (organic fertilizer, irrigation water, soil, and spray of pesticide and insecticide) and post-harvest practices (handling, collection, washing, processing, transportation, and packaging), thus innovative decontamination that can assure safety of the product is important [14]. For example, in spring 2018 there was an outbreak of *Yersinia enterocolitica* O:9 in Norway that presumable originated from RTE (washed) salad. In this outbreak, a total of 20 cases was registered all over Norway [5].

Thermal treatment is extensively used in the food industry nowadays for processing/preservation purposes, despite leaving a big footprint on the environment, due to high energy usage as well as possibly decreasing the nutritional value (vitamin loss) and affecting the color, firmness or other sensory attributes of the product [15, 16]. Consumers are also getting increasingly interested in the climate change and the need for a more sustainable food production [17, 18]. Efficient, profitable and sustainable non-thermal processing methods with minimum impact on nutritional and sensory quality, while extending product shelf-life have consequently gained much attention in recent years [19, 20]. Safer and healthier food will have a positive effect on the public health, by reducing the occurrence of diet-related diseases, food allergy, food poisoning, food recalls and other food associated health cost, thus reducing the overall cost on the public health service [21, 22]. Additionally, reduced food losses/waste via extended shelf life and sustainable packaging, as well as enhanced productivity and sustainable resource management will relieve pressure on limited agri-resources and foster better self-sufficiency [23]. Non thermal pasteurization methods include High Pressure

processing, Pulsed electric fields, UV-C light , High-Power Ultrasound (US), Cold plasma (CP) and Microwave Volumetric Heating [19, 21]. For High Pressure Processed food is subjected to pressure ranging between 150 and 600 megapascal (MPa) at room temperature for a certain period of time, usually less than 5 minutes, which effectively inactivates pathogenic and spoilage organisms [19, 24, 25]. UV is mainly effective for surface decontamination and have been reported to increase the shelf life of fresh produce, while also improving the organoleptic properties of fresh produce (e.g., increase of the antioxidant capacity) [26]. US waves are sound waves with a frequency ranging from 20 kHz to 10 MHz [27]. Low-power US (from 100 kHz to 1 MHz and high-power US (from 20 to 100 kHz) are the main types of US used for food applications [27, 28]. The high-power US has a direct effect on the inactivation of microbes during decontamination and processing treatments [28]. In pulsed electric fields, food is subjected to a pulsed high voltage field for less than a second [19]. Lastly, an interesting technology emerging is plasma, generated by applying energy to a gas, resulting in a ionized gas which contains free electrons, ions and neutral particles [29]. Due to these not involving significant heating, the sensory and nutritional quality of the processed product is comparable to that of the unprocessed counterpart, thus allowing the preservation of the sensory properties and nutritional value whilst successfully destroying bacteria and other microorganisms [19]. Nevertheless, the technologies do have some major bottlenecks for large-scale implementation in the industry, including e.g. development of process compatible technology design and scale-up, regulatory approval, acceptance from consumers and effective process control and validation [30].

According to FAO, due to climate change and a rapid development of urbanization, industrialization and world population a food shortage is three times more likely to happen [3]. One of the most viable processes to limit food shortages is to increase crop yields, which so far is limited by seed surface, by water and by soil contamination [31]. CP is considered to be an innovative and eco-friendly approach among solutions to face these challenges [31], which has proven effective in increasing seed activity, earlier germination and higher germination rate, faster growth [32], increased enzyme activity [33, 34] and increased yield of plants [35]. Additionally, CP systems has been shown to effectively decontaminate and disinfect plants [36]. An unexploited and sustainable alternative to terrestrial biomass that has gained increasing interest in recent years are macroalgae. However, major challenges arise with the use of macroalgae, as the high-water content favors high microbial proliferation once harvested, which further decreases the quality and increases the health risks [37].

1.2 Plasma technology

Plasma is referred to as the fourth state of matter, next to solids, liquids and gases [38]. It exists abundantly in the universe, with over 99% of visible matter appearing in the plasma state [39] and can be observed in forms as lightning, the northern lights and the sun [40, 41]. Plasma is a partially or fully ionized gas, consisting of a large number of different reactive species [15], such as electrons, positive and negative ions, free radicals, gas atoms and molecules (in ground state and as excited species) [42]. Most commonly manmade plasma is generated by applying electrical discharge to a gas substrate (e.g. room air) [43, 44]. Based on the properties of plasma, it is already commercially exploited in a widely spread variety of fields [43]; proven useful for antimicrobial purposes [45], upgrading surface features on textiles, glass or paper and in advanced materials and electronics [43, 46].

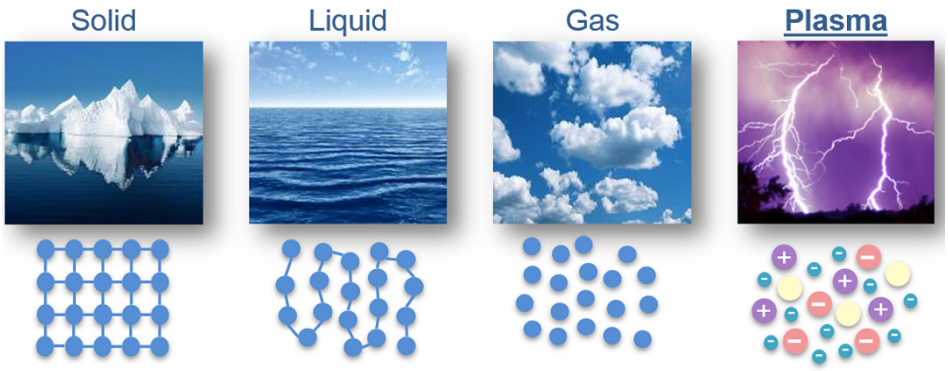

Figure 2. The four states of matter. (From ref [47])

Overall, plasma can be described based on density or thermodynamic equilibrium [48]. With regards to the thermodynamic equilibrium, plasma is classified into two major categories, high temperature and low temperature plasmas, with the latter being further divided into thermal and non-thermal plasma (Table 2) [49].

Table 2. Classification of plasma presenting temperature and density, adapted from Nehra et al. [42]

Plasma	State	Example
High temperature plasma	$T_e \approx T_i \approx T_g$, $T_p = 10^6$ - 10^8 K $n_e \geq 10^{20}$ m^{-3}	Laser fusion plasma
Low temperature plasma		
Thermal (quasi-equilibrium plasma)	$T_e \approx T_i \approx T_g$, $T_p \leq 2 \times 10^4$ K $n_e \geq 10^{20}$ m^{-3}	Arc plasma, plasma torches
Non-thermal plasma (Non-equilibrium plasma)	$T_e >> T_i \approx 300$ -10^3 K $n_e \approx 10^{10}$ m^{-3}	Corona, DBD

Thermal plasma indicates that a thermodynamic equilibrium between the species in the gas, i.e. the ions, electrons and the neutral species have the same temperature [50, 51]. For these types of plasmas, a high temperature is needed, usually between 4,000 and 20,000 K [50] with a typical density (i.e. electron density, n_e) of $\geq 10^{20}$ m^{-3} [42]. Non-thermal plasma however, presents a rather large temperature difference between the electrons and the gas, where the temperature of the electrons can be several 10,000 K with an electron density of $\approx 10^{10}$ m^{-3}, while there is little change in the temperature of the gas [51]. The temperature difference is due to most of the energy being focused on the electrons when the plasma is generated, keeping the total temperature of the gas ambient [51, 52]. The number density refers to the degree of ionization (charged particles per volume unit, i.e. number of electrons and ions). The electron temperature in the plasma affects the degree of ionization, thus weakly ionized plasma is also referred to as low-temperature plasma [48]. With regards to the density, the classification is high-density plasma with a number density of $n > 10^{15\text{-}18}$ m^{-3} and low-density plasma with a number density of $n < 10^{12\text{-}14}$ m^{-3} [48]. Figure 3 shows the typical naturally occurring and laboratory plasmas, including their number density and average kinetic energy [53].

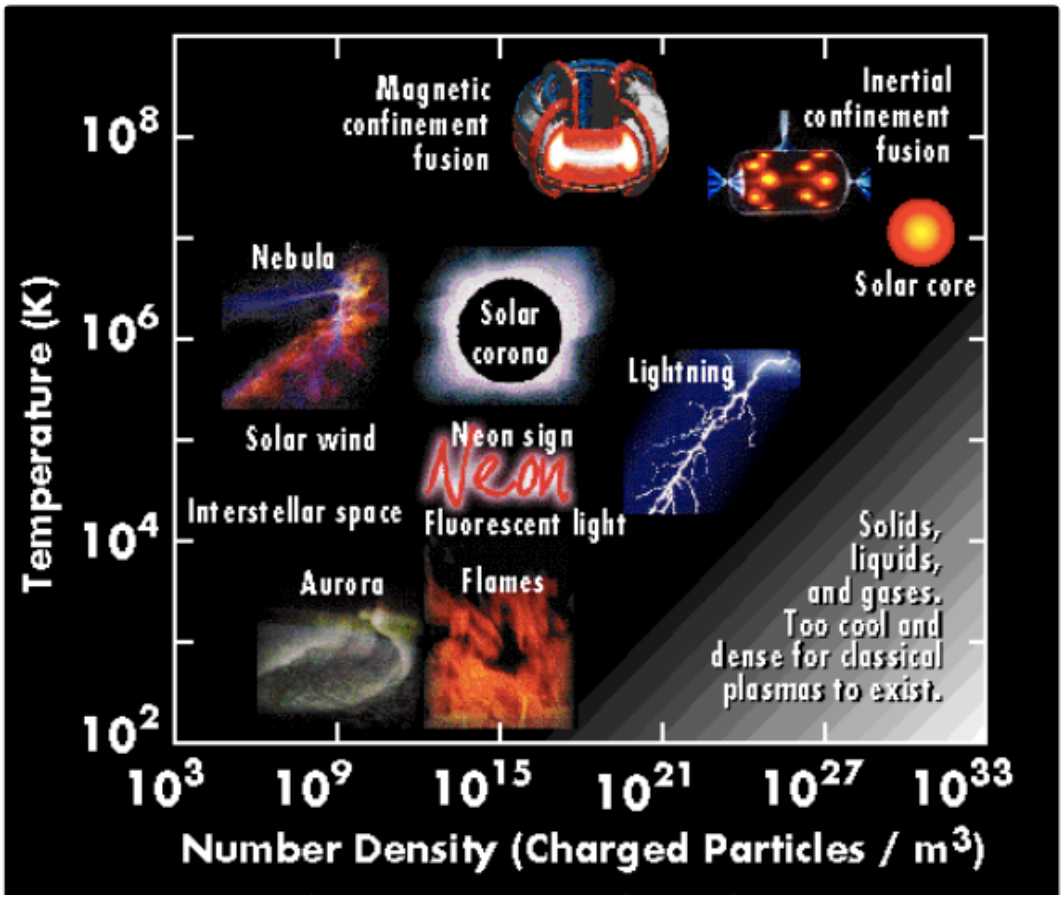

Figure 3. Correlations between plasma temperature and number density (charged particles per volume unit).(From ref [54])

The development of new plasma sources, able to generate cold plasma (CP) at atmospheric pressure, opened up for niche opportunities for bio-based applications towards food safety, public health standard and agriculture [43]. Including applications such as food decontamination, functionalization of food and food contact materials, plant growth enhancement, pest control, wastewater disinfection, or toxin removal [15, 43, 52]. The most common systems currently available for the generation of cold plasma includes corona discharge, dielectric barrier discharge (DBD), microwave discharge, gliding arc and plasma jet [55]. DBD are reactors that has two electrodes, with at least one of them covered by a dielectric barrier. Applying a high voltage between the two electrodes enables the production of an intense electric field that ionizes the gas (e.g. air or O_2) that are confined in the interelectrode gap (Figure 4) [31].

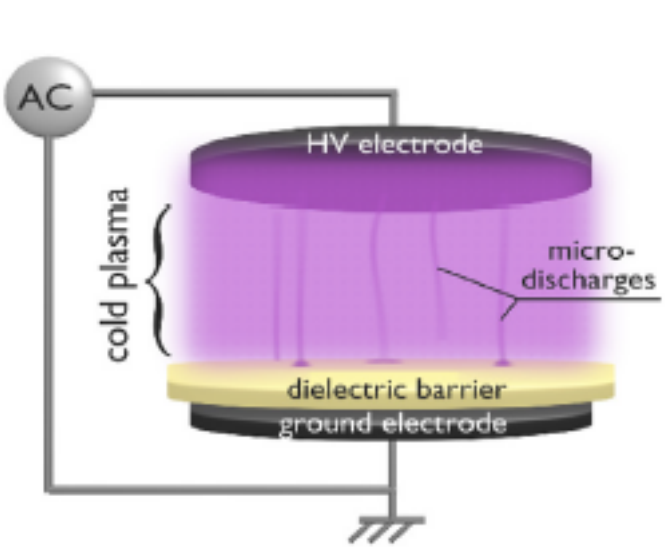

Figure 4. Basic scheme of a dielectric barrier discharge plasma generation system. (From Judée et al. (2018) [31])

The various plasma generation systems together with other processing variables have distinct effects on plasma efficacy. The plasma inducing gas (e.g. air or O_2) will e.g. determine the nature and quantities of reactive species formed [15], while the input voltage used affects the density, i.e. higher input voltage corresponds to higher density [56]. Additionally, direct or indirect plasma exposure to the matrix may result indifferent treatment effectiveness, i.e. an indirect approach decreases the amount of heat transmitted to the matrix, resulting in recombination of some of the charged particles before the samples is reached, due to their self-quenching nature [57].

1.3 Plasma activation of liquids

1.3.1 General

A recent application of cold plasma to overcome some of the challenges associated to this technology include the activation of liquids through their exposure to a plasma discharge (Figure 4) [58]. Plasma activated water (PAW) provides advantages such as e.g. dose control, storage capacity, on/offsite generation, sustainable production and possibility for self-sanitation and reactivation [43, 58]. The type and concentrations of reactive species in PAW rely on several conditions, e.g. the CP operating conditions (e.g. gas composition, plasma source, power and type of liquid), activation time, remote or direct generation and the distance between electrode and liquid surface for remote generation [43].

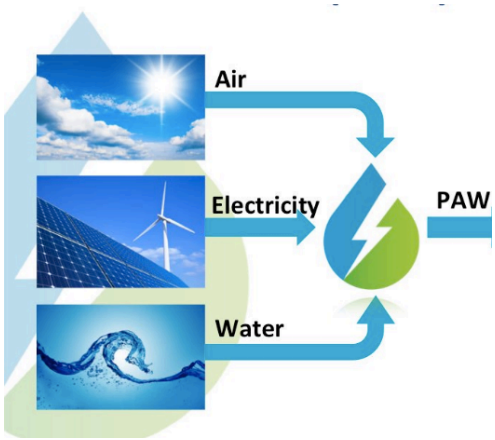

Figure 5. Illustration of the three components necessary for generation of plasma activated water (PAW). (From ref [59])

The existing set ups of PAW generating systems from literature are summarized in Table 3 [58]. The electrical discharge formed in gas phase that are in further contact with a liquid (e.g. over a surface, in a pre-existing bubble or interacting with water droplets and sprays) compared to the gas being in direct contact of the water results in different types and concentrations of reactive species. Regardless of the system, the generation of PAW generally leads to formation of reactive oxygen and nitrogen species, such as hydrogen peroxide, nitrates, nitrites and hydroxyl radicals [60].

Table 3. Available systems for PAW generation (adapted from Thirumdas et al., 2018) [58]

	Mode of operation	**Critical parameter**	**Chemistry**	**References**
- Plasma in contact with liquid **- Discharge over water and hydrated surfaces** **- Discharge with water spray** **- Gas discharge in bubbles**	Gliding arc plasma discharge formed above liquid solution Increase surface area cause by liquid spray Generation of the discharge within the bubbles	Air flow Gap distance of electrodes Distance between electrode and liquid Treatment time Type of gases Voltage source	H_2O_2 Nitrite Nitrates Superoxide anion radicals Singlet oxygen Hydroxide radicals Ozone •OH, O_2, O_2^-	Kamgang-Youbi et al. (2009) [61]; Naitali et al. (2010)[62]; Ma et al. (2015) [63]; Haghighat et al. (2017) [64]; Puač et al. (2017) [65]
- Plasma directly in water	Electric discharges directly in water	End plasma distance and water surface Gases Electrode types (e.g. Graphite, copper) Operating voltage Discharge current Frequency Electrode size	H_2O_2 Peroxide Nitrate Nitrite Superoxide anion (O_2) Ozone Nitric oxide radicals Hydroxyl radical	Ma et al. (2016) [66]; Naumova et al. (2011) [67]; Park et al. (2013) [68]; Shainsky et al. (2012) [69]; Shen et al. (2016) [70]; Zhang et al. (2016) [71];

PAW has been well-accepted for applications in several different fields, ranging from disinfection and decontamination to medicine and agriculture (Figure 6) [72]. Recently, numerous studies have reported great potential for PAW to inactivate bacteria, virus, biofilm and cancer cells [62, 72-75]. PAW has many attractive features as an anti-microbial agent, such as the absence of transport or storage of potential harmful chemicals, being eco-friendly and cost effective as well as having better control of reactive species and easy application [72]. Additionally, it can stimulate seed germination, improve seedling growth and increase crop yield [32, 58, 76], as well as maintaining postharvest quality of fresh products and inactivate foodborne microbes on food [63, 70-72]. It has also proved a rising trend in medical applications, not only for a direct approach as ablation or cauterization but also for more subtle modalities of medical therapy (tissue sterilization, blood coagulations, treatments of cancers) [77].

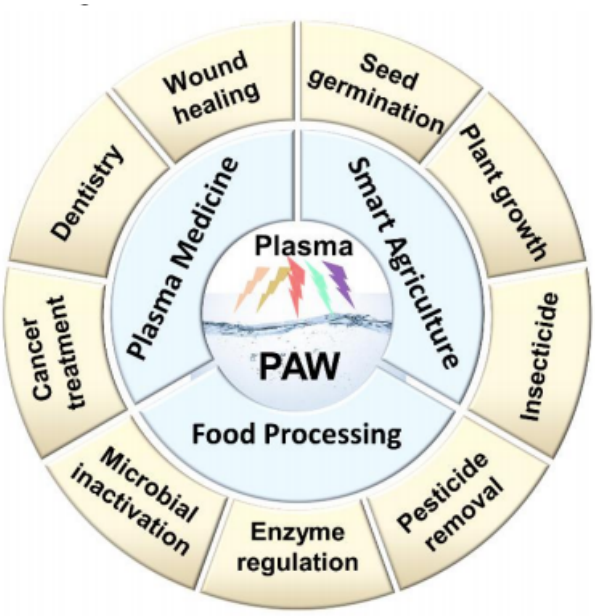

Figure 6. Overall illustration of PAW applied in plasma medicine, smart agriculture and food processing. (From Zhou et al. (2020) [72])

1.3.2 Chemical composition and storage stability

pH

Generally, the pH of water decreases when it is exposed to plasma [58, 62, 66, 70, 74, 78], where, to the knowledge of the author, the lowest pH reported from literature is 2, when pure deionized water (10 mL) was treated for 15 min at 17 kV with a DBD system [43, 69]. Vaka et al. (2019) [43] reported that the pH decreased with increasing exposure time and plasma power, with the most pronounced drop in pH to 2.4 ± 0.1, for 100 mL distilled water treated with a

SDBD system for 20 min with a plasma power of 36 W. Additionally, Ma et al. (2015) [63] observed that for activation with a plasma jet (Ar/O_2 as working gas) there was a rapid pH drop from 7 to 3.2 after 10 min activation, however, did not show any change after 10 min. On the other hand, Judée et al. (2018) [31] reported only negligible pH changes after 30 min activation of tap water with an initial pH of 7.8 using a DBD system (air as working gas), despite reporting high concentration of RONS present. Lukes et al. (2014) [79] conducted a study with phosphate buffer solutions at pH 3.3, 3.9 or 10.0 treated with plasma (Reticulated vitreous carbon electrode and air as feeding gas). Reporting that the concentration of reactive species, (i.e. hydrogen peroxide, nitrites and nitrates) was significantly dependent on the pH of the treated water, with a lower concentration of nitrites and a higher concentration of hydrogen peroxide with a lower pH. During the post-discharge period, concentrations of hydrogen peroxide and nitrites decreased, while the nitrates concentration increased, an effect attributed to the post-discharge reactions of nitrites formed through dissolution of NO_x species from the air discharge plasma into water [79]. Nitrites are not stable in acidic conditions (pH below 3.5) thus rapidly decompose into nitrogen oxide (NO) and nitrogen dioxide (NO_2) intermediates, which further react and form nitrates (NO_3^-) [58, 79]. Jung et al. (2015) [80] reported that when adjusting the initial pH of water with sodium pyrophosphate buffer 1% w/v (pH 9.7), the formation of nitrites over nitrates (782 and 358 mg/L, respectively) was favored after 120 min exposure time with a SBDB system.

ORP (Oxidation reduction potential)

The ORP is a measurement of one solutions ability to oxidize or reduce another substance, depending on the concentration of oxidizers and their strengths [58]. The ORP values provide rapid and single values for assessing the potential of PAW as a disinfectant [63]. Hydrogen peroxide is the ROS formed in PAW that are mainly involved in redox reactions where it can behave as an oxidant or reductant [58, 79]. Zhang et al. (2016) [71] reported that adding oxidizing chemicals resulted in a 63.3% increase in ORP values when distilled water was exposed to plasma for 20 min using Ar/O_2 gas. Ma et al. (2015) [63] reported a linear increasing pattern for ORP with respect to the activation time, with ORP levels of 450 and 550 mV after activation for 10 and 20 min, respectively (Ar/O_2 gas, plasma jet), while the control (distilled water) was 270 mV. Likewise, Vaka et al. (2019) [43] observed an increase in ORP values, in distilled water activated with a SDBD system, with higher plasma power and activation time, with values ranging between 200 and 292 mV for operating conditions of 26 W plasma power for 5 min activation and 36 W plasma power and 20 min activation, respectively. Xu et al.

(2016) [81] reported similar results, activation for 5, 10 and 15 min resulted in ORP of 341, 397 and 467 mV, respectively, while the control (distilled water) presented an ORP value of 146 mV.

Conductivity

Conductivity is a measurement of the ability water has to let electric current flow through it, a measurement that is greatly affected by the presence of extraneous ions [58]. In PAW, the RONS formed in the plasma gas rapidly dissolve in the water, which leads to an increase of the conductivity (μS/cm) [58]. Ma et al. (2015) [63] reported an increase in conductivity to 350 and 450 μS/cm after 10- and 20-min activation with Ar/O_2 gas plasma jet, respectively. Judée et al. (2018) [31] observed a decrease from 647.33 ± 15.07 mS/cm to 614 ± 10.50 mS/cm during the first 5 min of activation (tap water, DBD system with air as working gas), nevertheless, after 5 min the conductivity increased linearly with the activation time from 614 ± 10.50 mS/cm to 731.33 ± 19.37 mS/cm after 5 and 30 min activation, respectively. Likewise, Xu et al. (2016) [81] reported a linear increase in conductivity from 17 μS/cm (untreated water) to 218 μS/cm after 15 min generation with an atmospheric plasma jet. On the other hand, Tian et al. (2015) [82] observed a conductivity of 18.8 μS/cm after 20 min activation with similar feeding gas as Ma et al. (2016) [58], however, using a microjet. The microjet has a lower applied voltage, indicating that the higher applied voltage might be the reason for the increase in conductivity.

Temperature

Vaka et al. (2019) [43] reported an increase in the temperature alongside the increase of exposure time, which was attributed to the thermal effect of the SDBD electrode. Nevertheless, the temperature never exceeded 35 °C. Jung et al. (2017) [83] reported, from a study on meat batter, that the temperature increased from 2 to 20 °C after 60 min, and from 2 to 10 °C after 30 min activation. Judée et al. (2018) [31] observed a gradual increase in temperature upon plasma activation, from ambient (27 °C) to an increase of 3.60 ± 0.72 °C and 9.03 ± 1.26 °C after 5 and 30 min, respectively. Reporting a nonlinear increase in temperature where the heating slows down after 25 min activation, reaching a plateau, which in Judée et al. (2018) experiment was estimated to be 36.73 ± 1.26 °C.

RONS

The type and concentration of RONS formed in PAW is dependent on several conditions, e.g. the CP operating conditions (e.g. gas composition, plasma source, power and type of liquid),

activation time, remote or direct generation and the distance between electrode and liquid surface for remote generation [43]. ROS (i.e. hydrogen peroxide and hydroxyl ions) and RNS (i.e. nitrates, nitrites and peroxynitrites) has been reported as persistent species in PAW, regardless of operating system, the possible chemical reactions that can take place in generation of PAW that result in the formation of RONS are listed in Table 4 [43, 79]. In literature a wide concentration range of nitrates and nitrites levels have been reported. For instance, Vaka et al. (2019) [43] observed an increase in both nitrates and nitrites levels with higher plasma power and exposure time, reporting the highest yield after 30 min activation using a SDBD system with a plasma power of 36 W of 320 ± 47.8 mg/L and 7.2 ± 3.8 mg/L for nitrates and nitrites, respectively. Although, both species increased with higher exposure time and plasma power the maximum yield for nitrates was significantly higher than the maximum value for nitrites. As nitrites remain stable at alkaline conditions, Jung et al. (2015) [80] adjusted the initial pH of distilled water to 9.0 and generated PAW with a SDBD system (average power of 3.14 W; discharge area of 20 cm^2; frequency of 15 kHz), resulting in nitrites and nitrates levels of 782 and 385 mg/L, respectively, favoring the formation of nitrites. Judée et al. (2018) [31] reported a nitrite concentration of 175.4 ± 9.7 and 125.79 ± 6.85 μM after 10- and 30-min activation, respectively (DBD system, tap water and air as working gas), observing a decrease in nitrite levels after 10 min activation, whilst, the nitrate concentration increased almost linear to the activation time and reached a maximum concentration of 3.55 mM after 30 min.

With regards to the hydrogen peroxide, the concentration in PAW is dependent on initial treatment volume, direct/ remote treatment and electrode-liquid gap. Ikawa et al. (2010) [84] reported hydrogen peroxide concentrations up to 50 mg/L in 500 μL distilled water after 3 min exposure to a plasma jet, which is a direct treatment (a pulsed high voltage of -3.5 to +5.9 kV and a frequency of 13.9 kHz). Judée et al. (2018) [31] reported a quadratic trend for the increase of hydrogen peroxide concentration with increased activation time and achieved a maximum value of 1.85 ± 0.16 mM after 30 min (DBD system, voltage amplitude of 12.0 kV_{AC} at 500 Hz). Additionally, Shainsky et al. (2012) [69] reported concentrations of 2000 mg/L using a DBD system with a pulsed voltage of 17 kV on 100 μL distilled water with a 1.5 mm electrode-liquid gap. Taylor et al (2011) [85] reported hydrogen peroxide levels of 3.4 mg/L when using a DBD system operating at 5 kV for 20 min (10 mL distilled water). In literature the lowering of concentration rapidly after treatment is attributed to the rapid decomposition of hydrogen peroxide by nitrites under acidic conditions [79, 86].

Table 4. Chemical reactions that can take place during generation of PAW resulting in the formation of ROS and RNS. (Adapted from Thirumdas et al. (2018) [58])

$H_2O + e \rightarrow OH\bullet + H\bullet + e^-$
$H_2O + e \rightarrow H^+ + H\bullet + 2e^-$
$H_2O + e \rightarrow H\bullet + O\bullet + H\bullet + e-$
$O_2 + e \rightarrow O^+ + O + 2e$
$O_2 + e \rightarrow O_- + O$
$O + O_2 \rightarrow O_3$
$O_3 + NO \rightarrow NO_2 + O_2$
$N + O_2 \rightarrow NO + O$
$O + N_2 \rightarrow NO + N$
$2\ NO + O_2 \rightarrow 2\ NO_2$
$NO_2 + OH \rightarrow HNO_3$
$H_2O_2 + hv \rightarrow OH\bullet + OH\bullet$
$3\ NO_2 + H_2O \rightarrow 2\ HNO_3 + NO$
$H_2O_2 + H^+ + NO_2^- \rightarrow ONOOH + H_2O$
$OH\bullet + OH\bullet \rightarrow H_2O_2$
$NO + NO \rightarrow N_2 + O_2$
$NO + OH\bullet \rightarrow HNO_2$
$HNO2 + OH\bullet \rightarrow NO_2 - H_2O$
$NO_2 + hv \rightarrow NO + O\bullet$
$NO_3 + hv \rightarrow NO + O_2$
$NO_2 + NO_3 \rightarrow H_2O_3$
$N_2O_5 + H_2O \rightarrow 2\ HNO_3$
$2\ NO_2 + H_2O \rightarrow NO_2^- + NO_3^- + 2H^+$
$3\ NO_2^- + 3\ H^+ \rightarrow 2\ NO + NO_3^- + H_3O^+$
$OH + NO_2 \rightarrow [O=N-OOH] \rightarrow O=N-OO^- + H^+$

Stability during storage

The stability of PAW during storage has a big impact on the possibilities of industrial applications. If PAW keeps stable during storage it opens up for a lot more freedom when it comes to its usage. A recent study conducted by Vaka et al. (2019) [43], generated PAW with a SDBD and stored it in 4 °C for 14 days. This study reported no significant differences in the pH or the concentration of nitrates. In the graph with the nitrite concentration plotted against storage time, a decrease in concentration could be observed over time, nevertheless, from the statistical analysis, there was no significant difference. Shen et al. (2016) [70] assessed the bactericidal effect of PAW against *S. aureus* as a function of storage condition of 4 temperatures, -80, -20, 4 and 25 °C, for up to 30 days. The result showed a decrease in the reactive species (hydrogen peroxide, nitrites and nitrates) over time. In addition, this decrease

was greater for the higher storage temperature. In this study PAW was generated using a plasma jet in direct contact with the water. Niquet et al. (2018) [87] reported an increase in hydrogen peroxide concentration, while the concentration of nitrate remained constant for 24 h storage at 4 °C for PAW generated with DBD, although the nitrite levels was below detectable levels before and after storage. Julak et al. (2012) [55] conducted a study where PAW stability was assessed during four weeks storage at 4 °C, using water exposed to negative glow corona or positive streamer discharge for 60 min. Results from the positive streamer discharge showed a pronounced decrease in hydrogen peroxide concentration, however, there was still 50 mg/L left in 1 mL of exposed water. Moreover, for the negative corona, only negligible amount of hydrogen peroxide was left in the water. There were no significant differences in the pH for either systems.

1.3.3 Parameters for generating PAW

Activation time

The time the water is exposed to the plasma or activation time will have a great effect on the properties of the PAW, with the most typical activation times from literature ranging between 3 and 30 min. As mentioned in section 1.3.2, the pH and ORP of PAW have been reported to decrease/increase, respectively, as the activation time increases. Thus, according to Ma et al. (2015) [63] water activated for 20 minutes resulted in higher oxidation-reduction potential (ORP) (550 mV) than water activated for 10 min (450 mV). Xu et al. (2016) [81] reported similar observations, where the ORP values increased with longer exposure time (5, 10 and 15 min). For instance, Xu et al. (2015) [81] reported that the pH in PAW was lower after 15 min exposure than in 5 min exposure time. Vaka et al. (2019) [43] reported similar results when 5, 12.5 and 20 min activation times were assayed together with different plasma power values (16, 26 and 36 W). The PAW generated within the same plasma power values resulted in a lower pH with increased exposure time, additionally a higher concentration of RNS (i.e. nitrates and nitrite) was observed with increased exposure time. Numerous studies have indeed reported higher concentration of RONS with longer exposure times [31, 43, 80]. Additionally, Judée et al. (2018) [31] conducted an experiment assessing how the different activation time (i.e. 5, 10, 15, 20, 25 and 30 min) affected e.g. conductivity, temperature and concentrations of RONS in plasma activated tap water (DBD system). Resulting in a linear increase in conductivity for PAW activated for more than 5 min (decrease in the first 5 min), while a nonlinear regression was observed for the temperature, where the temperature increase slowed down after 25 min activation, reaching a plateau. With regards to the RONS, a quadric relation was suggested

between hydrogen peroxide concentration and activation time, while concentration of nitrates increased linear with longer activation times. Although, the nitrite concentration also increased the first 10 min, it decreased linearly after 15 min.

Voltage, current and frequency

Plasma process factors such as voltage, frequency and current can influence the pH, ORP and concentration of RONS, thus further influence microbial inactivation [88]. Typical frequency values from literature ranges between 10 – 20 kHz [66, 70, 74, 78, 81], although there are exceptions outside this range as well [79, 89]. Studies indicated that a higher voltage input resulted in a lower pH and higher concentration of reactive species. Vaka et al. (2019) [43] conducted an experiment with different input voltages that resulted in three different peak-to-peak values, 9, 10 and 11 kV, which corresponded to a plasma power of 16, 26 and 36 W, respectively. A significant increase in RNS concentration and ORP for the different plasma power can be observed for the same activation time, as well as a decrease in the pH.

Gas

The type of gas used is important, as the plasma chemistry is dependent on the properties of the gas medium [88]. Generally, any gas can be used, but the microbial efficiency will vary dependent on which one is used. For instance, the use of air, which is rich in oxygen and nitrogen, will result in formation of a number of primary species, including atomic oxygen, singlet oxygen, superoxide, ozone, hydroxyl radicals and atomic nitrogen. These will continue to react and form secondary species, including hydrogen peroxide, peroxynitrite, nitric oxide, nitrates and nitrites [58]. These are the main chemical reactions in PAW that processes antimicrobial activity. Typical gases used for PAW generation in literature includes atmospheric air [70, 73, 74], oxygen (O_2) [73] or a combination of Ar/O_2 [63, 81]. Zhang et al. (2017) [90] conducted an experiment, generating PAW with different feeding gas (i.e. argon, nitrogen, air and oxygen), assessing the amount of OH radicals, and concluded that the value is largely dependent on processing gas and was highest in the solution treated by oxygen plasma.

Water source and volume

Most research conducted with plasma activation of liquids, in literature, uses a volume ranging between 1 and 500 mL [63, 70, 74], although there have been studies with volumes up to 1600 mL [66]. The gap distance between plasma electrode and liquid surface typical ranging from 5 mm to 5 cm. Additionally, for most set ups in literature, distilled and deionized water are use,

due to its reproducibility in composition, unaffected by seasonality or occasional variations in the public water supply [43]. Literature is scarce for studies conducted up to date using Norwegian tap water. According to IVAR, which is an intercommunal company that operates municipal facilities for water, wastewater and general waste in the south-west of Norway, Norwegian tap water has on average a pH of 8, it is also considered to have a low hardness, where hard water has a high concentration of minerals, mostly calcium carbonate and magnesium bicarbonates [91]. The concentration of carbonic compounds, particularly carbonate and bicarbonate, is the main factor influencing the alkalinity of water and thus, its buffering capacity or ability to resist changes in pH, which will be of utmost importance with regards to the PAW composition [92]. Judée et al. (2018) [31] conducted an experiment with tap water from France, where it was observed that 30 min activation with a DBD system resulted in negligible changes in pH (initial pH of 7.8). At the same time was the bicarbonate and carbonate concentration determined to be 4.13 ± 0.09 mM and 13.1 ± 3.62 μM, respectively.

1.4 Applications of cold plasma technology in the food industry

As above mentioned, CP technology is already a well-accepted technology in many fields, and already commercially exploited for a variety of usages in electronics, surface decontamination, textiles, glass or paper. In addition, PAW is getting an increased amount of attention for exploitation in plasma medicine, food and agriculture applications [72]. In this section, the focus will be on microbiological food safety and agriculture applications. Indeed, CP have been demonstrated useful for disinfection in several studies, as well as having potential for many other purposes [93-95].

1.4.1 Plasma technology for food decontamination

In gas plasma, several mechanisms combine synergistically towards microbial decontamination, e.g. RONS, UV photons, electric field and charged particles (Figure 7) [96].

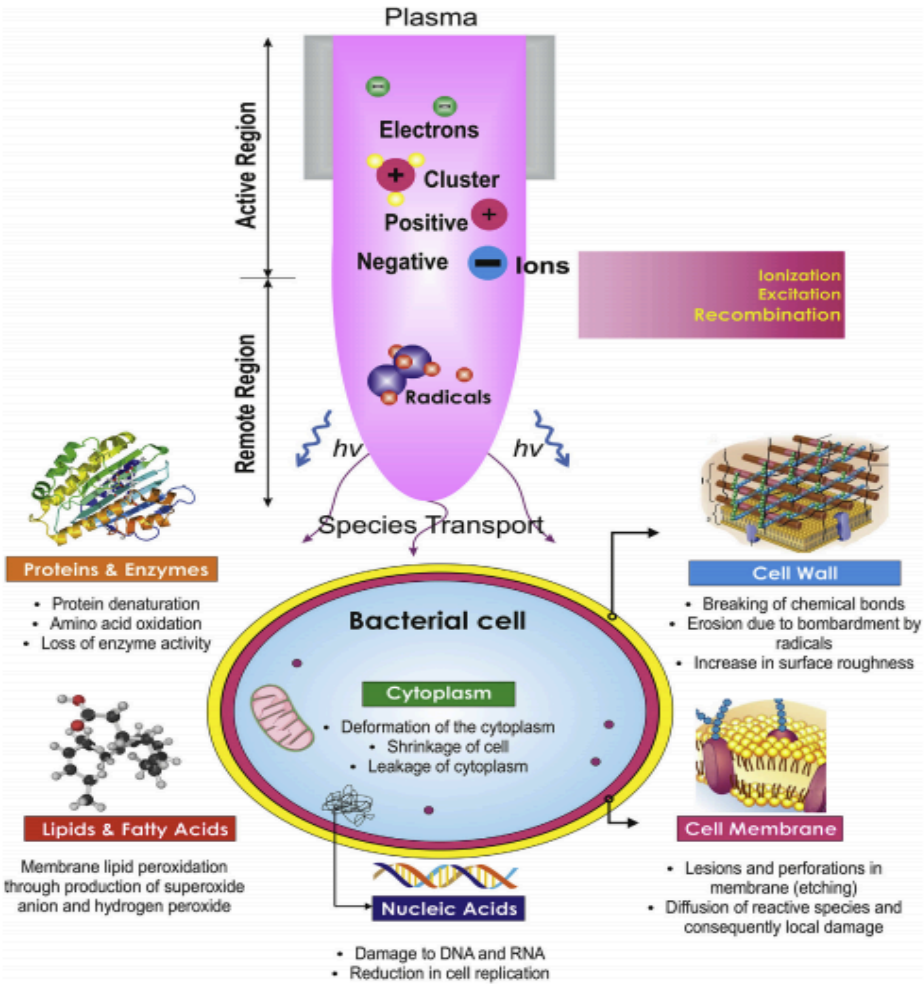

Figure 7. A schematic illustrating the action of cold plasma on cell structure resulting in loss of functionality and sterilization. (From Misra et al. (2017) [96])

Plasma reactive species are considered to play an important role in microbial decontamination [97]. Dependent on which gas is used, different reactive species are present in the plasma. The species that are commonly associated with antimicrobial activity are RONS [96]. The ROS from plasma interacts destructively with cellular biomolecules, such as DNA, proteins and enzymes and can potentially alter the function of biological membranes via interactions with lipids (causing formation of unsaturated fatty acid peroxides) and oxidation of amino acids [96, 98]. Exposure to intense electric fields can lead to rupture of the a bacterium cell membrane, caused by the electrostatic tension from the high electrical charge developed within [96]. UV light emitted from the cold plasma plays a smaller role in microbial decontamination [97]. With regards to the effectiveness of CP, the inherent properties of the microorganisms are important, as the sensitivity to CP treatment can vary within species or even strains. Furthermore, Gram-positive bacteria have been found to be less sensitive to CP treatment than Gram-negative bacteria, due to their lipopolysaccharide membrane and thicker peptidoglycan cell wall. In

addition, bacteria in the stationary phase are more sensitive than bacteria in the exponential phase [99, 100]. Sporulated bacteria have also been found to be less sensitive to CP treatment [93]. Moreover, high concentration of bacteria clusters reduce the penetration capacity of the reactive species and therefore the decontamination efficacy [101]. Table 5 presents a few selected studies on the antimicrobial effect of CP on different food matrices.

Table 5. Selected studies on the antimicrobial effect of CP on different food matrixes (adapted from Ekezie et al. (2017)) [15].

Food matrix	Microorganisms	Plasma source	Treatment conditions	Observation	References
Lettuce	*L. monocytogenes* *Pseudomona fluorescens*	DBD	V = 80 kV, f = 50 Hz, ET = 5 min	4 log cfu/g reduction of *L. monocytogenes*, 2.1 log cfu/g reduction of *P. fluorescens*	Patange et al. (2019) [102]
Tryptic soy agar (TSA) **Queso Fresco cheese (QFC)** **Cheese model (CM)**	*Listeria innocua*	DBD	V = 130 kV, f = 60 Hz, ET = 2 min	5.0, 3.5 and 1.6 log cfu/g reduction for RSA, CM and QFC, respectively.	Wan et al. (2019) [103]
Romaine lettuce	*Escherichia coli O157:H7*	DBD	V = 42.6 kV, RH = 22%, d = 5.0 cm, ET = 10 min	0.4-0.8 log cfu/g decrease in the number of *E.coli*	Min et al. (2017) [104]
Vacuum packed beef loin	*Staphylococcus aureus* *L. monocytogenes* *Escherichia coli*	DBD	f = 9 kHz, d = 2 cm, P = 29.9 W	≥2 log reduction	Bauer et al. (2017) [105]
Ham	*L. monocytogenes* *Salmonella typhimurium*	Two surface-micro-discharge-plasma	F = 2 kHz, V (peak – to – peak) = 10 kV, ET = 20 min	1.14 log reduction for *S. typhimurium* 1.02 log reduction for *l. monocytogenes*	Lis et al. (2018) [106]

However, applying CP gas directly on to the food products has some limitations, it may negatively affect product color, surface topography or bioactivity and the efficiency of the inactivation may also be dependent on the surface texture as CP does not have penetrating capabilities [43]. According to Noriega et al. (2011) [107], the surface properties of the product had a great impact on the plasma antimicrobial efficacy in chicken products, reporting that under same operating conditions, a 10 s treatment gave > 3 log reductions of *L. innocua* on membrane filters, an 8 min treatment gave 1 log reduction on skin, and a 4 min treatment gave > 3 log reductions on muscle. Noriega et al. (2011) suggest this may be due to the hidden spaces and irregularities on the surface where bacteria can be drawn to through capillary action, limiting the plasma reach and antibacterial efficacy. Likewise, Fernandez et al. (2013) [108]

reported that under the same operating conditions a 2 min treatment resulted in a 2.71 log-reduction of S. Typhimurium viability on membrane filters whereas a 15 min treatment was necessary to achieve 2.72, 1.76 and 0.94 log-reductions of viability on lettuce, strawberry and potato, respectively. Suggesting that the differing efficiency of CP treatment on the inactivation of *S. Typhimurium* on these different types of fresh foods is a consequence of their surface features. As already mentioned, PAW provides several advantages to direct CP treatment. It has the ability to penetrate the product, while not changing sensory properties, such as color, firmness or texture [43]. Additionally, PAW can be considered a green and prospective solution for biotechnology applications due to the transient nature of its biochemical activity, and potential economic and environmental benefits of using air rather than potentially toxic chemicals as the starting material and renewable energy to drive the discharge [72]. High food loss in the industry due to products with a short-shelf life or unsafe and withdrawn products has a high cost. PAW has the potential to reduce food loos, reduce water usage and reduce wastewater, resulting in a high recycling ratio [72, 109]

The mechanism mainly responsible for microbial inactivation are ROS and RNS, where the formation of these species further show an synergistic effect with high ORP and low pH, proved to possess anti-microbial activity [58, 71]. Hydrogen peroxide, hydroxyl ions and ozone are the chemical species formed in PAW considered to be strong anti-microbial agents [58]. ROS are responsible for lipid oxidation of the cell membrane, has the potential to break intra-molecular bonds of peptidoglycan which could further lead to cell wall breakdown, can cause cell shrinkage, cytoplasmic leakage and breakdown of spore membrane, as well as causing internal damage through breakdown of DNA, destruction of proteins and other internal components of the cell [58, 79]. Nitric oxide and its derived products (i.e. nitrates, nitrites and peroxynitrites) is the potent RNS species formed in PAW and their primary action of antimicrobial activity through the lowering of pH, where the formation of nitric, nitrous and formic acid cause the acidification [58]. Peroxynitrite ion is a very strong oxidizing agent, thus formation of this ion can also participate in the antimicrobial activity of PAW [58]. Important physical parameters responsible for microbial inactivation include pH, ORP, UV radiation, shock waves, photons and electric fields formed in PAW. Figure 8 is a schematic diagram of the PAW induced cell destruction, illustrating the different mechanisms caused by RONS and physical parameters (pH, ORP, UV radiation and shock waves) responsible [58].

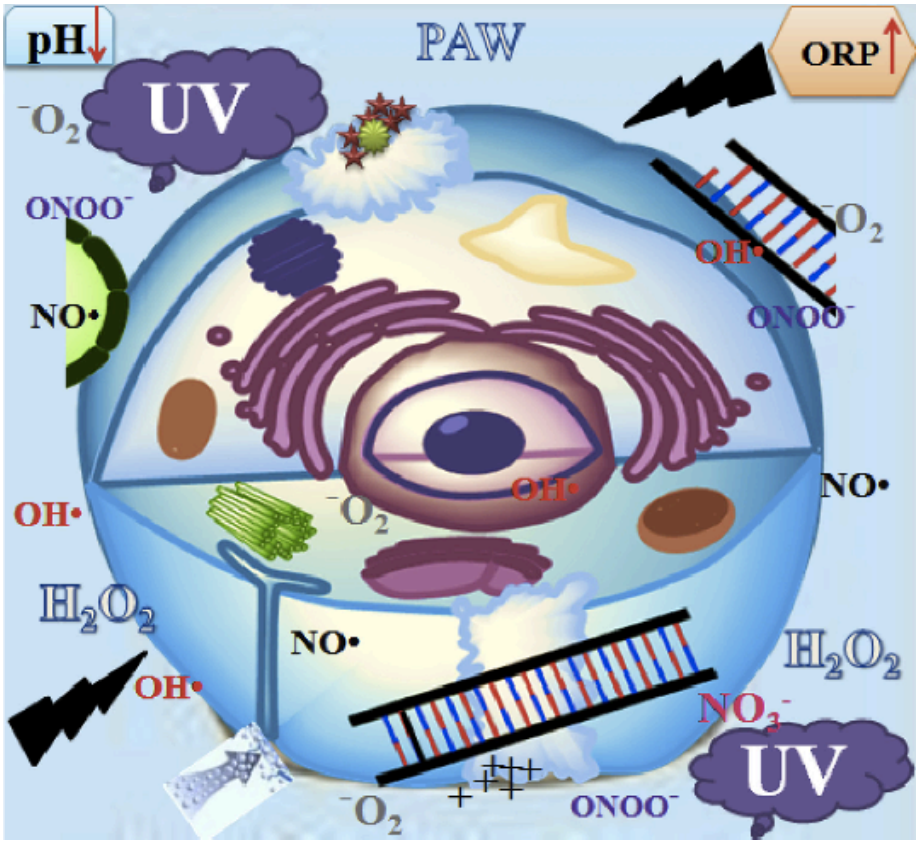

Figure 8. schematic diagram of the PAW induced cell destruction, the different mechanisms caused by RONS and physical parameters (pH, ORP, UV radiation and shock waves). (From Thirumdas et al. (2018) [58])

In literature, several studies have reported inactivation of different bacteria based on the different mechanisms responsible for the decontamination. For instance, Oehmigen et al. (2010) [78] conducted a study assessing the antimicrobial activity of PAW generated, using indirect surface DBD, from non-buffered physiological saline (NaCl: 0.85%) or phosphate buffered saline (PBS), where the pH in the non-buffered physiological saline decreased from pH 7 to values between 2 and 3 for the after 30 min activation, while the PBS solution kept a steady pH of around 7 after 30 min activation, resulting in complete inactivation of *E.coli* and *S. aureus* (initial concentration of 10^6–10^8 cfu/mL) after 5-15 min dependent on sample volume (1.5, 5 and 10 mL) for the non-buffered solution. Whereas for the PBS, only the smallest sample volume (1.5 mL) resulted in log reduction (3-log) after 15 min treatment. Oehmigen et al. (2010) concluded that with the use of buffered solutions, pH remains stable and an acidified environment is avoided, which reduces the antimicrobial plasma activity drastically. Furthermore, Tian et al. (2015) [82] conducted an experiment on the formation of intracellular ROS concentration in *S. aureus* treated with PAW (generated with direct/remote plasma jet), which resulted in a higher ROS concentration for PAW generated with direct contact between

the plasma jet and the water, which further led to more sever oxidation stress, drop in membrane potential, breach in integrity and cell death in *S. aureus,* thus more efficient sterilization. Ma et al. (2015) [63] reported that PAW activated for 20 min resulted in 3.5 log reductions of *S. aureus* in strawberries after 15 min treatment, observing that the ORP value increased with longer activation time, indicating more RONS are formed, thus a higher antimicrobial activity in PAW. Table 6 summarizes a few of the many studies conducted to assess the antimicrobial efficiency of PAW.

Table 6. Overview of selected studies on the potential of PAW for bacterial inactivation (adapted from Thirumdas et al. (2018) [58])

Food matrix	Microorganism	Plasma source	Treatment conditions	Observations	References
Strawberries	*S. aureus*	Plasma jet	80 mL distilled water, g = Ar – O_2, ET = 10 and 20 min, f = 10 kHz	PAW treatments achieved a reduction of S. aureus ranging from 1.6 to 2.3 log at day-0 storage, while 1.7 to 3.4 log at day-4 storage.	Ma et al. (2015) [63]
Fresh-cut apples	*Bacteria* *Mold* *Yeast* *Coliform*	DBD	Distilled water f= 7.0 kHz, V = 8 kV, ET = 10 min	Reduction of 1.05, 0.64, 1.04 and 0.86 log cfu/g for bacteria, molds, yeast and coliforms, respectively	Liu et al. (2020) [110]
Brines **Jerky**	*L. innocua*	Plasma jet	Brine solutions, f = 20 kHz, Power = 300 W, ET = 10 min	Reduction of 0.5 and 0.85 log for brines and jerky, respectively	Inguglia et al. (2020) [111]
Cell suspension	*E. coli* *S. aureus*	Micro-hollow cathode discharge	50 mL distilled water, g = oxygen or air, ET = 10, 15 and 30 min	Bacteria and biofilm were unable to survive in those PAWs after an exposure of 30 min and 3 h, respectively	Chen, Liang & Su (2017) [73]
Cell suspension	*E. coli*	DBD	1 mL N-Acetylcysteine solution, g = air, ET = 1, 2 and 3 min, f = 15 kHz, V = 31.4 kV	7 log reduction of E. coli	Ercan et al. (2015) [74]
Mung bean sprout	*Total aerobic bacteria* *Yeast*	Plasma jet	200 mL distilled water, g = compressed air, ET = 30 s, f = 40 kHz, V = 5 kV	2.32 log reduction bacteria 2.84 log reduction yeast	Xiang et al. (2019) [112]

The potential of CP as a food processing technology has been demonstrated for a range of processes and products, including microbial decontamination, pest control, toxin elimination, food and package functionalism, applications in agriculture, such as growth enhancement and

increased seed germination and much more [30]. Major challenges for implementing CP as a food processing tool by the industry includes the demonstration of product and process specific efficacies, development of process compatible technology designs and scale-up, effective process control and validation, regulatory approval and the acceptance of consumers [30].

1.4.2 Examples of product applications

Fresh produce

PAW is classified as purified water with promising applications in food industry, e.g. as a curing agent, fertilizer or postharvest sanitizer in the fresh produce industry [58, 113]. Minimally processed vegetables are increasingly important towards a healthy and balanced diet, which further leads to prevention of obesity, diabetes, cardiovascular diseases and cancer [114]. Additionally, fresh vegetables are rapidly growing as a convenience, ready to eat meal, thus the importance of technologies to keep the microbial safety and quality/freshness attributes. Nevertheless, major challenges face the fresh produce industry, such as the rapid deterioration and limited shelf-life in such products as compared to whole items, due to their high respiration and transpiration rates, and their susceptibility to enzymatic and microbial degradation [43, 115]. The color is one of the most important quality for the consumers acceptability [116], as the discoloration of green leafy vegetables is the first visible symptom of senescence [117]. Furthermore, the green leafy vegetable, such as spinach, are commonly linked as the source for foodborne illnesses, with washing step and surface cross-contamination being responsible as major sources for microbial contamination [114, 118]. Currently, several studies have proven enhanced shelf-life for fresh produce when being treated with PAW after the postharvest handling, as well as inactivating bacteria. Ma et al. (2016) [66] reported decreased fruit decay by 50% in Chinese bayberries treated with PAW compared to control samples. Chen, Liang (2017) [73] found that 30 min exposure to PAW completely inactivated *E. coli*, as well as 99.9 % inactivation of 1-day old biofilm with *S. aureus* exposed to PAW activated for 30.

L. monocytogenes is a Gram-positive bacterium responsible for the human illness listeriosis. Listeriosis has symptoms ranging from mild gastroenteritis to sever blood and central nervous system infections, including abortion in pregnant women [119]. Recently, several foodborne outbreaks have been linked to the presence of *L. monocytogenes in* fresh produce. For instance, in 2010, *L. monocytogenes* was accountable for the deaths of 10 people when there was a listeriosis outbreak originating from chopped celery in Texas [120]. *L. monocytogenes* is found extensively in soil, manure, water and other agriculture environments [121] and is generally

considered a high-risk in processed ready-to-eat, cold-stored meat and dairy products. Nevertheless, many studies have now detected *L. monocytogenes* in fresh produce samples and some minimally processed vegetables. It has been isolated from produce such as cabbage [122], lettuce [123-126], carrots [127-129], cucumbers [121, 130, 131] and salad vegetables [131-134]. Table 7 provides an overview of selected studies on the decontamination efficacy of CP and PAW on fresh produce.

Table 7. Overview of selected studies on the microbial decontamination efficacy of CP and PAW on fresh produce (adapted from Pan et al [135])

Microorganism	Treated matrixes	Treatment conditions	Salient results	References
L. monocytogenes	Lettuce and cabbage	Cold oxygen plasma (atmospheric air)	Cold oxygen plasma was effective on L. monocytogenes inactivation for both cabbage and lettuce	Srey, Park, Jahid, and Ha (2014) [136]
	Cabbage, lettuce, and dried figs	Microwave CP (400 to 900 W and 667 Pa), work gas (He: O2 = 99.8:0.2), flow rate (<20 standard L/min)	Microbial inhibition by CPT was linearly correlated with treatment time. CPT combined with lowering pH inhibited the pathogens synergistically	Lee, Kim, Chung, and Min (2015) [137]
	Fresh-cut dragon fruit	Atmospheric RF plasma (40 W, 60 s, 20 to 600 kHz), work gas (argon), and green tea extract (5.0%)	5.0% of green tea pre-treatment for 60 s followed by plasma exposure for 60 s could extend the shelf life of fresh-cut dragon fruit to at least 15 days at 4 °C	Matan et al. (2015) [138]
E. coli	Barley grains and wheat	A high voltage DBD plasma system (80 kV at 50 Hz, atmospheric pressure), working gas (atmospheric air), and discharge gap (10 mm)	Direct and indirect plasma treatment for 20 min followed by posttreatment storage for 2 hour resulted in 3.5 (undetectable levels) log10 cfu/g reduction and 3.3 log10 cfu/g reduction of E. coli on barley grains, respectively.	Los et al. (2018) [139]
S. aureus	Strawberry	PAW, work gas (Ar/O2), and flow rate (5 L/min)	Even for day 0 storage, PAW treatments achieved a reduction of S. aureus for 1.6 to 2.3 log Compared to control group, shelf life was obviously extended	Ma et al. (2015) [63]
Total microbial concentration	Baby spinach leaves	SDBD (air as feeding gas and atmospheric pressure), discharge gap = 44.8 mm, f = 12	About 1 log reduction in bacterial concentration, significantly lower microbial levels for samples treated	Noriega et al. (2019) [43]

	kHz, P = 12, 16 or 36 W	with PAW after eight days storage at 4 °C.

PAW has recently gained growing interest as a sustainable, cost-effective alternative to current disinfectants based on artificial chemical cocktails [55]. Nevertheless, further studies on PAW composition, stability and preservation ability on representative products, are still required towards technology upscaling and industrial uptake [43].

Macroalgae

Currently, the global seaweed production is largely dominated by Asian countries, where 87 % of the biomass is being used, either for direct human consumption (i.e. fresh or dried) or further processed as a food ingredient (i.e. alginate, phycocolloids, agar or carrageenan). Additionally, seaweed is being used for non-food applications, e.g. as a fertilizer, feed ingredients, pharmaceuticals and cosmetics [140]. Seaweeds are one of the largest unexploited global biomass resource, which is a suitable alternative to terrestrial biomass production, with the potential to sustain a sufficiently and healthy global food supply meeting the demand of a growing population [141]. Norway has a long and complex coastline with cold temperatures in the water which host over 400 species of brown, red and green seaweeds. Wild harvested *Laminaria hyperborea* and *Ascophyllum nodosum* and farmed *Sacharina latissima* are main macroalgal species processed at industrial scale in Norway nowadays [141].

Although seaweeds chemical composition depends on species, harvesting season and eco-habitat, macroalgae are naturally rich in valuable nutrients such as minerals, vitamins, polyunsaturated fatty acids (omega-3), polysaccharides (both structural and storage) and dietary fiber. Moreover, certain species contain relatively high protein levels (200-300 g/kg dry weight) and high-quality profiles of essential amino acids, lipids and minerals, besides a large variety of phytochemical constituents with potential in the prevention/treatment of health diseases [141, 142]. Coupled with high variations in shape, color, texture and taste, seaweeds nutritional content makes marine macroalgae highly relevant towards food applications. However, the high-water content of seaweeds [70-90%] poses a serious challenge for preserving and transporting large amounts of biomass from harvesting to processing sites, thus seaweeds are characterized by rapid microbial decomposition once harvested. For instance, algal susceptibility to contamination with heat-tolerant spore-forming pathogenic bacteria, resistant to prolonged freezing or anaerobic conditions, may challenge further operational settings [143-

145]. Although, algal bacterial pathogens associated with macroalgae are predominantly non-pathogenic to humans, there are some exceptions. they may act as reservoirs for faecal bacteria and if so the microbe-algae associating enhance the survival time of such bacteria in the marine environment [146]. Several of the human pathogenic vibrios are described associated with macroalgae, and even some environmental bacteria not having an aquatic habitat as its niche may also pose a challenge for food safety without giving a direct risk, of highest importance are the spore forming Bacillus sp. and clostridium sp., originating from soil by run of from land [146, 147]. Methods as drying can also stabilize seaweed biomass, however, the technology is not suitable for production on a large scale and may compromise product quality [148]. Thus, adoption of seaweeds as staple food items in the daily diet requires multi-target and mild processing schemes ensuring biomass safety, nutritional value and sensory-wise appealing attributes for human consumption, such as cold plasma technology. To the knowledge of the authors there is scarce literature available on the use of CP or PAW on seaweeds, with the exception of a few. For instance, the study Nisol et al. (2018) [149] conducted a study with HC discharge (Ar/O_2) directly bubbled into highly concentrated aqueous suspension of cyanobacteria Dolichospermum, green algae Scenedesmus and BMAA toxin, reporting that a short treatment time (up to 6 min) could greatly reduce the numbers of viable cells and completely destroy the BMAA toxin. Additionally, PAW was observed to continue its effectiveness after 24 h, even 4 days after terminating the discharge. Puligundla, Kim & Mok (2015) [150] conducted experiment using low pressure air plasma as an activating agent against surface microbial contaminants of sun-dried laver sheet and reported a 1-log reduction in viable cell count of aerobic bacteria was observed over a 20 min period. Lastly, Kim, Puliggundla & Mok (2015) [151] used atmospheric pressure corona discharge plasma jet for surface decontamination of thin sheets of dried laver, resulting in a greater than 2 log (99%) unit reductions in viable cell count of aerobic bacteria was observed over a 20 min period. Further studies would be required to assess the potential of PAW as a rinsing method for decontamination of seaweeds, including the impact it would have on the nutritional value and the quality attributes.

1.4.3 Agriculture applications

Agriculture is the process of producing food, feed and fiber and was the key to develop civilization and is as crucial today as it was 10 000 years ago. However, modern agriculture has advanced significantly and has over the last two centuries ensured a higher productivity [31]. Nevertheless, modern agriculture faces major challenges today, as FAO has predicted an 60%

increase in global food production is needed by 2050 and that a dramatically increase in food and fiber production is needed to meet the needs of a growing and modernizing population. As a result of the climate change and rapid development of urbanization, industrialization and world population food shortages is three times more likely. One of the most viable process to limit food shortages is, according to FAO, to increase crop yield [3].

To achieve optimal growth conditions for plants, they need a certain temperature, pH and essential nutrients. Essential elements are defined as elements that are needed as an intrinsic component in the structure or metabolism of a plant, who in its absence would cause severe abnormalities in a plant's growth, development, or reproduction. With these essential elements they can synthesize all compounds they need for normal growth, assuming they have access to water and sunlight. The elements can be divided into macronutritions and micronutritions, depending on the concentrations the plants need of each. The macronutritions are nitrogen, potassium, calcium, magnesium, phosphorus, sulphur and silicon [152]. Nitrogen is often the limited element, even though the air consists of 78% nitrogen, because the nitrogen appears in the air as N_2 making it unavailable to plants. The most used fertilizer today is therefore based on nitrogen and estimated calculations show that in 2008 synthetic nitrogen fertilizers fed 48 percent of the global populations [153]. The pH of the soil also has an effect on the uptake of the minerals due to the solubility of the minerals. In more acidic environments most minerals exist in a more soluble form, making them more available for the plants [152].

PAW has a great potential and can be considered as an innovative and eco-friendly approach as an alternative to mineral fertilizer [31]. PAW has been proven to enhance plants growth by modulating the signal transduction and metabolic regulation of the plant, it can stimulate seed germination, give hormone-like effects and have antimicrobial activity [58, 154]. The nitrogen concentration in PAW is between 1-10 mM, which is optimal for the plant and can therefore reduce the need for mineral nitrogen fertilizer. The production of mineral nitrogen fertilizer requires a large amount of fossil fuels, as well as human activity increase the input of reactive nitrogen in the atmosphere, thus, making high mineral nitrogen fertilization one of the main human agricultural practices with high environmental emission of pollutants into the atmosphere, soil and water [155]. In addition, studies have assessed the potential of PAW to increase the plants uptake of minerals and water, making it easier for plants to survive in stressful conditions (drought, nutrition defiance), is being exploited [67, 76, 156]. For instance, Ling et al. (2014) [76] conducted an experiment with cold plasma and reported enhanced seed

germination during draught stress periods. However, literature about PAW for enhancement of seed germination and plant growth is currently limited [58]. Nevertheless, Naumova et al. (2011) [67] reported a 50% increase in germinability in rye seeds when treated 5 min with an electric front-type discharger was used for the activation. It was also conducted an experiment were flowers of Zinnia elegance was watered with PAW which yielded a 15-20% increase of the degree of the cultures germinability and a 1.5- to 2-fold increase in the length of the plant roots. Furthermore, Lindsay et al. (2014) [156] conducted an experiment over 4 weeks with plants watered with only tap water, plants watered the first two weeks with tap water and week 3 and 4 with PAW and plants watered with PAW every week. Interestingly, the results did not show a significance difference in plant length the first two weeks, however, in week 3 and 4 plants watered with PAW was significantly longer than plants watered only with tap water. Table 8 summarizes the most recent papers currently available in regard to plant growth enhancement with the use of PAW.

Table 8. Overview of selected studies on the potential of PAW for plant growth enhancement (adapted from Ito et al., 2017)[157]

Target	Environment	Treatment	Plasma type	Exposure time	Evaluation	Reference
Watermelon **Zinnia** **Alfalfa Sprout** **Pole bean** **Shade champ grass** **Tomato** **Banana pepper** **Radish**	Humid air	Plasma activated liquids (Tap water)	In-water spark, transferred arc, gliding arc	2 min	Increase of nitrite and nitrate, showed a positive effect on plant growth	Park et al. (2013) [68]
Brassica rapa var. pervidrid (Chinese cabbage; Brassica campestris)	Air	Plasma activated liquid	In-water discharge	10 and 20 min	Increase of growth	Takaki et al. (2013) [158]
Tomato seedling	Air	Plasma activated water (de-ionized)	Plasma jet	15, 30 and 60 min	PAW can act as a plant growth inducer as well as immune inducer	Adihkari et al. (2019) [159]
Raddish seeds **Tomato plants** **Pepper plants**	Air	Plasma activated water (de-ionized)	Cyl-DBD	15 and 30 min	Increase of plant growth for Raddish seeds and pepper plants, but not for tomato plants.	Sivachandian & Khacef (2017) [160]
Soybean (G*licine max*)	Air	Plasma activated water (de-ionized)	DBD	1 and 5 min	Increase of plant growth	Lo porto et al. (2018) [139]

2. Objectives

The overall objective of this master thesis was to assess the potential of plasma activated water (PAW) for food and agricultural applications. Specific objectives include the following:

- To characterize the composition of PAW (pH, ORP, temperature, RONS and carbonic compounds) generated from tap water with different plasma systems, as a function of main operating conditions, i.e. plasma power and activation time.
- To determine the stability of PAW during four-week storage at different temperatures relevant for industrial settings (i.e. 10, 4 and -20 °C), which represent typical refrigeration and freezing temperatures, besides temperature abuse conditions.
- To assess the efficacy of PAW, alone or in combination with ultrasonication (US), for the inactivation of planktonic *Listeria monocytogenes* cells, responsible for foodborne outbreaks typically associated to minimally processed fresh produce. Moreover, it was initially planned to assess PAW decontamination potential on fresh-cut vegetables (baby spinach leaves) but due to *force majeure* (covid19 lockdown) these experiments were not completed.
- To evaluate the preservation potential of PAW, alone or in combination with US, on wild harvested macroalgal biomass (*Laminaria hyperborea*) as a sustainable alternative to current industrial practices.
- To determine the efficacy of PAW as a sustainable alternative to mineral nitrogen fertilizers, with regards to tomato plant growth enhancement

3. Materials and methods

3.1 Materials

3.1.1 Chemical reagents

The chemical reagent used in the present work, as well as their manufacturers, are listed in Table 1.

Table 9. The chemical reagent and their manufacturers.

Chemicals	***Manufacturer***
D-Sorbitol	SIGMA life science
Ethylenediaminetetraacetic (EDTA) acid disodium salt dihydrate	SIGMA life science
Griess' reagent	SIGMA-ALDRICH
Hydrochloric acid, 37%	SIGMA-ALDRICH
Hydrogen Peroxide standard solution, 30 wt. % in H_2O	SIGMA-ALDRICH
Iron (III) sulfate heptahydrate	SIGMA-ALDRICH
Nitrate standard solution, 1000 mg/L NO_3	Merck
Spectroquant® Nitrate test, 109713	Merck
Ringer tablets	Merck
Sodium Hydroxide	VWR CHEMICALS
Sodium Nitrite, ≥ 97.0%	SIGMA-ALDRICH
Sulfuric acid (95-98%)	SIGMA-ALDRICH
Titanium (IV) oxysulfate solution (1.8-2.1%)	SIGMA-ALDRICH
Xylenol Orange tetrasodium salt	SIGMA-ALDRICH

Besides the PAW generated and characterized in the context of this Master thesis, a commercial PAW with a different composition, and thus disinfection and fertilizing potential.

3.1.2 Microbial strains and culture media

The different culture media used for determining bacterial concentrations in the present work, as well as their manufacturers, are listed in Table 2. All media were prepared as instructed by the respective manufacturers.

Table 10. The Media used and their manufacturers

Media	Manufacturer
Bactopeptone	Difco
Brain heart infusion agar	Merck
Brain heart infusion broth	Merck
Marine agar	Difco
PALCAM	Merck
Tryptone soy agar	OXOID
Yeast extract, granulated	Merck

A *Listeria. monocytogenes* strain isolated from spinach leaves was kindly provided by BAMA GRUPPEN AS.

3.1.3 Raw materials

Samples of *Laminaria hyperborea* were kindly supplied by Dolmøy House of Seafood AS. They were harvested the day before the trials and shipped overnight at 4 °C under refrigerated conditions. Unwashed spinach leaves were kindly provided by BAMA GRUPPEN AS and stored overnight under refrigerated conditions before the trials. Tomato seeds *Solanum lycopersicum* cv. Heinz were kindly supplied by Professor Cathrine Lillo at Centre of Organelle research (CORE), Stavanger, Norway.

3.2 Methods

3.2.1 PAW generating systems and standard operating conditions

An electrode for relatively large treatment volumes (300 mL), built up by experts at the University of Liverpool (UK), was used in this Master thesis to characterize the PAW composition and stability during refrigerated/frozen storage, as a function of plasma operating conditions (plasma power and activation time). When assessing the efficacy of PAW as disinfectant or fertilizing agent, the plasma system experienced several technical issues, which affected its integrity, production capacity and properties of the PAW. Plasma technology for water/liquids activation is still at early stage of development (laboratory scale), with relatively low production capacity (from 1 to 500 mL). Moreover, only basic hand-crafted plasma electrodes were available on site, with relatively short life span before technical failure occurs (electric arc), also triggered by extensive use. After a maintenance attempt, it was eventually

replaced by a back-up system for smaller treatment volumes, able to generate PAW of similar characteristics. Technical details of both systems, as well as their use in different trials, are described in sections 3.2.1. Both systems operated at atmospheric pressure, with room air as the plasma-inducing gas.

System for large treatment volumes

The configuration of the PAW system for larger treatment volumes (Figure 9) include 1. Oscilloscope, Channel, 200 MHz, 2 GSPS, 16 Mpts (TENMA, Tokyo, Japan); 2. Function generator (AIM-TTI INSTRUMENTS, Direct Digital Synthesis, Cambridge, UK); 3. DC power supply (GW INSTEK, Ny Taipei, Taiwan), Switching DC Programmable, 1 Output, 0-60 V, 0-3.5; 4. High-voltage power supply. (University of Liverpool); 5. High-voltage probe, 75 MHz, 20 kV, 1000:1 (TEKTRONIX, Oregon, USA); 6. Current monitoring probe (PEARSON, London, UK), in addition to a SDBD electrode built by experts at University of Liverpool. A reactor, which consisted of a powered electrode and a ground electrode with a 1 mm thick quartz tape between them was set up to generate a surface barrier discharge (SBD). This configuration was coupled to the lid of the treatment chamber (150 x 300 x 25 mm), with a total discharge area of 306.3 cm^2. The system was not completely sealed, with a small gap between the lid and the treatment chamber (Figure 10).

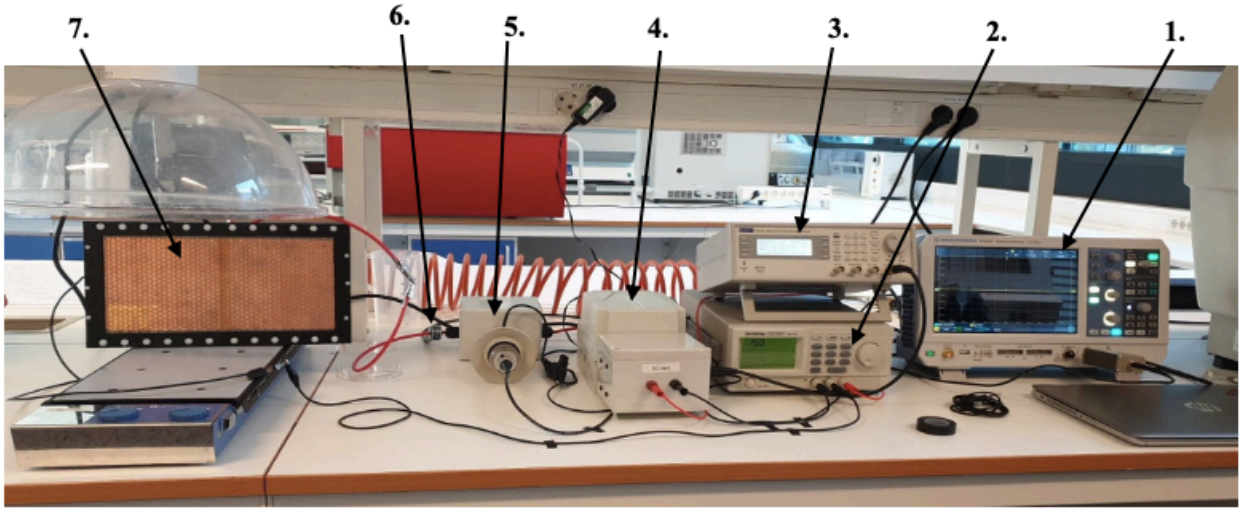

Figure 9. Set up of the plasma system for larger treatment volumes. 1. Oscilloscope; 2. Function generator; 3. DC power supply; 4. High-voltage power supply; 5. High-voltage probe; 6. Current monitoring probe; 7. Plasma electrode

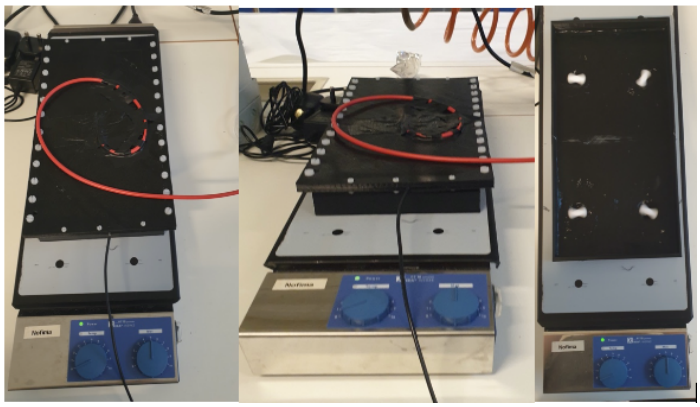

Figure 10. Set up of the electrode and treatment chamber on the magnetic stirring plate

Regarding the operating conditions, plasma power of 25 W (low mode, L) and 35 W (high mode, H) and activation times of 10 and 30 min (Table 11) were investigated based on the 2^2 full factorial design of experiment in independent triplicate runs, taking into account the variability of the tap water supply. The CP generating source produced a sinusoidal signal at a frequency of 11.8 kHz (high mode) and 11.9 kHz (low mode). For the trials, 300 mL tap water, with an initial temperature of 9 - 11 °C and pH of 8.0 ± 0.07 was used. The treatment chamber was located on the top of a magnetic stirring plate and four magnetic bars of 1 cm length were placed inside the water (Figure 10), with a speed of ≈ 500 rpm. For 300 mL treatment volume, the gap distance between the liquid surface and the electrode was 21.4 mm (6.6 mm water column).

Table 11. Combinations of plasma power and activation time tested with the PAW system for large treatment volumes based on the 2^2 full factorial design of experiment

Sample name	**Activation time (min)**	**Plasma power (W)**
H – 30	30	35
L – 30	30	25
H – 10	10	35
L – 10	10	25

Once the conditions listed in Table 11 were tested in terms of PAW composition and storability, the plasma electrode experienced technical failure (electric arc) attributed to extensive use. As a first maintenance attempt at the University of Liverpool, more robust materials were included in the original set-up, with the discharge area occurring as a purple glow in Figure 11. For this upgraded electrode, 200 mL tap water were used during the activation (35 W for 30 min) to

generate PAW with similar properties (H-30*). However, after certain period the performance of the electrode was severely affected, and it was replaced by the system for small treatment volumes.

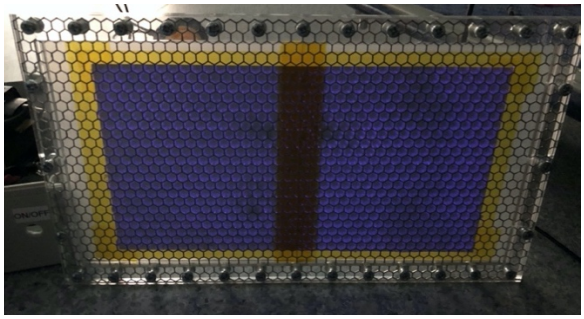

Figure 11. Plasma discharge

System for small treatment volumes

The setup of the plasma system for small treatment volumes included mainly the same components as mentioned for the system for larger treatment volumes; 1. Oscilloscope, Channel, 200 MHz, 2 GSPS, 16 Mpts (TENMA, Tokyo, Japan); 2. Function generator (AIM-TTI INSTRUMENTS, Direct Digital Synthesis, Cambridge, UK); 3. DC power supply (GW INSTEK, Ny Taipei, Taiwan), Switching DC Programmable, 1 Output, 0-60 V, 0-3.5; 4. High-voltage power supply. (University of Liverpool); 5. High-voltage probe, 75 MHz, 20 kV, 1000:1 (TEKTRONIX, Oregon, USA); 6. Current monitoring probe (PEARSON, London, UK), in addition to a SDBD electrode built by experts from University of Liverpool, however, with a smaller surface of 144 cm^2 (Univeristy of Liverpool). As with the reactor for the larger system, this reactor was also set up to generate a SDBD and consisted of a powered electrode and a ground electrode with a 1 mm thick quartz tape between them. This configuration was coupled to the lid (Figure 13b) of the treatment chamber (Figure 13a) and the system completely sealed during activation trials. The dimensions of the treatment chamber were 176 x 174 x 48 mm, with a total discharge area of 144 cm^2.

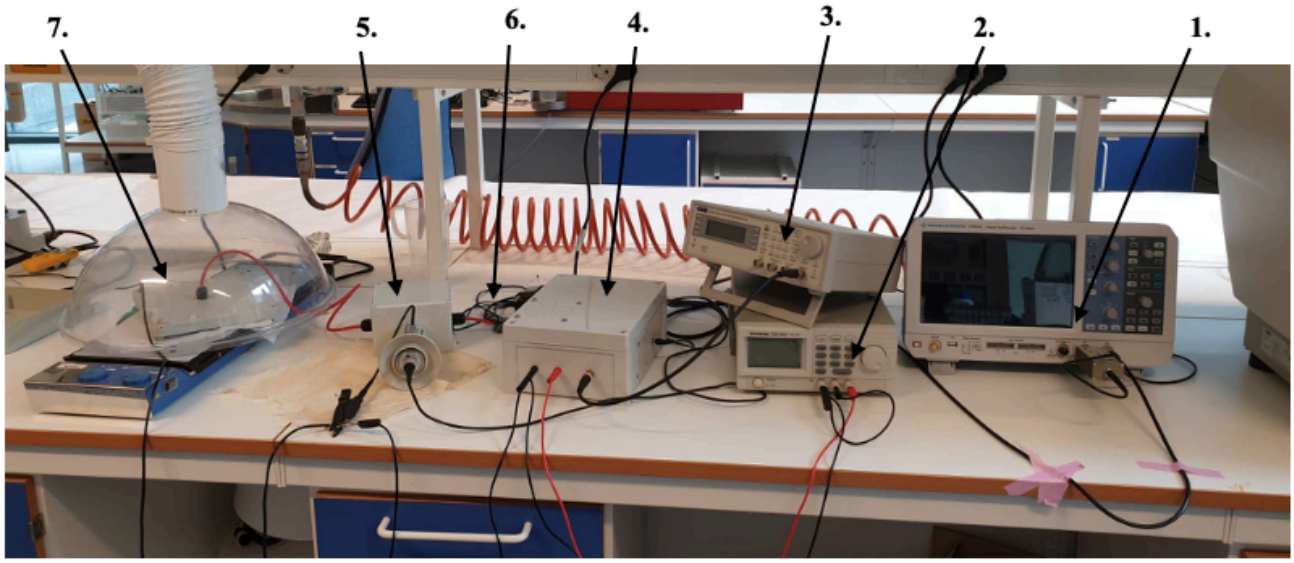

Figure 12. Set up of the plasma system for small treatment volumes: 1. Oscilloscope; 2. Function generator; 3. DC power supply; 4. High-voltage power supply; 5. High-voltage probe; 6. Current monitoring probe; 7. Plasma electrode

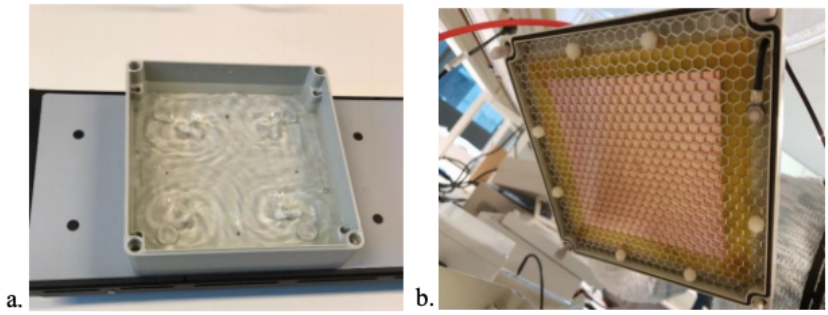

Figure 13a. Treatment chamber; b. Plasma electrode

Regarding the operating conditions, plasma power of 35 W, and activation times of either 5 or 30 min, were investigated as indicated in Table 12 as HS (High mode, system for small volume) following with the activation time. The CP generating source produced a sinusoidal signal at a frequency of 18 kHz. 100 mL tap water with an initial temperature of 9 - 11 °C was used for the trials. The initial pH of the tap water was 8.0 ± 0.7. During the activation, the treatment chamber was located on the top of a magnetic stirring plate and four magnetic bars of 1 cm length were evenly placed inside the water (Figure 13), with a speed of≈ 500 rpm. For 100 mL treatment volume, the gap distance between the liquid surface and the electrode was 44.8 mm (3.2 mm water column). The purpose of these trials was to assess the variability in the PAW composition at different exposure times when subjected to the highest plasma power based in Vaka et al. (2019) [43].

Table 12. Operating conditions of the plasma system for small treatment volumes

Sample name	Activation time (min)	Plasma Power (W)
HS – 5	5	35
HS – 30	30	35

Overview on the use of the different PAW systems for the application trials

As discussed above, two PAW generation systems and different operating conditions were used for PAW generation, besides the commercial PAW (PAW_IB). The system for larger treatment volumes was used to characterize PAW composition and storability as a function of plasma operating parameters, i.e. plasma power and activation time (Section 3.2.2). It was also used for the tomato plant trial denoted as #1, where PAW generated under the conditions listed in Table 11 were compared. After its maintenance at the University of Liverpool, the PAW generated from 200 mL tap water was used for the inactivation trials on *L. monocytogenes* (Section 3.2.4). The PAW generated with the system for small volumes was also characterized (conditions listed in Table 12)) and used for the decontamination of *L. hyperborea*, the inactivation of *L. monocytogenes* and tomato plant trial #3. The commercial PAW (IB) was characterized for its composition and used for the tomato plant trial #2 as well as for inactivation of *L. monocytogenes*. Table 13 provides an overview of the PAW generation systems, the treatment volume and the different experiments.

Table 13. Overview on the use of both PAW systems and the commercial PAW for different trials

Trials	Large volume (300 mL)	Large volume after maintenance (200 mL)	Small volume (100 mL)	PAW_IB
Characterization	x			
Storage stability	x			
Inactivation of *l. monocytogenes*		x	x	x
Tomato plant #1	x			
Tomato plant #2	x			x
Tomato plant #3			x	
Decontamination of *l. Hyperborea*			x	

3.2.2 Characterization of PAW composition

The composition of PAW, in terms of pH, ORP and RONS, was characterized as a function of the operating conditions (plasma power and activation time), as described in sections 3.2.1 for

both PAW generation systems. The different conditions were assessed in triplicate on independent days and time span, to take into account the variability of the tap water supply. Moreover, the properties of the commercial PAW (IB), used for further application trials, were also characterized. The analytical methods for the determination of RONS, pH and ORP are described hereafter.

pH, ORP and temperature

pH, ORP and temperature of the PAW were measured with the FiveGo pH meter F2 (Mettler Toledo, Columbus, Ohio, US). The ORP, expressed in mV, is a measurement of the degree a substance can oxidize or reduce another substance. A positive mV indicates that the substance is an oxidizing agent, with the higher the mV indicating the higher oxidizing power. The pH values and the temperature (T, °C) were used to estimate hydronium ion (H_30^+) and hydroxide (OH^-) concentrations in the PAW according to Equation 1 & Equation 2, respectively.

Equation 1. Formula used for calculation of the hydronium concentration.

$$[H_3O^+] = 10^{-pH}$$

As described by Judeé et al (2018) hydroxide concentration is estimated using the concentration of H_3O^+ and the ionic product of water, Kw. Kw is $[H_3O^+]$ * $[OH^-] = 10^{-14}$ at 25 °C [31]. The water exposed to plasma has an increase in temperature, to take account of this increase pKw can be estimated with the following formula (Harned and Owen, 1958).

$$pKw = 14.88 - 0.0335 * T$$

Combining the formula for hydronium ion and pKw leads to the following formula:

Equation 2. Formula used for calculation of the hydroxide concentration

$$[HO^-] = 10^{pH-0.0335*T-14.88}$$

Nitrates, Nitrites, nitric acid and nitrous acid

The concentration of nitrates and nitrites in the PAW was determined via standard spectrophotometric methods using a Shimadzu UV Mini 1240 UV/Vis Spectrophotometer (Shimadzu, Tokyo, Japan). The Spectroquant® test kit #109713 (Merck, New Jersey, USA),

analogous to DIN 38405-9, was used for the determination of nitrates in the PAW. In a sulfuric and phosphoric solution, nitrate ions react with 2,6-dimethylphenol (DMP) to form 4-nitro-2,6-dimethylphenol, which is determined spectrophotometrically at a wavelength of 340 nm. A calibration curve (0.5 – 100 mg/L) was determined in triplicate using distilled water as blank. The results of nitrates levels and pH in the PAW, together with the pKa value of the acid, were used to estimate the concentration of nitric acid according to Equation 3, as described by Judeé et al. (2018) [31].

Equation 3. Formula used for calculating the concentration of HNO_3.

$$[HNO_3] = \frac{[NO_3^-]}{10^{pH-pKa}} \qquad (\text{pKa} = -2)$$

The nitrites levels in the PAW were determined with the Griess method, based on the formation of a pink diazo dye through diazonium coupling reaction with *N*-(1-Naphthyl) ethylenediamine, which was spectrophotometrically determined at a wavelength of 548 nm. A calibration curve (0.02-0.2 mM) was determined in triplicate, using distilled water as blank. The experimental results of nitrites and pH in the PAW, together with the pKa value of the acid, were used to estimate the concentration of nitrous acid according to Equation 4, as described by Judeé et al. (2018) [31].

Equation 4. Formula used for calculating the concentration of HNO_2

$$[HNO_2] = \frac{[NO_2^-]}{10^{pH-pKa}} \quad (pKa = 3.39)$$

Hydrogen peroxide

Two spectrophotometric methods with different detection limits (mM *vs* µM range) were established for the determination of hydrogen peroxide in the PAW samples. The titanium sulphate colorimetric method [161] was used to determine concentrations of hydrogen peroxide within the mM range. If hydrogen peroxide is present in the sample, peroxide will react with titanium ions, giving rise to a yellow color that can be determined spectrophotometrically at a wavelength of 407 nm. A standard calibration curve (0.25-2.5 mM) was determined in triplicate, using distilled water as blank.

The ferric-xylenol orange assay as modified by Gay and Gebicki (2000) [162] was used to determine concentrations of hydrogen peroxide within the μM range. Hydrogen peroxide present in the sample gives rise to a purple complex, which can be spectrophotometrically determined at a wavelength of 560 nm. A standard calibration curve (25-250 μM) was determined in triplicate, using distilled water as blank.

Carbonic compounds (CO_3^{2-}, HCO_3^-, H_2CO_3)

The determination of carbonic compounds in tap water and PAW was based on either an acidic or basic titration, depending on whether the initial pH in the sample was higher or lower than 6.3, respectively. 0.1 M HCl or 0.1 M NaOH was used for acidic or basic titration, respectively. The volume required to reach the equivalence point (V_{eq}) was determined by the first derivative of the acid/base titration curve (i.e. pH versus added volume of acid/base) using the software Prism GraphPad version 8. The concentrations of CO_3^{2-}, HCO_3, H_2CO_3 were estimated from this value, the initial volume of the solution (Vs), the concentration of solution added (i.e. [HCl] or [NaOH]), concentration of hydroxide (θ) or hydronium ions (θ′), together with the pH and pKa for the corresponding compound. The reactions and formulas used differ based on acidic or basic titration, in a basic titration the addition of [HCl] to the water give rise to the possibility of the following reactions:

$$CO_3^{2-} + H_3O^+ \rightleftharpoons HCO_3^- + H_2O$$

$$CO_3^{2-} + 2H_3O^+ \rightleftharpoons H_2CO_3 + 2H_2O$$

$$HCO_3^- + H_3O \rightleftharpoons H_2CO_3 + H_2O$$

From the first derivative of the values obtained from the titration the equivalence point was determined and used to calculate the total concentration of carbonic compounds with the formulas below:

$$V_{solution} * ([OH^-] + 2[CO_3^{2+}] + [HCO_3^-]) = V_{eq} * [HCl]$$

Equation 5. Formula used for calculation of the total concentration of carbonic compounds after acidic titration.

$$[Total] = \frac{V_{eq}}{V_s} * [HCl] - \theta$$

Subsequently, the carbonate ion, bicarbonate and carbonic acid concentration can be calculated from the following equation 6-8, respectively:

Equation 6. Estimated concentrations of CO_3^{2-}

$$CO_3^{2-} = \frac{[Total]*10^{pH-pKa}}{1+2*10^{pH-pKa}} \quad (\text{pKa} = 10.32)$$

Equation 7. Estimated concentrations of HCO_3^-

$$[HCO_3^-] = [Total] - 2[CO_3^{2-}]$$

Equation 8. Estimated concentrations of H_2CO_3

$$[H_2CO_3] = \frac{[HCO_3^-]}{10^{pH-pKa}} \quad (pKa = 6.37)$$

Generally, water exposed to plasma results in an acidified environment (pH below 6.3), thus the reactions and formulas for a basic titration is listed below. The addition of a strong base (OH^-) can react to several carbonic compounds as following:

$$H_2CO_3 + OH^- \rightleftharpoons HCO_3 + H_2O$$
$$H_2CO_3 + 2OH^- \rightleftharpoons CO_3^{2-} + 2H_2O$$
$$HCO_3 + OH^- \rightleftharpoons CO_3^{2-} + 2H_2O$$

The total concentration of carbonic compounds can be calculated from the equivalent point with Equation 9, deduced as followed:

$$V_{solution} * ([OH^-] + 2[CO_3^{2+}] + [HCO_3^-]) = V_{eq} * [NaOH]$$

Equation 9. Formula used to calculate the total concentration of carbonic compounds after basic titration.

$$[Total] = \frac{V_{eq}}{V_s} * [NaOH] - \theta'$$

From the total concentration of carbonic compounds, carbonate ion, bicarbonate and carbonic acid can be calculated by equation 10 - 12:

Equation 10. Estimated concentration of H_2CO_3

$$[H_2CO_3] = \frac{[Total]}{2*10^{pH-pKa}} \quad (pKa = 6.37)$$

Equation 11. Estimated concentration of HCO_3^-

$$[HCO_3^-] = [Total] - 2[H_2CO_3]$$

Equation 12. Estimated concentration of CO_3^{2-}

$$[CO_3^{2-}] = [HCO_3^-] * 10^{pH-pKa} \quad (pKa = 10.32)$$

3.2.3 Storage conditions (Volume, temperature and duration)

The stability of PAW, in terms of pH, ORP and concentration of RONS, was assessed during 1-month storage at 4, 10 and -20 °C, which represent typical refrigeration and freezing temperatures, besides temperature abuse conditions. The PAW generation conditions (4 combinations of plasma power and activation time) are listed in Table 11. Three replicates of each condition, generated on independent days and time span, were stored at each different temperature (i.e. in total 9 replicates per condition). Samples were taken after 24 h, one, two, three and four weeks of storage to analyze the concentration of reactive species (nitrates, nitrites, hydrogen peroxide, carbonic compounds), as well as the pH and ORP.

3.2.4 Application trials with PAW

The potential of PAW for inactivation of *L. monocytogenes*, plant growth enhancement, and macroalgae decontamination was assessed in this Master thesis. The experimental design and analytical methods involved in the different trials are described hereafter.

Potential of PAW for inactivation of L. monocytogenes

The antimicrobial activity of PAW, either alone or in combination with ultrasonication, was assessed on planktonic cells (cell suspension) of *L. monocytogenes*. The effect of the treatment on the PAW composition and treatment time was also assessed. The different types of PAW used is summarized in Table 14. The sample and inoculum size were optimized in preparation for the trials toward the inactivation of *L. monocytogenes* on spinach leaves was also optimized. However, due to *major force*, it was not possible to complete the full factorial design for the inactivation of planktonic cells and further disinfection trials on spinach leaves were dismissed.

Table 14. The different types of PAW used for inactivation of l. monocytogenes

Inactivation of *l. monocytogenes*	Plasma power (W)	Activation time (min)	Large volume after maintenance (200 mL)	Small volume (100 mL)	PAW_IB
HS-5	35	5		x	
HS-30	35	30		x	
H-30*	35	30	x		
PAW_IB					x

Planktonic cells

Preparation of frozen stock cultures - A *L. monocytogenes* strain isolated from spinach leaves was kindly provided by BAMA GRUPPEN AS. A colony was resuspended in 5 mL sterile BHI broth (37 g/L) and incubated at 37 °C for 24 h. Subsequently, the inoculum was centrifuged (4500 rpm at 4 °C for 6 min) (Hettich® ROTINA 420/420R, Tuttingen, Germany) and the supernatant was carefully removed before the pellet was resuspended in 5 mL sterile BHI broth (74 g/L). 0.5 mL aliquot was distributed into sterile cryovials containing 0.5 mL glycerol prepared at 40% v/v and vortexed before they were stored at -80 °C.

Inoculum preparation – The strain was recovered from the stock solution by streaking it onto a BHI agar plate followed by incubation at 37 °C for 24 h. After the incubation the plate was stored at 4 °C and was kept for a maximum of two weeks prior to further use. The inoculum was made by transferring one colony from the BHI agar plate to 5 mL BHI broth (37 g/L), followed by incubation at 37°C for 24 h to obtain stationary phase pre-cultures with a cell density of approximately 10^9 cfu/mL.

Inactivation trials - The 24-hour inoculum was centrifuged (4500 rpm at 4 °C for 6 min) (Hettich® ROTINA 420/420R, Tuttingen, Germany) and the cell pellet was resuspended in 5 mL of Ringer solution. A 100 µL aliquot was transferred and vortexed into 10 mL of either tap water as control (stored at 4 °C) or PAW (HS-5, HS-30, H-30* or PAW_IB stored at 4 °C) with the treatment times of 5, 15 and 30 min in duplicate.

Moreover, additional 2.5 min treatments were conducted in duplicate in either tap water (control) or PAW (HS_30 or H-30* stored at 4 °C) to mimic industrial settings [43], so that *L. monocytogenes* cells were recovered after the first 2.5 min treatment by centrifugation (4500 rpm at 4 °C for 6 min) and then resuspended in fresh 10 mL media for another 2.5 min. Furthermore, either tap water (control) or PAW (HS_30 or H-30* stored at 4 °C) inoculated

with *L. monocytogenes* were treated for 5 min in an ultrasonic water bath (BT 130H, UPCORP, Illinois, USA) at 8-10 ºC operating at 68 kHz and 500 W in duplicate.

Microbiological analysis – After treatment, the samples were centrifuged (4500 rpm at 4 °C for 6 min), the supernatant was carefully removed, and the pellet resuspended in 10 mL Ringer solution. Serial decimal dilutions were prepared in Ringer solution and spread onto BHIA plates, followed by incubation at 37 ºC for 24 h prior to enumeration of viable counts.

Sample and inoculum size on spinach leaves

Unwashed spinach leaves were kindly provided by BAMA GRUPPEN AS and stored overnight at 4 ºC. As a ratio of 5 g sample in 100 mL rinsing media was set up to mimic relevant industrial conditions [43], the number, size and individual weight of spinach leaves needed to obtain 5 g samples were determined. Thus, all the spinach leaves from a 150 g commercial batch were sorted into three categories according to size, i.e. small, medium and big sized leaves. As medium sized leaves showed the highest occurrence, three batches of 5 g were prepared with medium sized leaves, recording the number and individual weight of the leaves per batch. Moreover, 100 µL water was pipetted and spread using a cotton swab onto the surface of three leaves from each size category, and allowed to dry for a maximum of 30 min under the laminar flow cabinet, to confirm whether such a standard inoculum volume was enough to cover the entire surface of the samples, while absorbing into the leaves in a reasonable time period.

Finally, the inoculation conditions were optimized towards a target initial concentration of 10^7 cfu/g spinach leaves per 5 g samples (triplicates) of medium sized spinach leaves when inoculated with 100 µL of two different dilutions, 1:10 and 2:3 v/v, the 2:3 dilution was tested directly and with a centrifuging step before dilution, of the 24-hour *L. monocytogenes* inoculum in Ringer solution. The samples were allowed to dry for 30 min, then placed in a stomacher bag with 45 mL of Ringer solution and homogenized for 2 min. Serial decimal dilutions were prepared in Ringer solution, plated onto PALCAM agar plates and incubated at 37 °C for 24 h, prior to enumeration of viable counts.

Potential of PAW for macroalgae decontamination

Fresh wild-harvested *L. hyperborea* was kindly provided by Dolmøy House of Seafood AS (Frøya, Norway). The samples were harvested the day before the trials and shipped overnight under refrigerated conditions with ice accumulators. The supply of macroalgae samples was

severely affected by adverse weather conditions, logistic challenges and seasonal epiphytic biofouling (ideal harvesting season in May-June). Thus, only two batches delivered on different weeks (21st January and 13th February 2020) were available for screening trials, so that a full factorial design was not completed. The conditions of the two types of PAW used in the trials are listed in Table 15.

Table 15. Overview of the two types of PAW used for decontamination of macroalgae

PAW used for macroalgae decontamination	**Plasma power (W)**	**Activation time (min)**	**Small volume (100 mL)**
HS-5	35	5	x
HS-30	35	10	x

Immediately after the delivery, the stipe and holdfast were removed with a sterile scalpel and the macroalgae leaves were cut into 5 g pieces avoiding damaged areas, and placed into sterile glass jars closed with aluminum lids (Figure 14). The samples were treated immediately (in triplicate) with 100 mL of either tap water (control), different PAW solutions, or 0.1 M EDTA dihydrated salt, an authorized food additive in the EU with antimicrobial and antioxidant properties [163]. The PAW was generated the day before and stored at 4 °C prior to the experiments as the tap water used as control. All the treatments were performed in triplicate. The following experimental conditions were tested: (A) Tap water (5, 15, 30 or 60 min) and PAW HS-5 and HS-30 (30 min) on a rotatory shaker at a speed of 1 (Heidolph Reax Incl 2 Universal adaptor; Schwabach, Germany) (Figure 15A); and (B) Tap water (30 or 60 min), EDTA salt dihydrate 0.1 N (30 or 60 min) and PAW HS-5 and HS-30 (30 min) in a BT 130H ultrasound bench top system (UPCORP, Illinois, USA). The samples were placed at a standard central position inside the ultrasonic water bath (8-10 °C) (Figure 15B) and treated at a dual frequency of 68/170 kHz and 1000 W ultrasonic power.

A.  B. 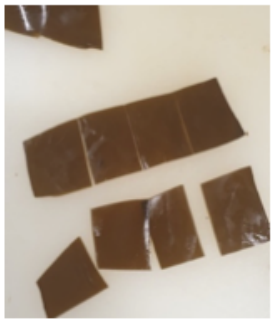 C. 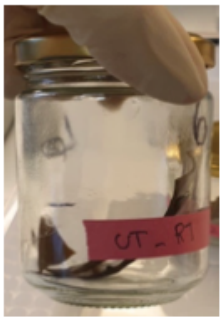

Figure 14. A) Layout of a seaweed plant; B) The sizes of the seaweed were cut into; C) Glass jar the seaweeds were treated in.

A.  B. 

Figure 15. A) The Rotatory shaker used for the trials with macroalgae, displaying their placement in the shaker; B) US used for the macroalgae trials, displaying their placement inside the bath.

After treatment, the content of the glass jars was poured onto a sieve and the samples were carefully placed in a sterile stomacher bag (Grade, UK) containing 45 mL peptone saltwater (0.1% w/v bactopeptone and 0.85% w/v NaCl) and homogenized (Smasher blender, Biomérieux, France) for 2 min. One mL aliquot of the cell suspensions was sampled, serially/decimally diluted in peptone saltwater and spread onto MA plates, which were incubated at 25°C for 72 h prior to enumeration of total viable counts. To determine whether there were lactic acid bacteria present in untreated samples, the samples were spread onto MRS plates after serial decimal dilutions in peptone saltwater and incubated at 30°C for 48 h in the anerobic culture jars containing an Oxoid™ AaeroGen™ gas pack and a Thermo Scientific™ Oxoid™ resazurin anaerobic indicator (ThermoFisher, Massachusetts, USA). Furthermore, with the aim to determine the presence of bacterial spores in the samples, 10 mL of the cell suspensions after stomaching was heated at 80 °C for 12 min to inactivate vegetative cells. The samples were spread onto TSAYE agar plates and incubated at 30°C for 8 days in the anaerobic

culture jars containing an Oxoid™ AaeroGen™ gas pack and a Thermo Scientific™ Oxoid™ resazurin anaerobic indicator (ThermoFisher, Massachusetts, USA).

PAW as a fertilizer

Three different trials were conducted to assess the potential of PAW as a fertilizing agent on tomato plants. The purpose of trial #1 was to assess the effect of PAW generated under different operating conditions (plasma power and activation time) on plant growth. Trial #2 was conducted with PAW to evaluate the isolated effect of the nitrogen compounds and the high hydrogen peroxide in high concentrations on plant growth. Furthermore, the aim of trial #3 was to unravel a potential synergistic effect of PAW combined with a multi-nutrient solution on plant growth. Table 16 gives an overview of the conditions of PAW used for the different tomato trials.

Table 16. Overview of the different types of PAW used in the tomato trials

Trial nr.	PAW used for tomato trials	Plasma power (W)	Activation time (min)	Large volume (300 mL)	Small volume (100 mL)	PAW_IB
1	L-10	25	10	x		
1	H-10	35	10	x		
1 & 2	L-30	25	30	x		
1	H-30	35	30	x		
2	PAW_IB					x
3	HS-5	35	5		x	
3	HS-30	35	30		x	

Trial #1 – Two seeds of *S. lycopersicum* (tomato) cultivar Heinz (Figure 16) were initially sown in Magenta boxes (Sigma-Aldrich, Missouri, USA), to ensure the germination of at least one seed. The boxes contained 200 mL Vermiculite Agra Grad 3-100 L (LOG AS, Oslo, Norway) as a substrate (Figure 16), either with tap water or PAW, 120 mL, generated under the four conditions listed in (Table 11), with 25 or 35 W for 10- and 30-min activation time) with 5 replicates per conditions. The Magenta boxes were incubated in a plant growth room with a regime of 16 h light followed by 8 h dark, with a 35 cm gap distance maintained between the top of the magenta box and the light source (OSRAM L58W/77, FLUORA, Recyciable Germany). The plants in the magenta boxes were watered with either 50 mL tap water or PAW two days after the germination and subsequently once every week for three weeks. Approximately one week after the germination one plant from the magenta boxes, where both

seeds germinated, was plucked based on which one was closest to the average plant height. Three weeks after germination the plants were harvested. When harvested, each plant was carefully removed from the vermiculite and the roots were rinsed with tap water and dried before a series of measurements were taken including the total length (cm), root length (cm), total weight (g) and root weight (g).

A. 

B. 

Figure 16. A) Set up of the magenta boxes containing vermiculite and tomato seeds used for the trials. B) The tomato seeds used in present work (S. lycopersicum cv. Heinz*)*

*Trial #*2 – Two seeds of *S. lycopersicum* (tomato) cultivar Heinz were again initially sown in Magenta boxes containing 200 mL Vermiculite, and 120 mL of either tap water, PAW generated under L-30 conditions (25 W for 30 min activation), PAW_IB or 50 μM NH_4NO_3 in tap water (nitrogen solution) were added in triplicates. For evaluating the isolated effect of nitrogen compounds, the plasma power and activation time for the generation of PAW were selected to achieve the highest concentration of these compounds while ensuring a sustainable production (low energy consumption). PAW_IB was included to assess the effect of a high hydrogen peroxide concentration (142 ± 5.53 mg/L) in PAW. The samples were incubated in the same plant growth room as in Trial #1, with the same light/dark regime and light source. Furthermore, the plants were watered with 50 mL tap water, PAW or nitrogen solution four days after the germination and subsequently once every week for four weeks. The harvest protocol described above for trial #1 was followed.

Trials #3 - With an experimental set-up similar to previous trials, two different conditions were assed in Trial #3; PAW or tap water combined with a diluted multi-nutrient solution (Hoagland solution). Hoagland solution (Hoagland D. R. & Arnon D.J (1950)) is used for growing plants without soil and the recipe for the Hoagland solution, including the concentration of each nutrient before and after dilution are listed in Table 17 [164]. Either 120 mL of diluted

Hoagland solution (12 mL Hoagland solution + 108 mL tap water) or 120 mL PAW with Hoagland solution (12 mL Hoagland solution + 108 mL PAW) was initially added to the 200 mL Vermiculite (5 replicates). The plasma power and activation time for the generation of PAW was selected based on a compromise of trial #1 and the PAW available due to *major force*. The light/dark regime and light source was the same as the previous trials. For the first two weeks after germination the plants were watered with 50 mL diluted Hoagland solution in tap water or PAW HS-5 (5 mL Hoagland solution + 45 mL tap water or PAW HS-5). Subsequently, the next two weeks they were watered with 100 mL diluted Hoagland solution in tap water or PAW HS-30 (10 mL Hoagland solution + 90 mL tap water or PAW HS-30). Harvested following the same protocol as for trial #1 and #2.

Table 17. Recipe of the multi-nutrient solution (Hoagland solution) needed to make 10 x concentrated solution, including the concentration of the minerals in a 1 x solution (used for plants) and diluted 0.1 x solution (used in present work)

	1 L 1 x concentrated solution (mL)	**Final concentration in 1 x solution**	**Final concentration in 0.1 x solution**
1 M KH_2PO_4	1	1 mM PO_4^-	0.1 mM PO_4
1 M KNO_3	5	5 mM NO_3^-	0.5 mM NO_3^-
1 M $Ca(NO_3^-)_2$:$4H_2O$	5	10 mM NO_3^- 5 mM Ca^{++}	1.0 mM NO_3^- 0.5 mM Ca^{++}
$MgSO_3$:$7H_2O$	2	2 mM Mg^{++} 2 mM SO_4^-	0.2 mM Mg^{++} 0.2 mM SO_4^-
1% Fe-EDTA	1		
Micronutrients	1		

1 L Micronutrients solution includes 2.86 g H_3BO_3, 1.81 g $MnCl_2$:$4H_2O$, 0.099 g $CuSO_4$:$5H_2O$, 0.22 g $ZnSO_4$:$7H_2O$, 0.029 g H_2MoO_4: H2O

3.2.5 Statistical analysis

Statistical analysis was performed using the IBM SPSS statistics software package version 25 (SPSS Inc., Chicago, IL, USA). General linear model Univariate procedure was used to examine the significant main effects of the operating parameters (plasma power and activation time) and storage conditions (temperature, time) and their interaction effects. One-way ANOVA with Tukey HSD as post hoc analysis was used to examine significant difference for simple main effects. The level of significant was set at 95 % ($P \leq 0.05$).

4. Results and discussion

4.1 Physico-chemical characterization of PAW

4.1.1 Standard curves for the determination of reactive species

Figure 17 displays the standard curves for the reactive nitrogen species (nitrites, nitrates) and hydrogen peroxide, according to the Titanium sulphate (mM) and Ferric-xylenol orange (µM) methods, using distilled water as blank. The concentration range was set between the detection and quantification thresholds for each specific analytical method, Spectroquant® test kit for nitrates, the Griess method for nitrites, the Titanium sulphate colorimetric method and the Ferric-xylenol orange colorimetric method for hydrogen peroxide. The absorbance reading of the spectrophotometer was set to zero before every measurement, and the reading for each sample was adjusted by the blank after reading.

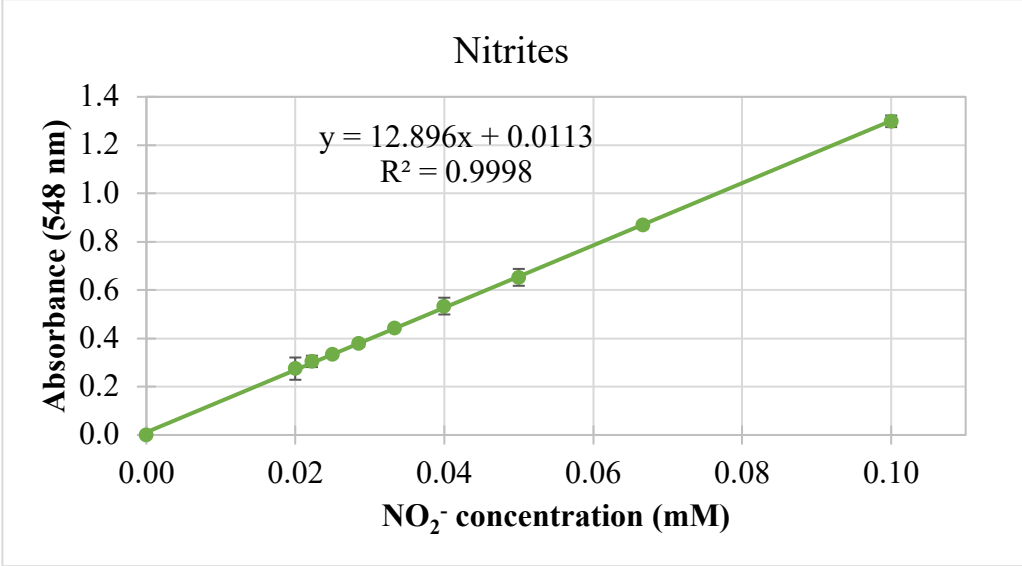

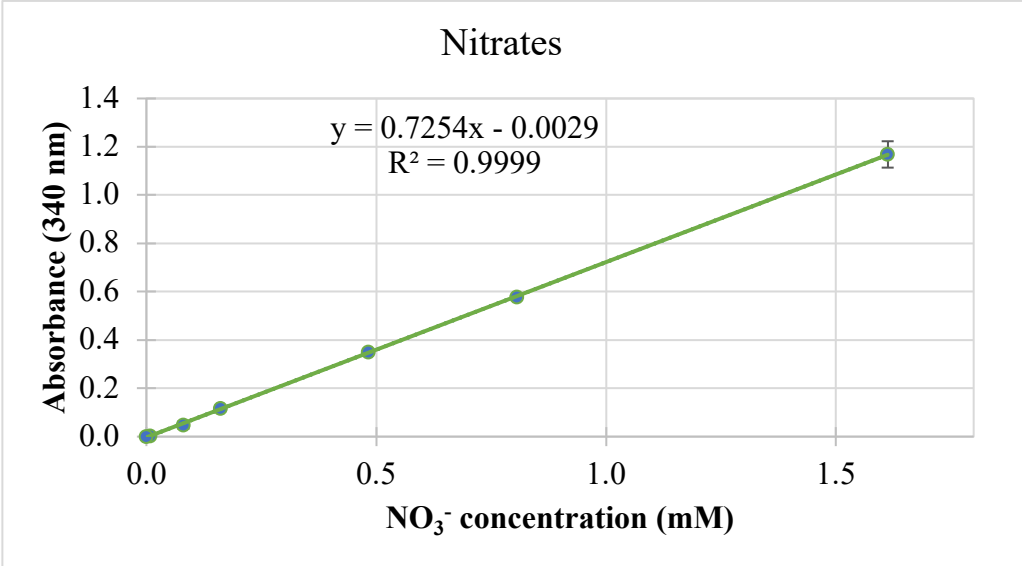

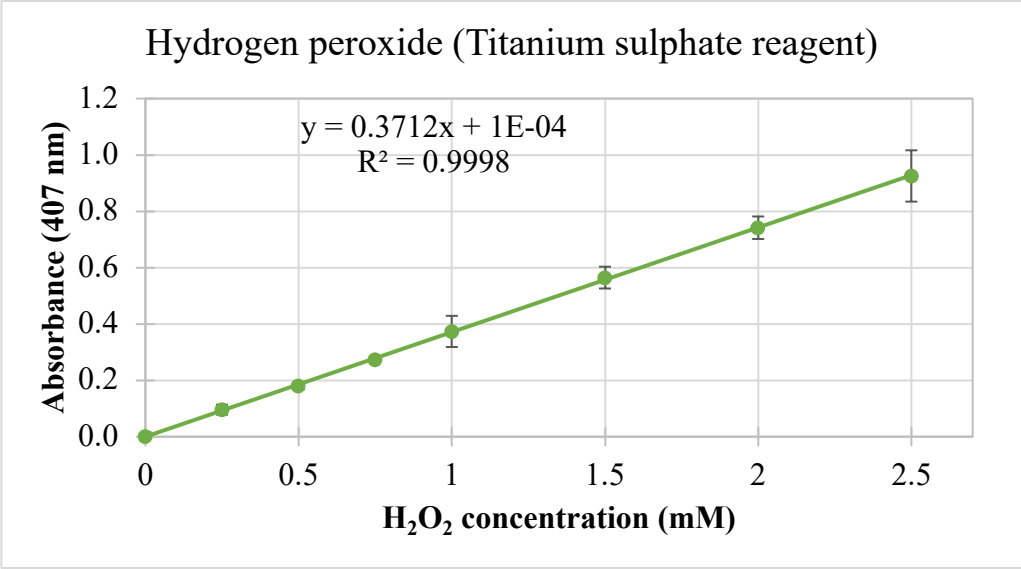

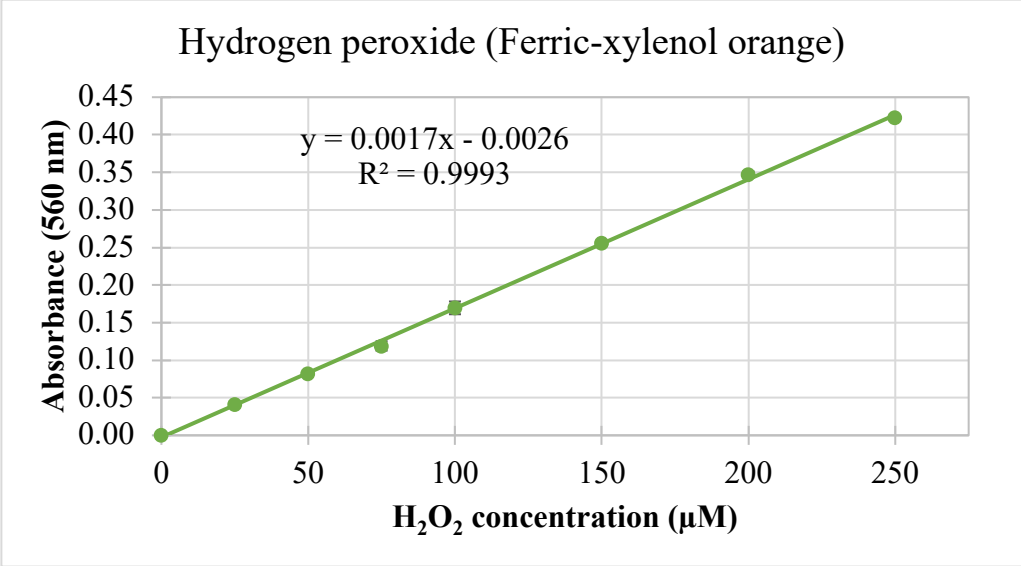

Figure 17. Standard curves (in distilled water) for the determination of reactive species (nitrites, nitrates and hydrogen peroxide) in tap water and PAW samples (n=3)

4.1.2 Characterization of the tap water for plasma activation trials

The composition of tap water (Norway) used for generation of PAW is presented in Table 18, including the pH, ORP, concentration of reactive species (nitrate, nitrite and hydrogen peroxide) and carbonic compounds. The pH and ORP were 8.0 ± 0.1 and -45.2 ± 2.4 mV, respectively. The negative value of ORP indicates reducing properties of the tap water, while positive values would refer to high oxidation potential. The concentration of the reactive oxygen and nitrogen species was below the detection limit of the different analytical methods used in the present work. Carbonic compounds in water function as a buffer, a weak acid with its correspondent weak base, in this case H_2CO_3 and HCO_3^-. Thus, with a low pH the formation of H_2CO_3 is favored as HCO_3^- works as a H^+ donor. The carbonic compounds in the tap water

were determined by acidic titration (pH above 6.3) using HCl 0.1 M as a titrant (Figure 18A). Subsequently, the equivalent point or volume needed to reach the equivalence point was determined from the first derivative of the titration curve (the lowest value), as shown in Figure 18B. Moreover, the equivalent point was used to determine the total concentration of carbonic compounds, CO_3^{2-}, HCO_3^- and $H_2CO_3^{2-}$ according to the equations 5-8 (Section 3.2.2.). The total concentration of carbonic compounds and bicarbonate (HCO_3^-) were 1.06 ± 0.03 mM and 1.05 ± 0.03 mM, respectively, which indicates very low presence of carbonic acid or carbonate. Judée et al. (2018) [92] reported the concentration of bicarbonate and carbonate to be 4.13 ± 0.09 mM and 13.1 ± 3.62 μM, respectively with a pH of 7.8 in untreated tap water (France), which were used for the generation of PAW. The concentration of carbonic compounds, particularly carbonate and bicarbonate, is the main factor influencing the alkalinity of water and thus, its buffering capacity or ability to resist changes in pH, which will be of utmost importance with regards to the PAW composition. Comparing the concentration bicarbonates (the compound with the highest concentration) in the Norwegian tap water and the tap water from France, it can be observed that the concentration was four times higher for the tap water from France, suggesting a higher alkalinity and stronger resistance to changes in pH.

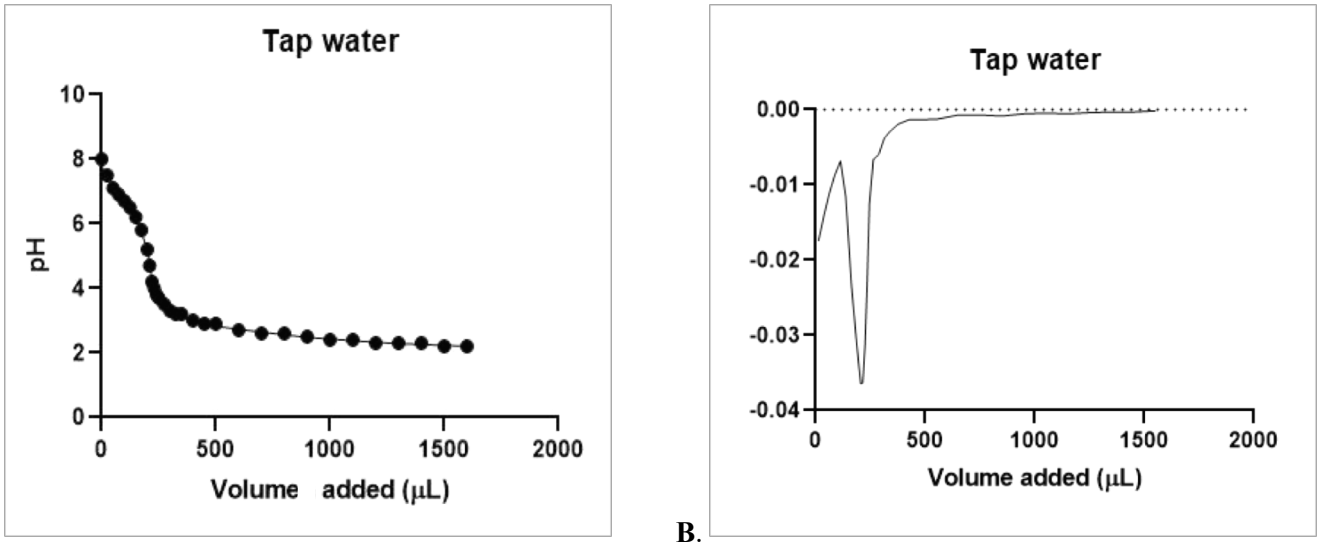

Figure 18. ***A)*** *Titration curve (acidic) of tap water (Norway)* ***B)*** *First derivative of the acidic titration curve of tap water*

Table 18. Characterization of the initial composition of Norwegian tap water used for generation of PAW

Composition of tap water	
pH	8.0 ± 0.1
ORP (mV)	-45.3 ± 2.4
Nitrate (mg/L)	ND
Nitrite (mg/L)	ND
Hydrogen peroxide (mg/L)	ND
Total carbonic compounds (mM)	1.06 ± 0.03
CO_3^{2-} (mM)	0.0040 ± 0.0001
HCO_3^- (mM)	1.05 ± 0.03
H_2CO_3 (mM)	0.03 ± 0.01

4.1.3 Characterization of PAW as a function of plasma power and activation time

The composition of PAW right after generation with the large plasma system was characterized in terms of pH, ORP, temperature and RONS levels, as described in section 3.2.2. Figure 19 displays the results (average and standard deviation, n=3) corresponding to the effect of plasma power and activation time on the pH, temperature (immediate reading) and ORP. The initial pH of the tap water was 8.0 ± 0.1 (Table 18), thus the pH of the PAW samples significantly decreased as the activation time and the plasma power increased (Figure 19). The drop in pH was significantly more pronounced with regards to the activation time (10 and 30 min) for a constant plasma power, rather than for different plasma powers (25 and 35 W) at a constant activation time. Nevertheless, both activation time and plasma power had a significant effect on the drop in pH (up to 2.5 ± 0.1 in the present study). The drop in pH is typically related to the generation of reactive species. RONS in the CP discharge have been reported to diffuse into the water and react with the water molecules giving rise to reactive species, whose generation causes the release of hydrogen ions [79, 80]. Such a correlation between pH and reactive species has been observed in the present work (Figure 19 - Figure 21). Shen et al. (2016) [70] reported similar results (pH drop from 6.8 to 2.3) with PAW generated from distilled water with a plasma microjet (frequency of 20 kHz; Activation time of 20 min). Similar to present work, Vaka et al. (2019) [43] reported a pH of 2.4 ± 0.1 in PAW generated with a SDBD system for 20 min (plasma power of 36 W; frequency of 12 kHz). In addition, Lin et al. (2019) [165] reported a decrease in pH in PAW generated with tap water and plasma jet for 10, 20 and 30 min activation time and plasma power of 40, 50 and 60 W, where the longer the activation time and the higher the plasma power resulted in the most pronounced pH drop. On the contrary, Judée et al. (2018) [31] used tap water at pH 7.8 (France) for the generation of PAW and reported only negligible

variations in pH after 30 min activation time using a DBD system (voltage amplitude of 12.0 kV_{AC} at 500 Hz). The tap water in France has a higher alkalinity and buffering capacity than Norwegian tap water. As mentioned in section 4.1.2, the carbonic compounds, mainly bicarbonate and carbonate ion, are working as a buffer in tap water to keep the pH stable, and Judée et al. (2018) reported a four times higher concentration of bicarbonate in untreated tap water from France (4.13 ± 0.09 mM) than that from Norway (1.06 ± 0.03 mM).

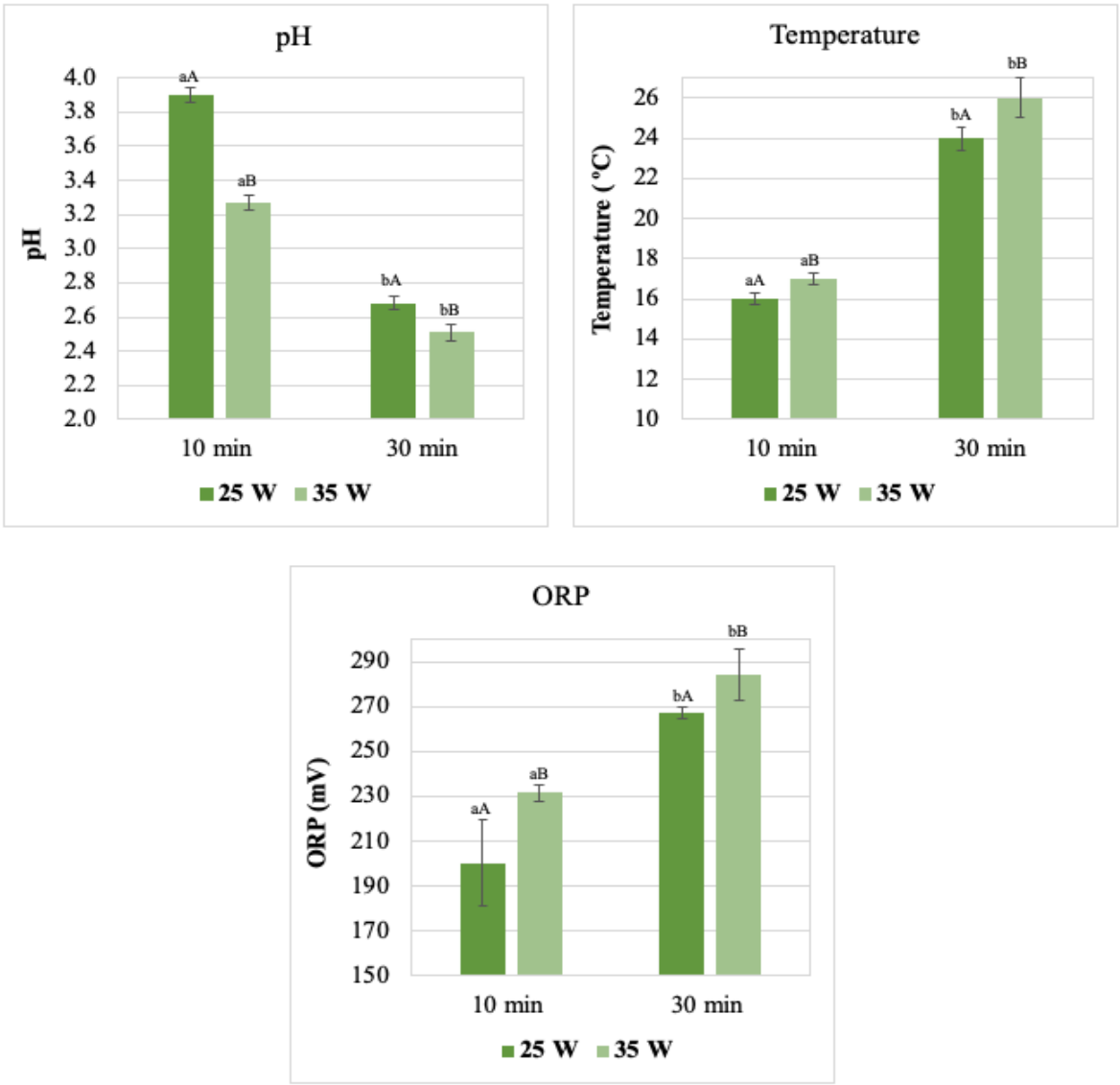

Figure 19. pH, temperature (immediate reading) and ORP of PAW as a function of plasma power (25/35 W) and activation time (10/30 min). Different upper-case letters indicate a significant difference in the concentration of the reactive species with regards to plasma power. Different lower-case letters show a significant difference with regards to activation time (n=3, P-level ≤ 0.05) (Numeric values in Appendix A)

Additionally, the ORP values increased with the activation time and plasma power (Figure 19). Similarly to pH, significant differences were observed for both activation time and plasma power with regards to the ORP values, although the activation time for constant plasma power exhibited the most pronounced effect. In the present work, the ORP increased from -45.3 ± 2.4 (tap water) to values ranging between 200.2 ± 19.0 and 284.1 ± 11.5 mV for extreme operating conditions (25 W/10 min and 35 W/30 min), thus the reducing tap water transformed into PAW with a high oxidation potential. Similarly, Vaka et al. (2019) [43] generated 100 mL PAW with a SDBD system and reported ORP values of 200 and 292 mV for operating conditions of 26W/5 min and 36W/20 min, respectively. Ma et al. (2015) [63] also reported an increase in ORP when generating PAW with a plasma jet (frequency of 10 kHz; Peak to peak voltage of 18 kV; volume of 80 mL) from 270 mV in untreated water to 450 and 550 mV after 10 and 20 min activation, respectively. Similarly, Abuzairi et al. (2018) [166] reported that longer activation time led to higher ORP and RONS levels. As described in section 1.4.1, the ORP plays an important role in the disinfection potential of PAW [167].

Furthermore, the temperature of PAW (immediate reading after treatment) increased with the activation time and plasma power (Figure 19), due to a thermal effect attributed to the SDBD electrode. In the present work the maximum temperature right after PAW generation reached 26 ± 1 °C (35 W for 30 min) from an initial temperature of the tap water of about 11.0 °C (Table 18), with Vaka et al. (2019) [43] reporting a maximum value of 30.9 ± 1.2 °C for PAW generated at similar power for 20 min. Likewise, Judée et al. (2018) [31] reported an increase in the PAW temperature for longer activation times, with an increase of 3.6 ± 0.7 and 9.0 ± 0.8 °C after 5 and 30 min, respectively, reaching a maximum temperature of 36.15 ± 1.26 °C (DBD system, voltage amplitude of 12.0 kV_{AC} at 500 Hz). However, the temperature did not increase in a linear manner, after 25 min activation (90% response time) the temperature reaches a plateau, keeping steady at 36.15 ± 1.26 °C. Room temperature has typically been used for PAW generation even though this could affect the solubility of RONS. Thus, Vaka et al. (2019) [43] reported an increase in pH and nitrites levels and a slight decrease in the temperature after treatment (28 °C) for PAW generated (SDBD system; 36 W for 20 min) from distilled water at 4 °C as compared to 10 °C, although nitrates levels remained unaffected. It is noteworthy that in present work the PAW was stabilized at room temperature before any further parameter was determined, with the pH and ORP meter integrating a temperature compensation probe.

Additionally, the concentration of hydronium ions and hydroxide in PAW was estimated with equations 1 and 2, respectively, as described in section 3.2.2 (Figure 20), which are based on the pH of the PAW and the corresponding temperature at the time of measurement. The concentration of hydronium ions increased towards the activation time and plasma power, with both parameters showing a statistically significant effect, which is directly correlated with the pH drop. On the other hand, a decrease in the average hydroxide concentration with increasing activation time and plasma power was observed, however, significant differences were not obtained from the statistical analysis. Nevertheless, the concentration of hydroxide could be considered negligible (pM), which is attributed to the acidic pH of PAW.

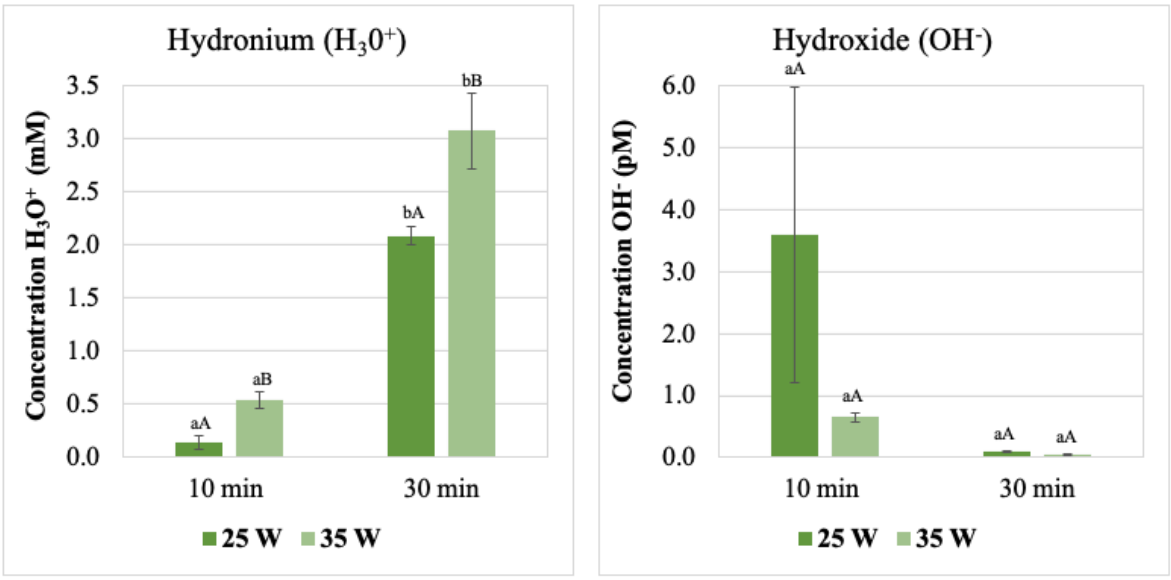

Figure 20. Concentration of hydronium and hydroxide in PAW, based on the pH and temperature directly after treatment, as a function of plasma power (25/35 W) and activation time (10/30 min). Different upper-case letters indicate a significant difference in the concentration of the reactive species with regards to plasma power. Different lower-case letters show a significant difference with regards to activation time (n=3, P-level ≤ 0.05) (Numeric values in Appendix A)

Regarding the effect of activation time and plasma power on RNS in PAW, both nitrate and nitrite concentrations increased significantly with the longest activation time (30 min) and highest plasma power (35 W) reaching a maximum concentration of 342.5 ± 13.5 and 1.57 ± 0.12 mg/L, respectively (Figure 21). The concentration of nitrates is significantly higher than that for nitrites due to the instability of nitrites in acidic environment, forming nitrous acid, which later decomposes into nitrates and nitrogen oxide. Nitrate levels in PAW have often been reported to be higher than nitrite levels [43, 70, 74]. For instance, Vaka et al. (2019) [43] reported similar results as present work with PAW generated at 36 W for 20 min (SDBD

system) yielding the highest concentration of nitrates and nitrites (320 ± 47.8 and 7.2 ± 3.8 mg/L, respectively). On the contrary to present work, Judée et al. (2018) [31] reported a nitrite concentration of 175.4 ± 9.7 and 125.79 ± 6.85 μM after 10- and 30-min activation, respectively, observing a decrease in nitrite levels after 10 min activation. However, the nitrate concentration increased almost linear to the activation time, similar to the present work, and reached a maximum concentration of 3.55 mM after 30 min. On the other hand, since nitrites remain stable at alkaline conditions, Jung et al. (2015) [80] adjusted the initial pH of distilled water to 9.0 and generated PAW with a SDBD system (average power of 3.14 W; discharge area of 20 cm^2; frequency of 15 kHz), resulting in nitrites and nitrates levels, much higher than those in present work, of 782 and 385 mg/L, respectively, favoring the formation of nitrite. In addition, the concentration of nitrous and nitric acid in PAW was estimated according to equations 3 and 4 (section 3.2.2) and displayed in Figure 22. The concentration of both HNO_2 and HNO_3 increased towards activation time and plasma power, however, unlike the trend for nitrates and nitrites, the formation of HNO_2 was favored due to the pKa of HNO_3 being very low (-2.00) as compared to the pKa of HNO_2 (3.39) [31]. The maximum concentration achieved at 35 W for 30 min was 258 ± 37 mM and 171 ± 25 μM, for HNO_2 and HNO_3 respectively. Judée et al. (2018) [31] reported a maximum concentration of 10.72 ± 5.78 nM and 1.15 ± 0.69 pM for HNO_2 and HNO_3, respectively after 10 min activation with a DBD system (voltage amplitude of 12.0 kV_{AC} at 500 Hz). Similar to present work, the concentration of HNO_2 was higher than the concentration of HNO_3, even though the concentration of nitrate was higher than nitrite. Nevertheless, both HNO_2 and HNO_3 was much higher in present work compared to the values reported by Judée et al. (2018).

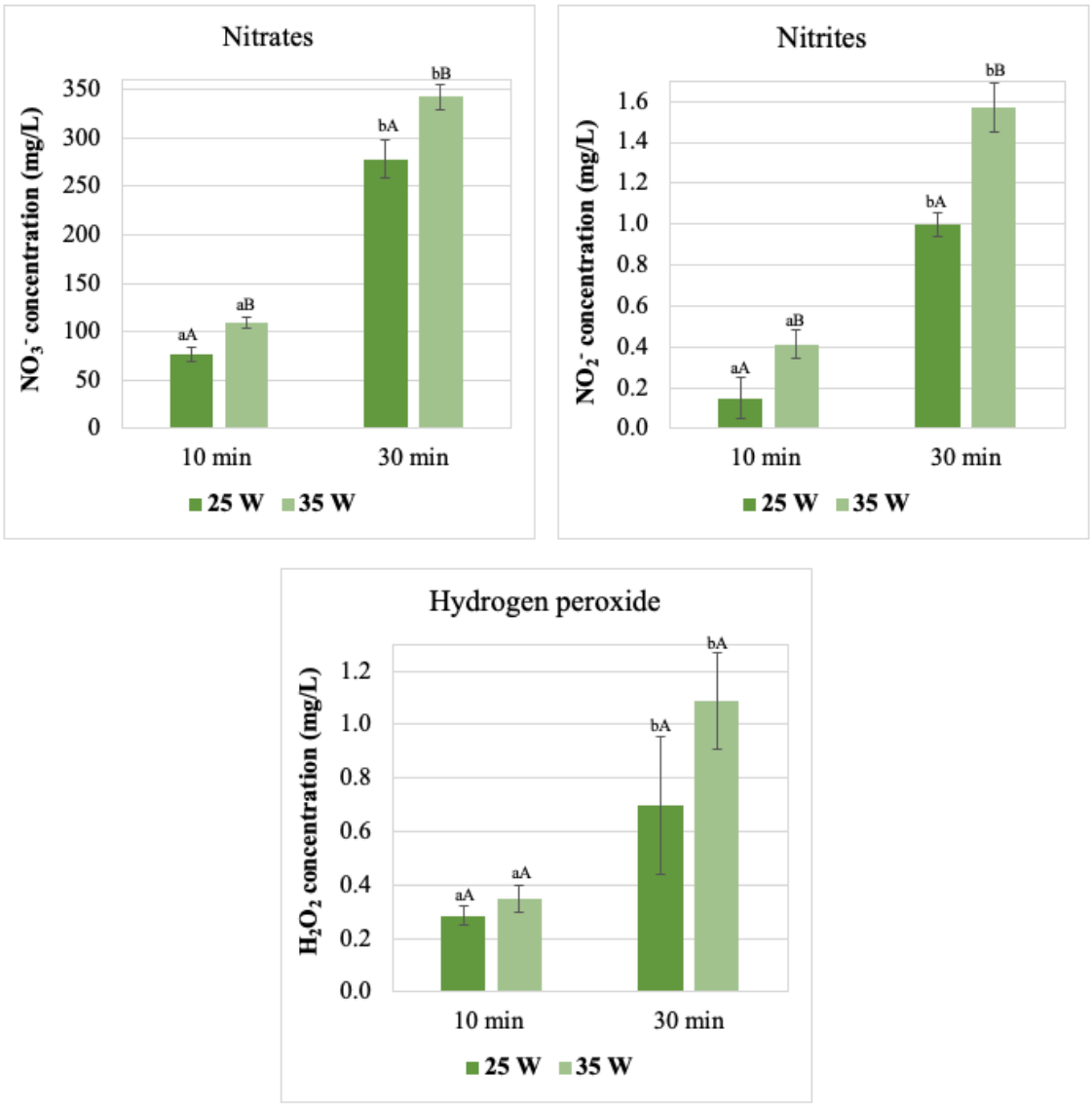

Figure 21. Concentration of reactive species (nitrates, nitrites and hydrogen peroxide) in PAW as a function of plasma power (25/35 W) and activation time (10/30 min). Different upper-case letters indicate a significant difference in the concentration of the reactive species with regards to plasma power. Different lower-case letters show a significant difference with regards to activation time. (n=3, P-level ≤ 0.05) (Numeric values listed Appendix A)

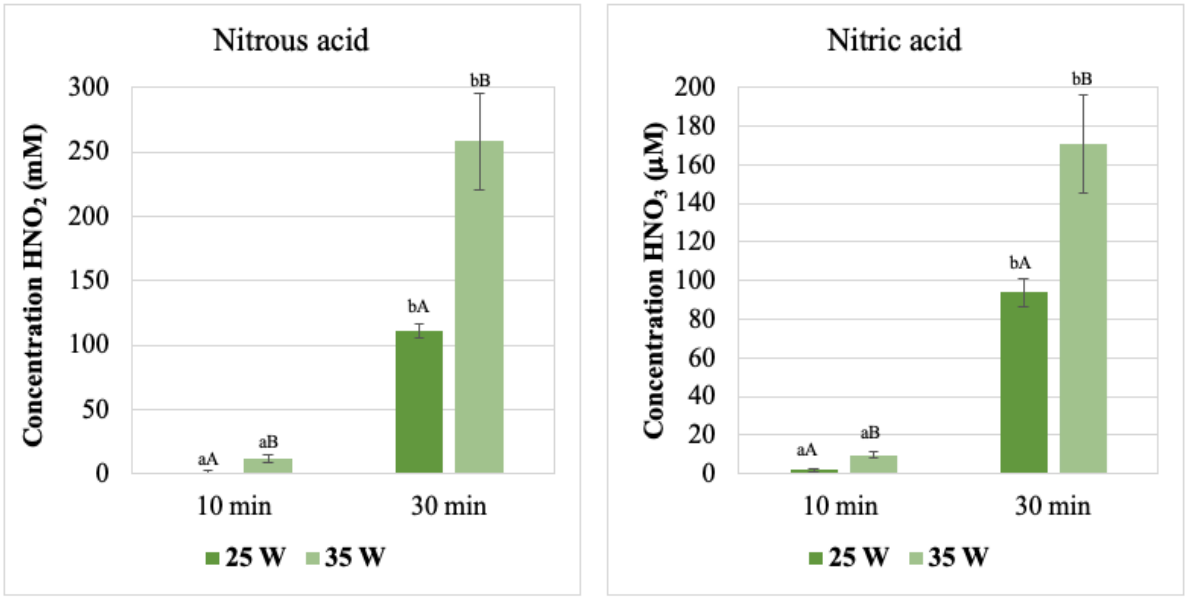

Figure 22. Estimated concentration of HNO_2 and HNO_3 in PAW as a function of plasma power (25/35 W) and activation time (10/30 min). Different upper-case letters indicate a significant difference in the concentration of the reactive species with regards to plasma power. Different lower-case letters show a significant difference with regards to activation time. (n=3, P-level ≤ 0.05) (Numeric values listed in Appendix A)

With regards to hydrogen peroxide in PAW, the average concentration increased towards plasma power and activation time (Figure 21). However, only the activation time resulted in statistically significant differences. Thus, hydrogen peroxide levels were higher for longer activation times (30 min). Similarly, Judée et al. (2018) [31] reported a quadratic trend for the increase of hydrogen peroxide concentration with increased activation time and achieved a maximum value of 1.85 ± 0.16 mM after 30 min (DBD system, voltage amplitude of 12.0 kV_{AC} at 500 Hz). In the present study, hydrogen peroxide levels were relatively low, reaching a maximum of 1.1 ± 0.2 mg/L for extreme operating conditions (35 W/30 min). In literature this has been attributed to the rapid decomposition of hydrogen peroxide by nitrites under acidic conditions [79, 86]. The remote PAW generation (i.e. electrode not immersed in the water), the relatively long exposure times (10 and 30 min) and the electrode-liquid gap (21.4 cm) affected by the treatment volume, may have affected the availability of hydrogen peroxide due to the suppression of decomposition reactions by radicals from the gas and at the interface [168]. Interestingly, concentrations of 2000 mg/L were reported by Shainsky et al. (2012) [69] (DBD system with a pulsed voltage of 17 kV; 100 µL volume; 1.5 mm electrode-liquid gap), although this value dropped to 10 mg/L after 10 min. Furthermore, Ikawa et al. (2010) [84] reported hydrogen peroxide concentrations up to 50 mg/L after 3 min exposure to a plasma jet (direct treatment, using a pulsed high voltage of -3.5 to +5.9 kV and a frequency of 13.9 kHz), much

higher than those in the present work, although the treatment volume was significantly lower (500 μL). On the other hand, Taylor et al (2011) [85] reported hydrogen peroxide levels in the range of the present work(3.4 mg/L) with a similar DBD system operating at 5 kV for 20 min, although the treatment volume (10 mL) was much lower.

Similarly, to hydrogen peroxide, the initial treatment volume, affecting the electrode-liquid gap, plays a decisive role with regards to the RNS levels. Initial volumes of water, ranging from 1 mL to 1.6 L have been assessed in the literature, including different gap distances between the plasma electrode and the water surface ranging from 5 to 50 mm. A study from Vaka et al. (2019) [43] showed that an increase in treatment volume from 100 to 500 mL (44.8 to 32.0 mm gap) significantly altered pH (2.4 ± 0.1 to ≈7.0), temperature (30.9 ± 1.2 to ≈22 °C) and nitrates levels (320.0 ± 47.8 to ≈40 mg/L) in the PAW generated with a SDBD system at 36 W for 20 min. In this work, the magnetic stirring was kept constant at 500 rpm; however, adjusting this factor may result in enhanced diffusion of RONS into the water. A study conducted with a similar SDBD system and 500 mL water resulted in significantly higher nitrites and nitrates levels (782 and 358 mg/L, respectively) using magnetic stirring at 300 rpm. However, the longer treatment time (2-h) and much higher initial pH of the water (adjusted to 9.7) could be responsible for the higher concentrations [113].

The concentration of carbonic compounds in PAW was determined by basic titration (pH below 6.3) using NaOH 0.1 M, as described in section 4.1.2 and according to equations 10-12 (Section 3.2.2.). As illustrated in Figure 23, the total concentration of carbonic compounds in the PAW increased with increasing activation time and plasma power, reaching a maximum value of 1.39 ± 0.26 mM. However, statistically significant differences were only observed for the activation time. While the levels of H_2CO_3 presented a similar trend to that of total carbonic compound, a slight decrease in the average concentration of bicarbonate with increasing plasma power and activation time was observed. Interestingly, the increase of H_2CO_3 levels towards both operating conditions is correlated to the acidification of the media. Although the CO_3^{2-} values were practically negligible (pM), a decrease with increasing plasma power and activation time was observed, with a maximum value of 152.5 ± 172.7 pM for the lowest power and activation time (L-10). Likewise, Judée et al. (2018) [31] reported that bicarbonate decreased rapidly with activation time, from 4.13 ± 0.09 mM (untreated) to 0.98 ± 0.25 mM after 30 min activation. Additionally, both H_2CO_3 and CO_3^{2-} concentration decreased from 121.3 ± 30.8 and 6.34 ± 0.99 to 41.0 ± 16.6 μM and 2.20 ± 0.88 μM, respectively, for untreated and 30-min activation. The

fast decrease of bicarbonates in PAW is not fully understood, nevertheless Judée et al (2018) suggested that as carbon dioxide dissolved in water decreases with a rise of the water temperature, the DBD activation heating the plasma water very locally at a temperature high enough to converse carbonate and bicarbonate ions into gaseous carbon dioxide. However, in present work the carbonic acid concentration increases, whilst bicarbonate decreases, as discussed carbonic acid is favored in acidic environments and the pH for PAW in present work was in the range 2.5 ± 0.1 to 3.9 ± 0.0, compared to the non-changeable pH that Judée et al. (2018) reported (7.8), suggesting that in present work the bicarbonate are conversed to carbonic acid.

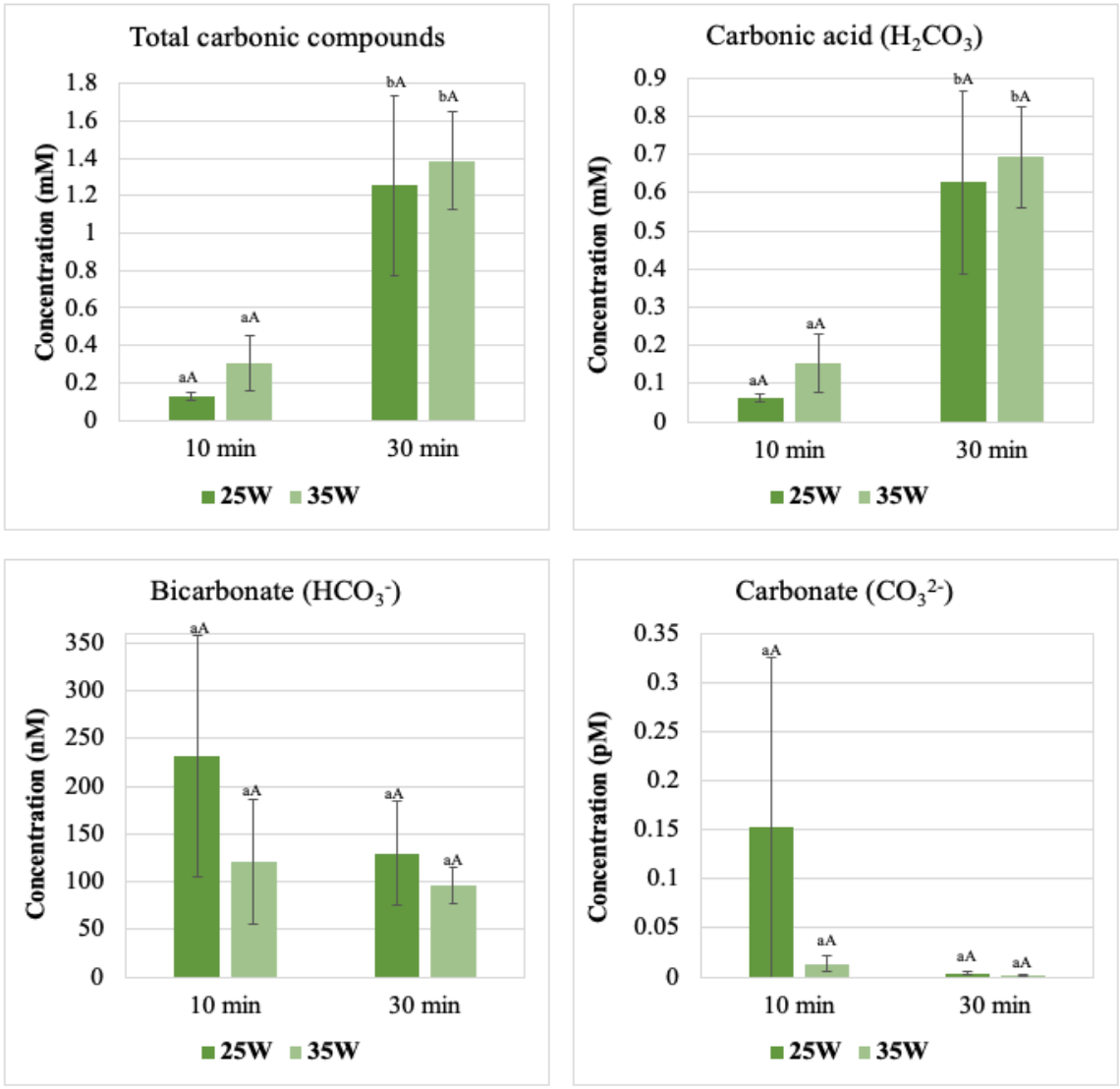

Figure 23. Estimated concentrations of total carbonic compounds, carbonic acid, bicarbonate and carbonate ion in PAW as a function of plasma power (25/35 W) and activation time (10/30 min). Different upper-case letters indicate a significant difference in the concentration of the reactive species with regards to plasma power. Different lower-case letters show a significant difference with regards to activation time. (n=3, P-level ≤ 0.05) (Numeric values listed in Appendix A)

4.1.4 Overview of PAW composition as a function of different generation system

In the present work two different plasma systems, suitable for larger and smaller volumes, were used for the generation of PAW, as compared to commercial PAW (IB). Table 19 provides an overview of selected parameters (i.e. pH, nitrates, nitrites and hydrogen peroxide) for the PAW generated with different operating system and conditions. The plasma power (i.e. 35 or 25 W), the activation time (i.e. 5, 10 or 30 min) and the generation system (system for large volumes before/after maintenance and system for small volumes) with the corresponding volume (100, 200 or 300 mL) are listed.

Table 19. An overview of selected parameters (i.e. pH, nitrates, nitrites and hydrogen peroxide) for the PAW generated with the different systems, with different volumes and the commercial PAW(IB)

	Plasma Power (W)	Activation time (min)	Generation system / volume	pH	Nitrates (mg/L)	Nitrites (mg/L)	Hydrogen peroxide (mg/L)
H-30	35	30	Δ 3	2.5 ± 0.1	342.5 ± 13.6	1.6 ± 0.1	1.1 ± 0.2
L-30	25	30	Δ 3	2.7 ± 0.0	278.3 ± 19.8	1.0 ± 0.1	0.7 ± 0.3
H-10	35	10	Δ 3	3.3 ± 0.0	109.2 ± 6.0	0.4 ± 0.1	0.4 ± 0.1
L-10	25	10	Δ 3	3.9 ± 0.0	76.9 ± 7.7	0.2 ± 0.1	0.3 ± 0.0
HS-5	35	5	◊ 1		78.1 ± 11.8	24.2 ± 7.8	
HS-30	35	30	◊ 1	2.3 ± 0.0	459.6 ± 2.1	30.2 ± 0.7	7.7 ± 0.9
H-30*	35	30	□ 2	2.2 ± 0.0	458.5 ± 3.0	1.9 ± 0.1	0.4 ± 0.1
PAW_IB			Commercial	2.4 ± 0.0	310.8 ± 7.2	0.4 ± 0.0	142.6 ± 5.5

Δ = System for larger volumes, ◊ = System for smaller volumes, □ = System for larger volumes after maintenance and 1, 2, 3 = 100, 200 and 300 mL, respectively.

Interesting remarks from Table 19 refer to the average hydrogen peroxide concentration in PAW_IB being significantly higher (142.6 ± 5.5 mg/L) than the maximum levels achieved with the SBDB systems used in present work (7.7 ± 0.9 mg/L for HS-30). Additionally, HS-30 (system for smaller volumes) presented the highest average levels of nitrates and nitrites, with values of 459.6 ± 2.1 and 30.2 ± 0.7 mg/L, respectively. Although the H-30* (system for larger volumes after maintenance) reached similar average levels for nitrates (458.5 ± 3.0 mg/L), the average nitrites concentration was significantly lower (1.9 ± 0.1 mg/L). With regards to the pH, H-30*, HS-30 and PAW_IB resulted in values between 2.2 ± 0.0 and 2.4 ± 0.0 Thus, the system for smaller volumes (100 mL) operating at 35 W for 30 min gave rise to the PAW with the

highest concentration of RONS, which in principle makes it the most favorable setting for application into products.

4.2 PAW storage stability

The stability of PAW generated with the system for larger volumes at a plasma power of 25 or 35 W and activation times of 10 or 30 min was assessed at 10, 4 and -20 °C (representing temperature abuse condition, typical refrigeration and freezing temperatures, respectively) for 28 days, with compositional analysis directly after activation (0) and after 1, 7, 14, 21 and 28 days of storage. Figure 24 and Figure 25 display the results (average and standard deviation; n=3) corresponding to the stability of pH and ORP in PAW, respectively. Both pH and ORP values remained stable after 28 days of storage for all the generation conditions, with no significant differences between the different temperatures assayed. Similarly, Vaka et al. (2019) [43] reported no significant differences in the pH of PAW stored at 4 °C for two weeks. Additionally, Shen et al. (2016) [70] observed a stable pH for 30-days storage at 25, 4, -20 and -80 °C, however, the ORP dropped from 540 to 400-450 mV after 30 days of storage, with the highest drop recorded for the highest storage temperature.

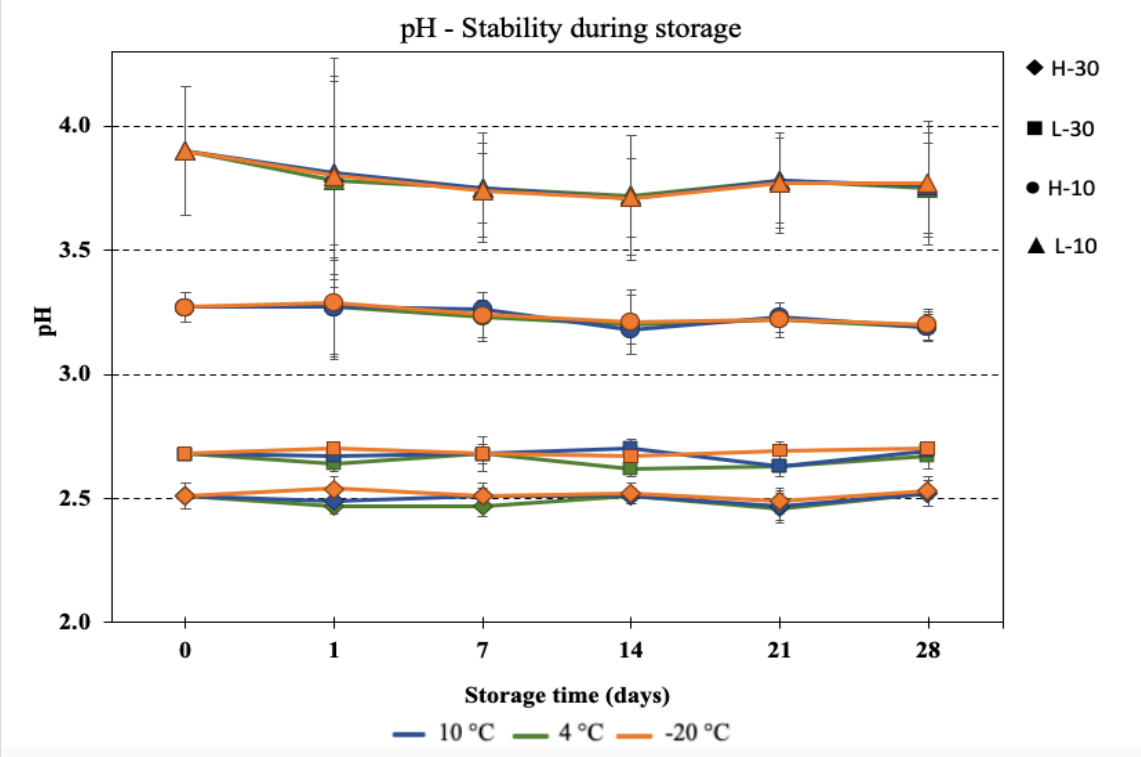

Figure 24. pH of PAW during storage at 10, 4 and -20 ℃ as a function of the plasma power (25/35 W) and activation time (10/30 min) for 28 days storage, measured after 0 (directly after activation), 1, 7, 14, 21 and 28 days. Statistical analysis performed between PAW stored at different temperatures or between the weeks with a significant level set at 95 % (P≤0.05, n=3) (Numeric values listed in Appendix A)

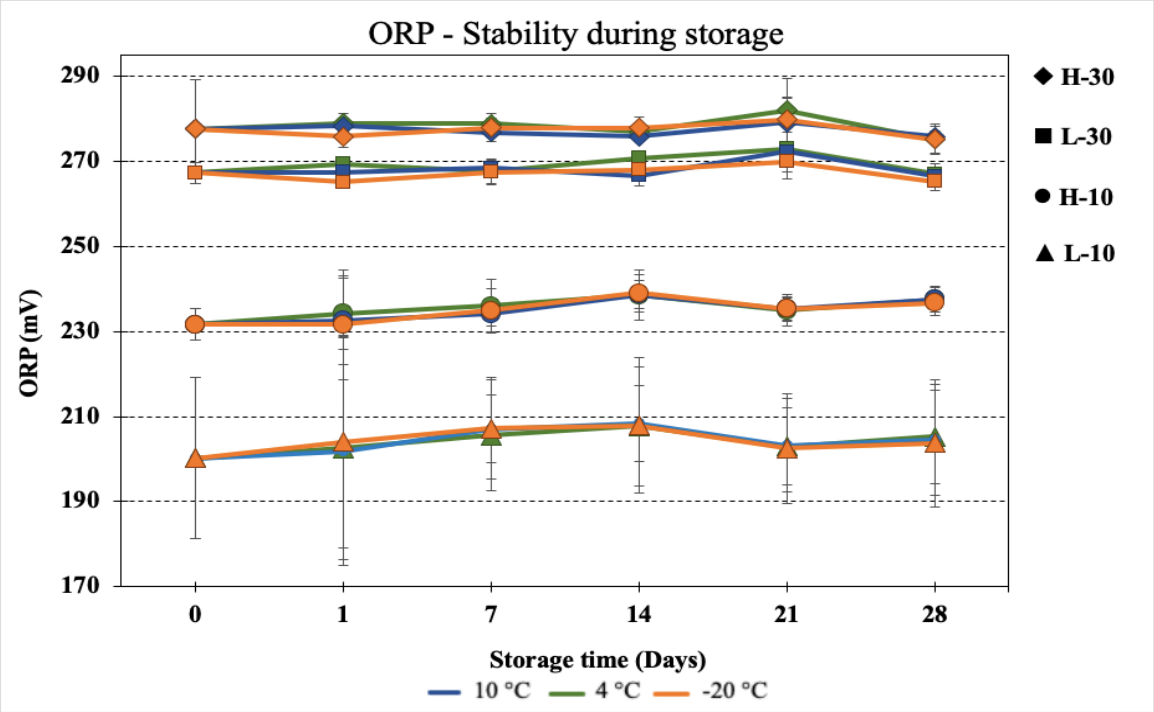

Figure 25. The ORP of PAW during storage at 10, 4 and -20 ℃ as a function of the plasma power (25/35 W) and activation time (10/30 min) for 28 days storage, measured after 0 (directly after activation), 1, 7, 14, 21 and 28 days. Statistical analysis performed between PAW stored at different temperatures or between the weeks with a significant level set at 95 % ($P \leq 0.05$, n=3) (Numeric values listed in Appendix A)

The hydronium ion and hydroxide concentrations in PAW, based on the pH and the corresponding temperature at the measurement point, are presented in Figure 26 and Table 20, respectively. No significant differences were found in the hydronium ion concentration in PAW stored for 28 days at the three different temperatures for all the generation conditions. Nevertheless, a slight variation in the average values with the storage period was observed, especially for the H-30 and L-30, which could be attributed to small differences in the sample temperature, as the pH of PAW remained stable (Figure 23). As already mentioned in section 4.1.3, the hydroxide levels (pM) were practically negligible due to the acidic environment. During storage, no statistically significant variability was observed with regards to the storage period and temperature, for all the generation conditions, which is directly related to the pH stability. However, a slight decrease in the average values for L-10 between 0 and 28 days, independently of the temperature.

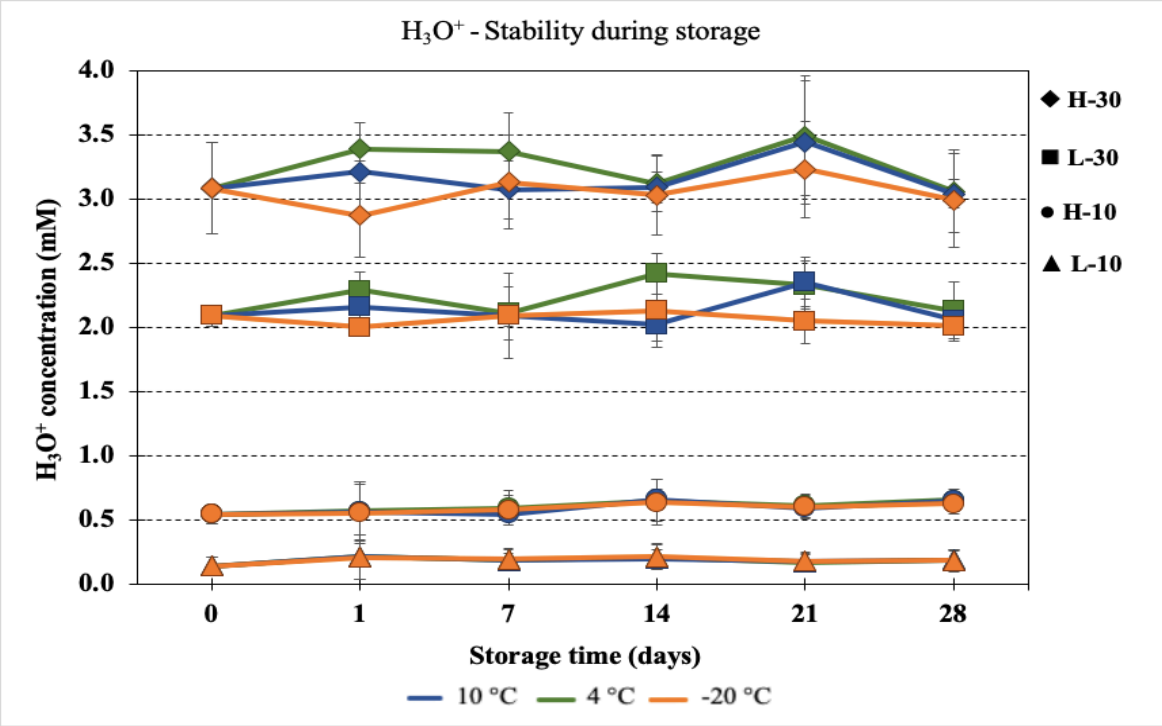

Figure 26. Stability of hydronium concentration during storage at 10, 4 and -20 ℃ as a function of the plasma power (25/35 W) and activation time (10/30 min) for 28 days storage, measured after 0 (directly after activation), 1, 7, 14, 21 and 28 days. Statistical analysis performed between PAW stored at different temperatures or between the weeks with a significant level set at 95 % (P≤0.05, n=3 (Numeric values in Appendix A)

Table 20. Stability of hydroxide concentration during storage at 10, 4 and -20 ℃ as a function of the plasma power (25/35 W) and activation time (10/30 min) for 28 days storage, measured after 0 (directly after activation), 1, 7, 14, 21 and 28 days. Statistical analysis performed between PAW stored at different temperatures or between the weeks with a significant level set at 95 % (P≤0.05, n=3

		OH^- (pM)					
		0 D	1 D	7 D	14 D	21 D	28 D
H-30	4 ºC	0.059 ± 0.012	0.066 ± 0.10	0.078 ± 0.0069	0.079 ± 0.0044	0.057 ± 0.029	0.087 ± 0.013
	10 ºC	0.059 ± 0.012	0.078 ± 0.0006	0.081 ± 0.0074	0.080 ± 0.0044	0.067 ± 0.023	0.085 ± 0.0036
	- 20 ºC	0.059 ± 0.012	0.086 ± 0.0067	0.082 ± 0.0073	0.082 ± 0.0076	0.066 ± 0.023	0.086 ± 0.011
L-30	4 ºC	0.10 ± 0.004	0.11 ± 0.004	0.12 ± 0.011	0.10 ± 0.007	0.085 ± 0.036	0.12 ± 0.010
	10 ºC	0.10 ± 0.004	0.12 ± 0.012	0.12 ± 0.004	0.13 ± 0.011	0.091 ± 0.030	0.13 ± 0.006
	- 20 ºC	0.10 ± 0.004	0.13 ± 0.01	0.12 ± 0.016	0.12 ± 0.010	0.098 ± 0.034	0.13 ± 0.006
H-10	4 ºC	0.65 ± 0.078	0.40 ± 0.073	0.45 ± 0.09	0.39 ± 0.11	0.46 ± 0.07	0.40 ± 0.054
	10 ºC	0.65 ± 0.078	0.50 ± 0.22	0.46 ± 0.04	0.39 ± 0.08	0.46 ± 0.06	0.40 ± 0.047

	- 20 ºC	0.65 ± 0.078	0.53 ± 0.29	0.44 ± 0.09	0.42 ± 0.14	0.44 ± 0.03	0.42 ± 0.053
L-10	4 ºC	3.59 ± 2.39	2.02 ± 1.73	1.59 ± 0.99	1.46 ± 0.87	1.82 ± 0.77	1.55 ± 0.72
	10 ºC	3.59 ± 2.39	2.4 ± 2.39	1.48 ± 0.61	1.35 ± 0.56	1.74 ± 0.84	1.61 ± 0.89
	- 20 ºC	3.59 ± 2.39	2.04 ± 1.79	1.45 ± 0.77	1.45 ± 0.92	1.78 ± 0.92	1.75 ± 1.14

The stability of RNS levels in PAW during storage is displayed in Figure 27 andFigure 28. The concentration of nitrates in PAW remained stable for all the generation conditions, independently of the storage temperature and period. Interestingly, Vaka et al. (2019) [43] reported a slight increase in nitrates level for two weeks storage at 4 °C, whilst Shen et al (2016) [70] reported a decrease in the concentration of nitrates as the storage time increased, with that decrease being more pronounced at higher temperatures. With regards to nitrites, the levels in PAW H-30 stored at 4 and 10 °C significantly decreased after 24 h, and then remained relatively stable until the end of the storage period. Nevertheless, for storage at -20 °C, the concentration of nitrites in PAW H-30 was not detectable after 24 h, which confirms the key role of the storage temperature on PAW stability. Additionally, for L-30, H-10 and L-10, nitrites levels were not detectable after 24 h storage for any of the assayed temperatures, thus resulting in significant differences with regards to H-30 stored at 4 and 10 °C, but not to H-30 stored at -20 °C. Similarly, Vaka et al. (2019) [43] reported a slight decrease in nitrite concentration over a storage period of two weeks at 4 °C. Additionally, Traylor et al. (2011) [85] assessed the long-term antibacterial activity of PAW (7-day storage, temperature nondisclosed) and reported a decrease in nitrites and hydrogen peroxide to below the detection limit within two days while keeping a constant pH, similar as the results reported in present work. The decrease in nitrites levels has been attributed to this compound being unstable at low pH, leading to decomposition into nitrogen oxide and nitrate [169, 170].

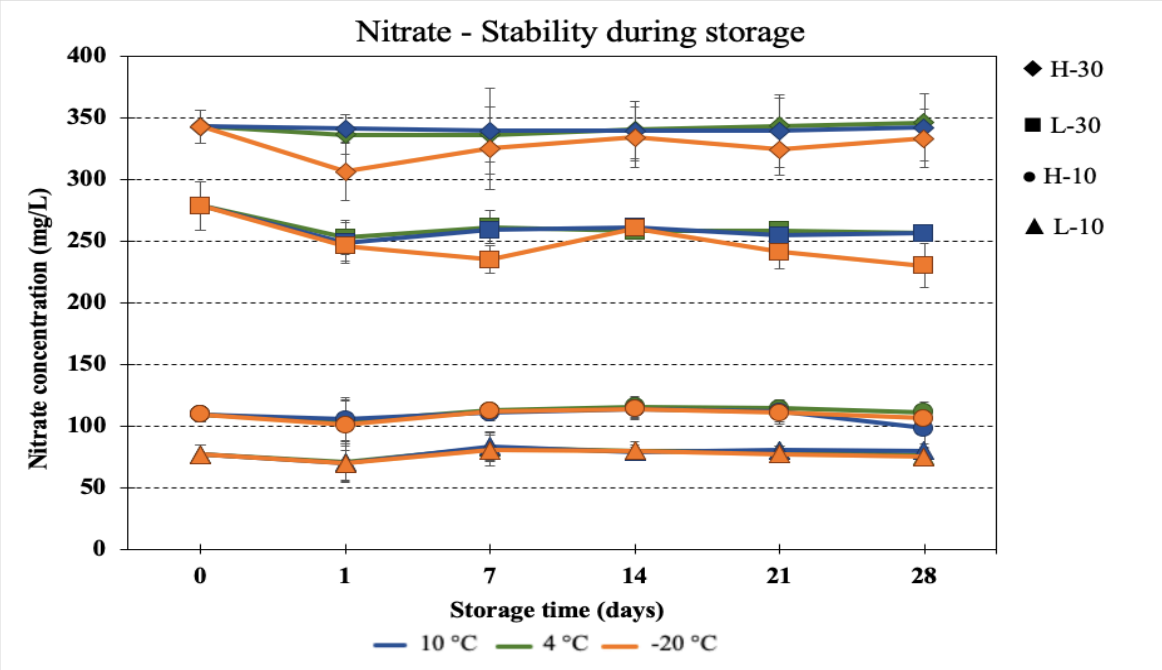

Figure 27. Stability of nitrate concentration during storage at 10, 4 and -20 ℃ as a function of the plasma power (25/35 W) and activation time (10/30 min) for 28 days storage, measured after 0 (directly after activation), 1, 7, 14, 21 and 28 days. Statistical analysis performed between PAW stored at different temperatures or between the weeks with a significant level set at 95 % (P≤0.05, n=3) (Numeric values listed in Appendix A)

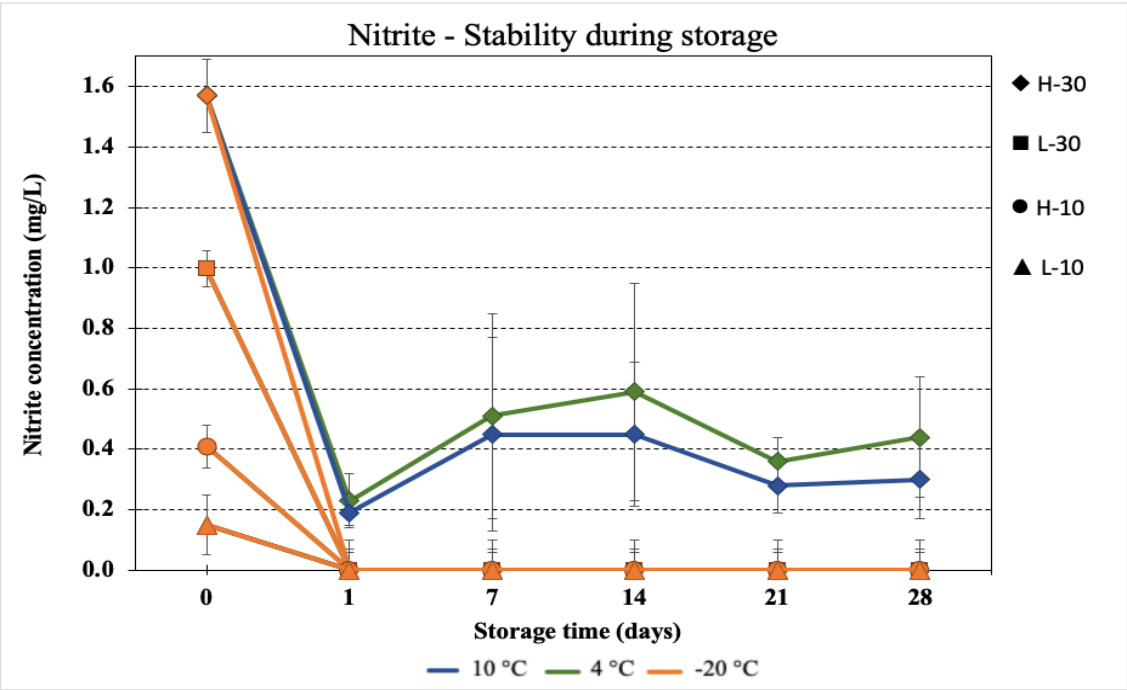

Figure 28. Stability of nitrite concentration during storage at 10, 4 and -20 ℃ as a function of the plasma power (25/35 W) and activation time (10/30 min) for 28 days storage, measured after 0 (directly after activation), 1, 7, 14, 21 and 28 days. Statistical analysis performed between PAW stored at different temperatures or between the weeks with a significant level set at 95 % (P≤0.05, n=3) (Numeric values listed in Appendix A)

The concentrations of nitric and nitrous acids were estimated according to Equation 3 and Equation 4, respectively, and the results are listed in Table 21. The HNO_3 concentration remained stable over four weeks of storage, independently of the temperature and generation conditions, as these values were based on the concentration of nitrates, they are following the same trend as nitrates (although a much lower concentration). The HNO_2 levels showed the same trend as the nitrites concentration during storage, indeed, PAW H-30 stored in 10 and 4 °C decreased significantly after 24 h and kept relatively stable until the end of storage. On the other hand, H-30 stored at -20 °C as well as the L-10, H-10 and L-30 decreased to below the detectable limits after 24 h. Estimated HNO_2 concentration gave a much higher concentration than HNO_3, as discussed in section 4.1.3 this has been contributed to the low pKa level of nitrate (-2) compared to the one of nitrite (3.37)

Table 21. Stability of HNO_2 and HNO_3 concentration during storage at 10, 4 and -20 ℃ as a function of the plasma power (25/35 W) and activation time (10/30 min) for 28 days storage, measured after 0 (directly after activation), 1, 7, 14, 21 and 28 days. Statistical analysis performed between PAW stored at different temperatures or between the weeks with a significant level set at 95 % ($P \leq 0.05$, n=3

		Storage time (Days)					
		0	1	7	14	21	28
				L-10			
HNO2 (mM)	10 ºC	1.3 ± 1.3	ND	ND	ND	ND	ND
	4 ºC	1.3 ± 1.3	ND	ND	ND	ND	ND
	-20 ºC	1.3 ± 1.3	ND	ND	ND	ND	ND
HNO3 (µM)	10 ºC	1.8 ± 1.0	2.7 ± 2.7	2.5 ± 0.9	2.6 ± 0.1	2.3 ± 0.9	2.4 ± 1.1
	4 ºC	1.8 ± 1.0	2.7 ± 2.6	2.6 ± 1.3	2.7 ± 1.3	2.3 ± 0.8	2.4 ± 1.0
	-20 ºC	1.8 ± 1.0	2.6 ± 2.6	2.5 ± 1.1	2.8 ± 1.5	2.3 ± 0.9	2.3 ± 1.1
				H-10			
HNO_2 (mM)	10 ºC	12.0 ± 2.7	ND	ND	ND	ND	ND
	4 ºC	12.0 ± 2.7	ND	ND	ND	ND	ND
	-20 ºC	12.0 ± 2.7	ND	ND	ND	ND	ND
HNO_3 (µM)	10 ºC	9.6 ± 1.8	10.0 ± 5.0	9.8 ± 1.3	12.2 ± 2.3	10.8 ± 2.05	10.5 ± 3.21
	4 ºC	9.6 ± 1.8	9.9 ± 5.2	10.9 ± 2.9	12.3 ± 3.8	11.3 ± 2.3	11.7 ± 1.6
	-20 ºC	9.6 ± 1.8	9.6 ± 5.4	10.8 ± 2.9	11.9 ± 4.1	10.8 ± 2.5	10.8 ± 2.0
				L-30			
HNO_2 (mM)	10 ºC	111.0 ± 5.8	ND	ND	ND	ND	ND
	4 ºC	111.0 ± 5.8	ND	ND	ND	ND	ND
	-20 ºC	111.0 ± 5.8	ND	ND	ND	ND	ND
HNO_3 (µM)	10 ºC	93.8 ± 7.3	86.6 ± 10.9	87.3 ± 4.2	85.0 ± 7.8	96.4 ± 7.3	85.0 ± 2.5
	4 ºC	93.8 ± 7.3	93.6 ± 10.0	89.2 ± 13.5	101.0 ± 5.6	97.4 ± 10.3	88.1 ± 9.8
	-20 ºC	93.8 ± 7.3	79.1 ± 3.9	78.9 ± 3.9	89.5 ± 3.9	79.7 ± 8.9	74.9 ± 9.5

			H-30				
HNO_2 (mM)	10 ºC	258.0 ± 37.5	33.2 ± 10.0	74.9 ± 50.0	74.0 ± 40.0	51.4 ± 20.0	48.2 ± 20.0
	4 ºC	258.0 ± 37.5	42.5 ± 20.0	91.1 ± 60.0	99.1 ± 60.0	67.2 ± 20.0	72.5 ± 30.0
	-20 ºC	258.0 ± 37.5	ND	ND	ND	ND	ND
HNO_3 (µM)	10 ºC	171.0 ± 25.3	177.0 ± 9.7	169.0 ± 28.8	170.0 ± 18.3	189 ± 41.1	168 ± 17.8
	4 ºC	171.0 ± 25.3	184.0 ± 19.3	183.0 ± 25.9	172.0 ± 23.3	194 ± 37.7	171 ± 29.2
	-20 ºC	171.0 ± 25.3	133.0 ± 5.6	165.0 ± 37.2	164.0 ± 23.9	170 ± 30.8	161 ± 29.4

As discussed in section 4.1, the concentration of hydrogen peroxide in PAW immediately after generation was remarkably low (maximum value of 1.1 ± 0.2 mg/L). With regards to its storage stability, hydrogen peroxide in PAW, for all the generation conditions, was not detectable after 24 h, independently of the storage temperature. On the other hand, Scholtz et al. (2012) [55] reported a decrease in hydrogen peroxide levels from 300 to 50 mg/L in PAW after storage for four weeks at 4 °C.

The concentration of carbonic compounds (total), H_2CO_3, HCO_3^- and CO_3^{2-} during four weeks of storage at 10, 4 and -20 °C is displayed in Figure 29 - 30 and Table 22 , respectively (average and standard deviation, n=3). The total concentration of carbonic compounds, H_2CO_2 and HCO_3^- did not result in a statistically significant different with regards to the storage temperature and period. However, a slight variability in the average values of the total carbonic compounds and H_2CO_2 was observed with regards to the storage time, especially for PAW H-30 and L-30. Interestingly, while PAW H-30 and L-30 presented much lower concentrations of HCO_3^- than PAW H-10 and L-10 directly after activation, this trend was not obvious after 24 h when bicarbonate concentration of H-10 and L-10 decreased slightly and no specific trends could be observed for the different temperatures. Nevertheless, the levels of HCO_3^- were very low (nM range). Regarding CO_3^{2-}, no statistically significant differences were observed for all the different operating conditions with regards to the different storage temperatures or over time, although the concentrations were practically negligible (pM). Nevertheless, a slight decrease in the average levels was observed for PAW H-10 and L-10, with regards to storage time (from day 0 to 28). As the carbonic compounds work as a buffer in water, the concentrations are dependent on the alkalinity of the PAW (buffering capacity), and therefore ability to resist changes in pH, which can be seen in present work as the pH kept stable during the four weeks storage.

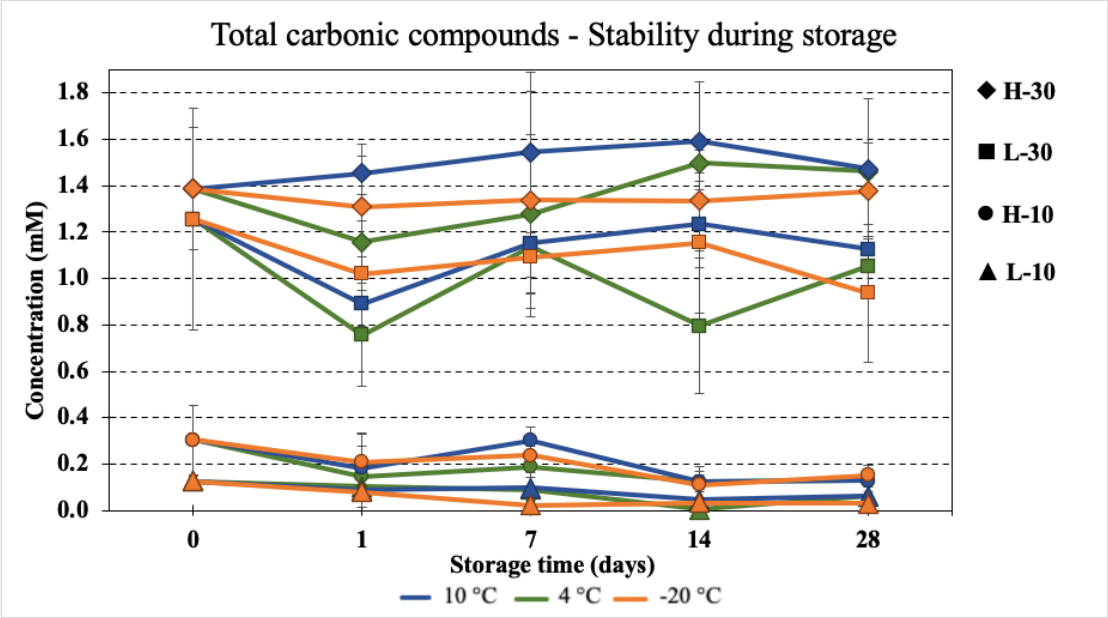

Figure 29. Stability of the total concentration of carbonic compounds in PAW during storage at 10, 4 and -20 ℃ as a function of the plasma power (25/35 W) and activation time (10/30 min) for 28 days storage, measured after 0 (directly after activation), 1, 7, 14, 21 and 28 days. Statistical analysis performed between PAW stored at different temperatures or between the weeks with a significant level set at 95 % (P≤0.05, n=3) (Numeric values in Appendix A)

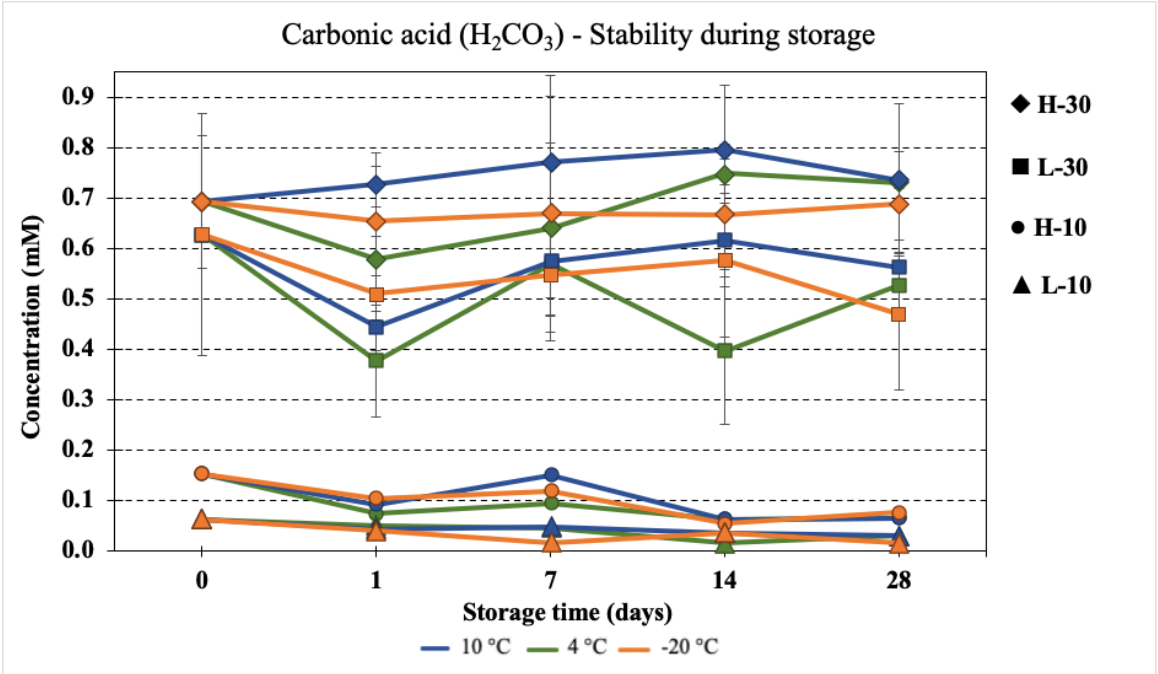

Figure 30 Stability of the concentration of carbonic acid in PAW during storage at 10, 4 and -20 ℃ as a function of the plasma power (25/35 W) and activation time (10/30 min) for 28 days storage, measured after 0 (directly after activation), 1, 7, 14, 21 and 28 days. Statistical analysis performed between PAW stored at different temperatures or between the weeks with a significant level set at 95 % (P≤0.05, n=3 (Numeric values in Appendix A)

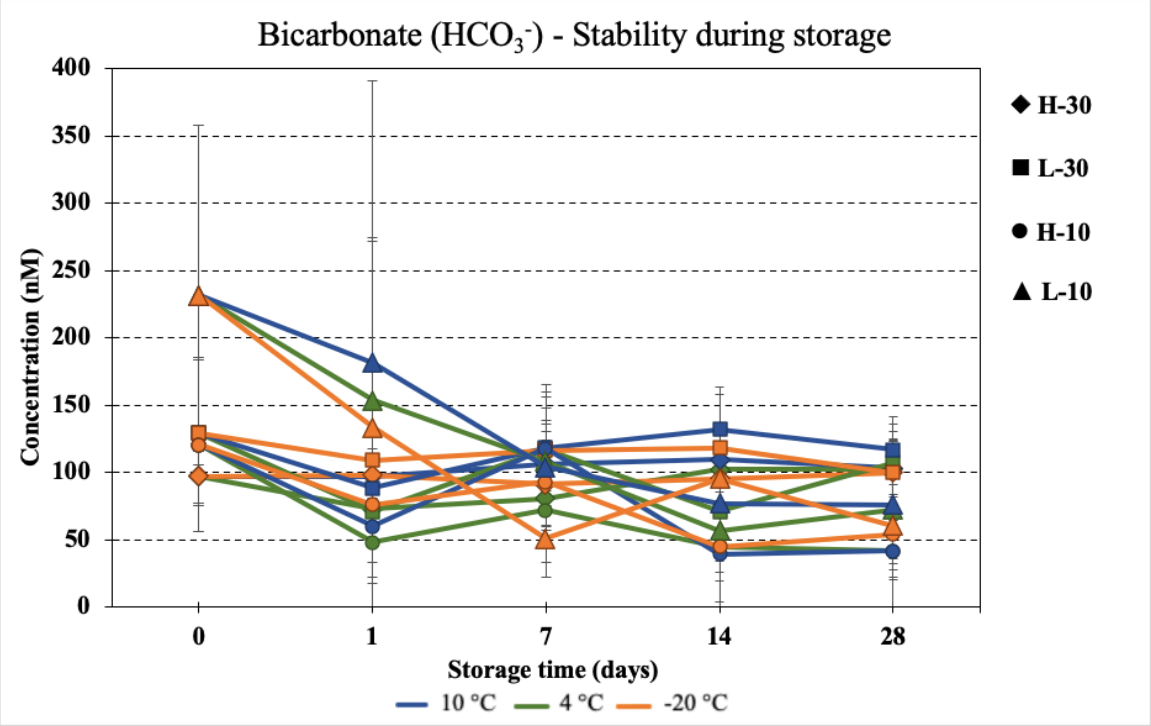

Figure 31. Stability of bicarbonate concentration in PAW during storage at 10, 4 and -20 ℃ as a function of the plasma power (25/35 W) and activation time (10/30 min) for 28 days storage, measured after 0 (directly after activation), 1, 7, 14, 21 and 28 days. Statistical analysis performed between PAW stored at different temperatures or between the weeks with a significant level set at 95 % (P≤0.05, n=3) (Numeric values in Appendix A)

Table 22. Stability of carbonate ion during storage at 10, 4 and -20 ℃ as a function of the plasma power (25/35 W) and activation time (10/30 min) for 28 days storage, measured after 0 (directly after activation), 1, 7, 14, 21 and 28 days. Statistical analysis resulted in no significant difference between PAW stored at different temperatures or between the weeks with a significant level set at 95 % (P≤0.05, n=3)

Concentration of carbonate (CO_3^{2-}), pM						
		0 D	1 D	7 D	14 D	28 D
H-30	4 ºC	1.9 ± 0.5	1.3 ± 0.4	1.4 ± 0.4	1.9 ± 0.2	2.0 ± 0.5
	10 ºC	1.9 ± 0.5	1.8 ± 0.2	2.0 ± 0.2	2.1 ± 0.2	2.0 ± 0.5
	-20 ºC	1.9 ± 0.5	2.0 ± 0.5	1.7 ± 0.7	1.9 ± 0.6	2.0 ± 0.7
L-30	4 ºC	3.7 ± 1.7	1.8 ± 0.7	3.3 ± 1.1	3.3 ± 0.9	3.4 ± 0.9
	10 ºC	3.7 ± 1.7	2.4 ± 0.4	1.8 ± 0.6	3.9 ± 1.3	3.3 ± 0.3
	-20 ºC	3.7 ± 1.7	3.2 ± 0.7	3.0 ± 1.6	3.3 ± 1.4	3.0 ± 1.2
H-10	4 ºC	13.3 ± 8.0	4.8 ± 1.4	7.8 ± 4.7	4.7 ± 3.9	3.8 ± 2.3
	10 ºC	13.3 ± 8.0	5.7 ± 2.2	12.7 ± 0.4	3.5 ± 0.05	3.7 ± 1.0
	-20 ºC	13.3 ± 8.0	8.6 ± 2.5	10.5 ± 7.5	5.2 ± 5.7	5.2 ± 2.7
L-10	4 ºC	152.5 ± 172.7	104.6 ± 146.4	40.8 ± 25.8	30.3 ± 37.8	26.2 ± 19.1
	10 ºC	152.5 ± 174.7	175.3 ± 278.9	31.8 ± 14.4	24.0 ± 7.0	30.9 ± 28.4
	-20 ºC	152.5 ± 172.7	99.1 ± 150.9	22.9 ± 20.8	41.2 ± 30.4	37.0 ± 57.9

4.3 PAW for Inactivation of *Listeria. monocytogenes* on baby spinach leaves

4.3.1 Inactivation of *L. monocytogenes* in cell suspension

The inactivation of planktonic cells of *L. monocytogenes* by different types of PAW and PAW combined with US bath compared to tap water was assessed, all types of water used for treatment was at 4 °C. The purpose of these trials with planktonic cells was to optimize the operating conditions (i.e. type of PAW, treatment time, potential of synergistic effect with US) for inactivation of *L. monocytogenes* in light of further decontamination experiment with baby spinach. Figure 32 shows the bacterial concentration (cfu/mL) after treatment with tap water, PAW L-10 (large system before maintenance), PAW_IB and PAW H-30* (large system after maintenance) for 5, 15 and 30 min, including HS-30 (small system) for 5 min treatment, with an initial concentration of $2.05 \times 10^7 \pm 2.1 \times 10^6$ cfu/mL (average and standard deviation, n=2). Such high concentration is not realistic in fresh produce, however, to demonstrate the extent of reduction in challenge organisms it is usually necessary to use a high inoculum lever (e.g. 10^6 or 10^7 cell/g of product). Typically, validation protocols require the plating method, which has a detection limit of 10^2 cfu/mL, thus the inoculum level must be at least 10^6 to measure the extent of reduction within statistical limits of this enumeration method [171]. The treatment times used in these trials are chosen as 5 min treatment is the reasonable value for industrial rinsing of fresh produce, while 15- and 30-min treatments are abusive values to explore the antimicrobial activity of PAW. In addition, 15- and 30- min treatment could give an indication about the potential of using PAW as a disinfectant for food contact surfaces, seeing as for these applications the treatment times are often longer.

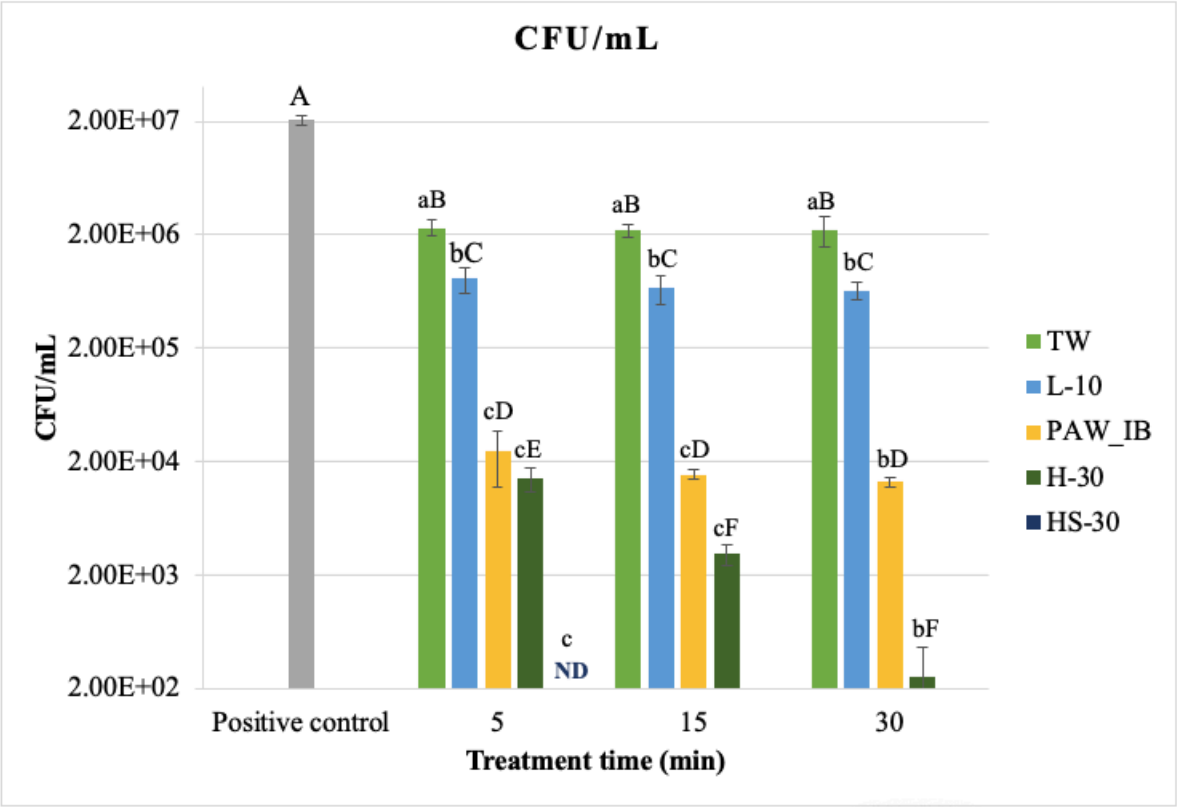

Figure 32. The bacterial concentration of L. monocytogenes in cell suspension after treatment with tap water (TW), PAW L-10, PAW_IB and PAW H-30 for 5, 15- and 30-min. Including HS-30 for 5 min treatment. Statistical analysis preformed for each water where different upper-case letter resents significant difference in regard to the treatment times, while the lower-case letters represent each treatment time, indicating significant differences between the different types of water ($P \leq 0.05$, $n = 3$) (numeric values in Appendix B)

With regards to the positive control, the treatment with tap water resulted in approximately a 1 log reduction after 5 min treatment, and did not increase with longer treatment time, thus there was no statistically significant difference in regard to the different treatment times (Figure 32). Furthermore, treatment with PAW L-10 gave approximately a 1.5 log reduction, a statistically significantly higher log reduction for each treatment time compared to treatment with tap water, however, likewise as with tap water there was no significant difference between the different treatment times when treated with PAW L-10. PAW_IB resulted in an even higher reduction of approximately 3 logs for 5 min treatment, which increased slightly for 15- and 30-min treatment (approximately to a 3.2 log reduction). This reduction was statistically higher than both tap water and L-10 for 5- and 15-min treatment, however, not for the 30 min treatment. Nevertheless, from Figure 31 it is clear that the PAW_IB did result in a higher log reduction for 30 min treatment than with tap water or L-10. Comparing treatment with PAW_IB for 5, 15 and 30 min resulted in no significant difference. Treatment with PAW H-30* gave the most pronounced drop between the treatments time 5, 15 and 30 min, with a reduction of

approximately 3.2, 3.8 and 4.8 log, respectively. Additionally, there was a statistically significant difference observed between 5 min treatment and 15 / 30 min treatment. For each treatment time, PAW H-30 had a significant difference to treatment by tap water and L-10, and although an increase in log reduction can be observed compared to PAW_IB as well, there was no significant difference between these types of PAW. The characterization of the different types of PAW shows that the H-30 has a lower pH, higher ORP and a higher concentration of nitrogen compounds than L-10 and PAW_IB, thus indicating that these factors have an impact on the antimicrobial effect. On the other hand, the PAW_IB have a much higher concentration of hydrogen peroxide, which indeed has been attributed to have a great antimicrobial effect, nevertheless in present work it does not seem to play such an important role as the H-30* did result in a higher log reduction with lower concentration of hydrogen peroxide present.

Moreover, the most effective treatment was with PAW HS-30 which gave such a log reduction that it was below the detection limit (10^2 cfu/mL) (Figure 32) . Interestingly, the main difference in PAW HS-30 compared to H-30* is the nitrite and nitrate concentration, which is much higher in HS-30, thus suggesting that the nitrites/nitrates may have an essential role in regard to the antimicrobial activity. In addition, the hydrogen peroxide concentration was somewhat higher in HS-30 than in H-30* (7.69 ± 0.91 and 0.35 ± 0.05 mg/L, respectively), nevertheless, much lower than in PAW_IB (142.6 ± 5.5 mg/L). Similar to present work, Baek et al. (2020) [172] conducted a study with plasma activated fine droplets (PAD) produced from arc discharge plasma on *L. monocytogenes* and *E. coli* O157:H7 resulting in a 0.58 and 3.1 log reduction of *L. monocytogenes* concentration after 1 and 5 min respectively. For the *E. coli* O157:H7 a 4.14 log reduction was reported after 1 min, but no additional decrease with a longer treatment time, thus suggesting that the *E. coli* O157:H7 was more susceptible to PAD than *L. monocytogenes,* possibly due to the different outer structures of the gram positive and gram negative cells. Nevertheless, PAD treatment did disrupt both the outer cell wall and the membrane of both *E. coli* and *L. monocytogenes* causing deformation and leakage of the cell. Similar to the increase in reduction from 5 to 30 min for treatment with H-30* in present work, Kamgang-youbi et al. (2009) [61] reported a 50% and 75% antimicrobial reduction after application time of 5 and 20 min, respectively. Furthermore, Smet et al. (2019) [173] conducted experiments with *L. monocytogenes* and *S. thypimurium* (gram negative) exposed to plasma activated liquid (PAL) made generated using helium with 0 or 1% oxygen as feeding gas. Similar to Baek et al. *L. monocytogenes* proved to be the most resistant to PAL treatment, as well as biofilm being more resistant than platonic cell. Additionally, Smet et al. reported that the PAL generated with

oxygen in the feeding gas and longer activation time resulted in a higher inactivation efficiency, as well as a higher concentration of reactive species and a higher drop in pH, thus further indicate the relationship between antimicrobial efficiency and reactive species. Likewise, Matan et al. (2015) [138] reported findings of completely reducing the growth of *E. coli*, *S. typhimurium*, and *L. monocytogenes* on the surface of inoculated fresh cut dragon fruit by approximately 5.6 log cfu/g with PAW generated with a plasma jet and Ar as the feeding gas.

To mimic industrial settings with regards to the rinsing of fresh produce, *L. monocytogenes* was treated for 2.5 + 2.5 min with the rinsing media being renewed between treatments, the water used for rinsing was 4 °C. Figure 33 displays the result for two subsequent treatments of 2.5 min (2.5 min x2) and 5 min treatment (average and standard deviation, n=2) for tap water, PAW H-30* and PAW HS-30. The 2.5 min x2 treatment was more effective for tap water as compared to tap water treatment for 5 min (approximately 3 and 1 log, respectively), nevertheless, statistically, there was no significant difference. Additionally, for H-30* there was no significant difference between the 5 min treatment and the 2.5 min x2 treatment, a small decrease in the average concentration can, however, be noticed for the 2.5 min x2 treatment. The concentration of *L.* monocytogenes treated with HS-30 was not detectable for either the 5 min or the 2.5 min x2 treatment. Thus, PAW HS-30 shows a great potential to replace tap water and reduce the number of rinsing steps. Future research could also investigate whether PAW HS-30 could be used for shorter times, resulting in the same efficacy. Additionally, it would be interesting to further investigate the isolated effect of pH and the different RONS compared to the synergistic effect of PAW. Already in the literature, Naitali et al. (2010) [62] conducted an experiment on the isolated effects of the reactive species and an acidified environment for inactivation of *Hafnia alvei*, nevertheless, findings showed that the synergic effect the reactive species has together with low pH and other parameters in PAW resulted in a higher log reduction than any of the other isolated treatments. Thus, suggesting that the synergistic effect of all parameters and reactive species is indeed more efficient than the isolated effect when using PAW as a disinfectant, however, more research is required.

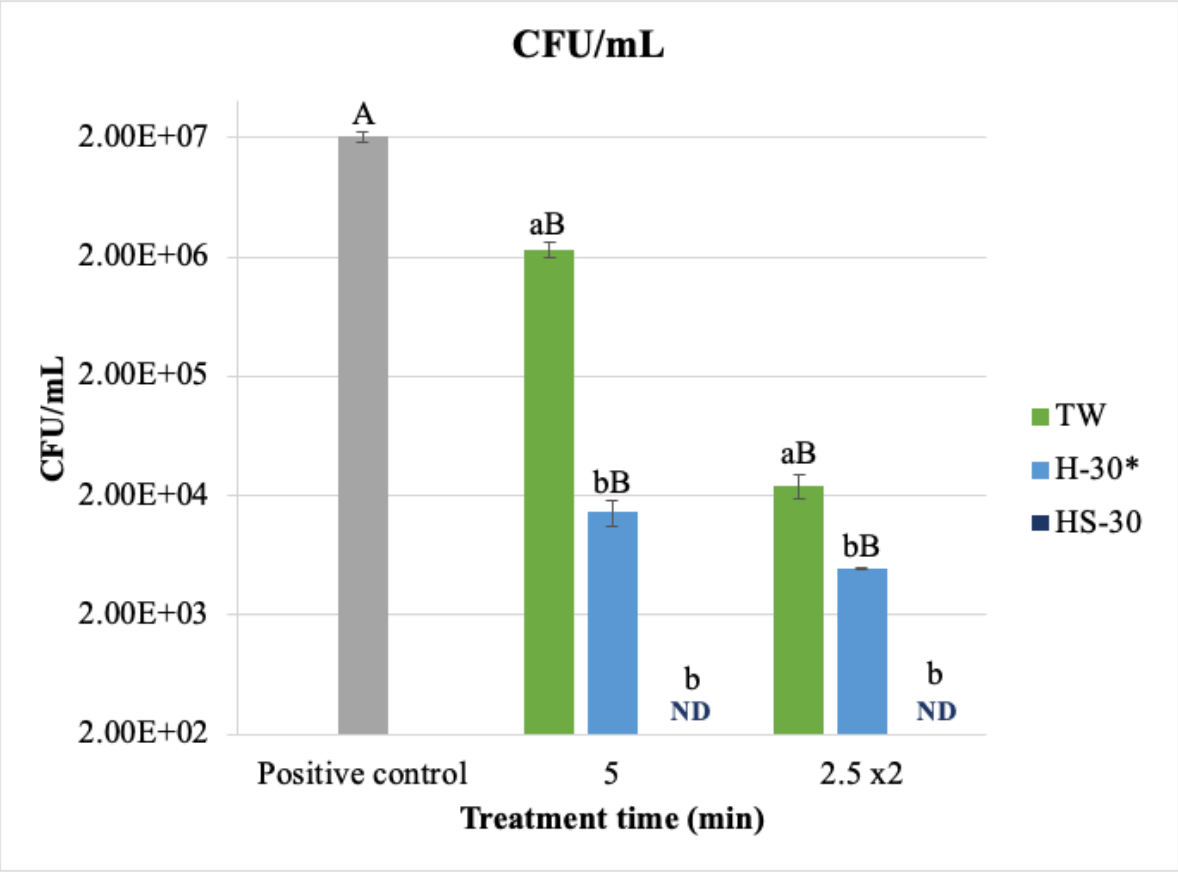

Figure 33. Concentration of L. monocytogenes after treatment with tap water, PAW H-30 and PAW HS-30 for 5 min or two subsequent treatments of 2.5 min. Statistical analysis preformed for each water where different upper case letter resents significant difference in regards to the treatment times, while the lower case letters represent each treatment time, showing significant differences between the different types of water (P≤0.05, n = 3) (Numeric values in Appendix B)*

Ultrasound waves are sound waves with a frequency ranging from 20 kHz to 10 MHz and can be further divided into subdivisions based on the frequency they are generated at. The high-energy low frequencies US are often used in food technologies and has been proven useful for several food applications, e.g. processes as drying, freezing, sterilization, filtration and cooking [174]. Especially for pasteurization in the dairy industry it has been proven effective for the removal of *E. coli, P. fluorescens* and *L. monocytogenes* without damaging the total protein content [175]. At low frequencies, the effect caused by unstable cavitation predominates, and the bubbles collapse with increasing violence as the frequency approaches 20 kHz [27].

In the present work (Figure 31), the effect of PAW H-30* and tap water combined with US treatment on the concentration (cfu/mL) of *L. monocytogenes* (average and standard deviation, n=2) was determined. Two US conditions were tested, either a frequency of 68 kHz or a dual frequency of 68/170 kHz, with a power of 500 and 1000 W, respectively, both for a 5 min

treatment time, with the PAW and tap water being tempered to 4 °C and the temperature in the US bath being 8-10 °C. The initial concentration of *l. monocytogenes* was 10^7 cfu/mL indicating that the cell suspension treated with tap water experienced approximately 2.8 log reduction (for both conditions) (Figure 31), while the cell suspensions treated with tap water for 5 min without the US treatment only gave approximately a 1 log reduction (Figure 32). In addition, the PAW H-30* treated in the US bath gave approximately a 3.4 and 3.5 log reduction for the 68 kHz frequency and the dual frequency, respectively. The cell suspension treated with H-30* for 5 min without the US treatment had approximately a 3.2 log reduction, thus the reduction was slightly larger for the treatment with PAW together with the US treatment, nevertheless, not large enough to conclude that there is a synergic effect between PAW and US. Furthermore, for the dual frequency there was a statistically difference between the tap water as compared to PAW H-30*, yet for the use of 68 kHz frequency there was no significant difference between the types of water (Figure 34). Mason et al. (2003) [176] conducted an experiment with a push-pull system on *bacillus subtilis* in water and suggested that to inactivate the *b. subtilis* it would have to be treated with ultrasound for a long time, after 60 min 73 % of the viable bacteria were destroyed or inactivated. Such long treatment times are not realistic when dealing with fresh produce. On the other hand, Royintarat et al. (2020) [177] reported an increase in log reduction from the synergistic effect of PAW and the US (40 Hz and power output of 220 W) compared the techniques alone. For this trial H-30* was chosen as the PAW to be tested as it is generated with the larger system and therefore has a higher production capacity as compared to the small system (HS-30). Nevertheless, the inactivation obtained with the HS-30 resulted in no detectable viable bacteria after 5 min treatment, thus giving much better values than using H-30* combined with the US.

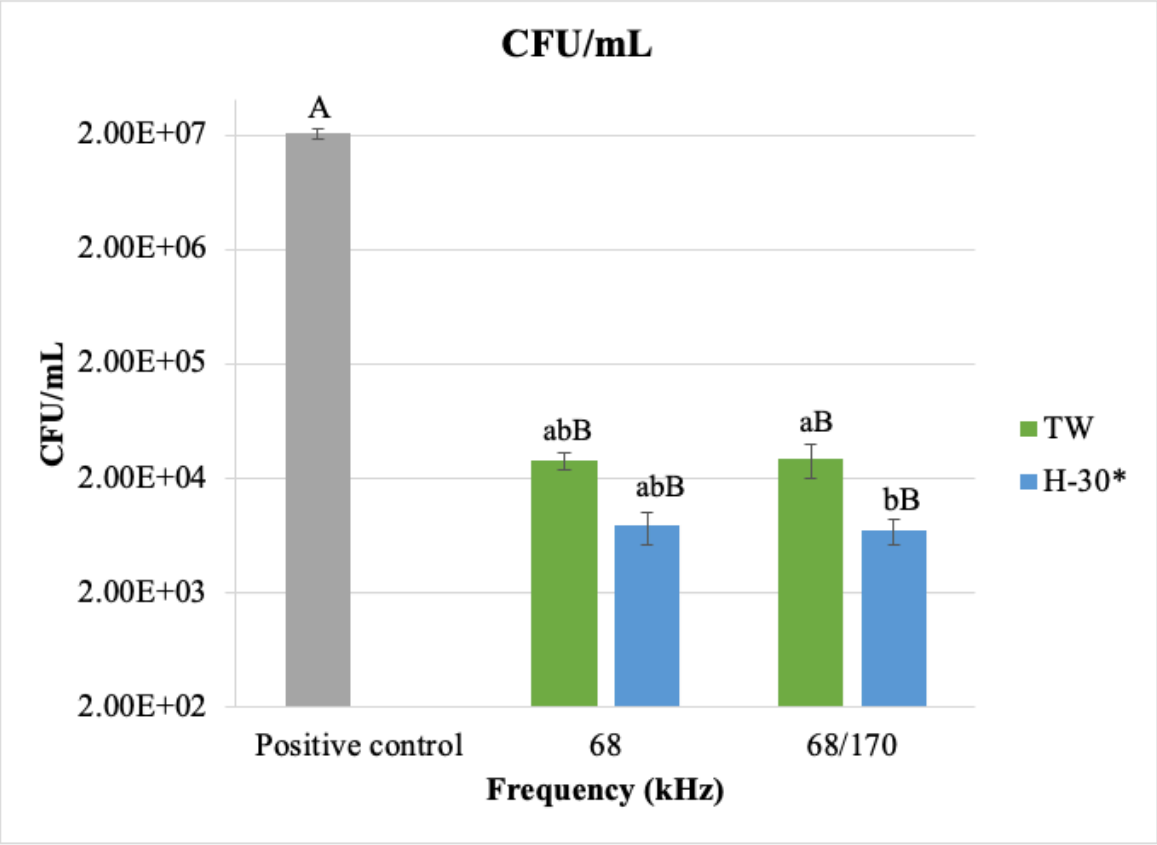

Figure 34. Concentration of L. monocytogenes after 5 min treatment of tap water (TW) and PAW HS-30 (PAW) in the US bath with a frequency of 68 and dual 68/170 kHz, corresponding to a power of 500 and 1000 W, respectively. Statistical analysis preformed for each water where different upper-case letter resents significant difference in regard to the frequency used, while the lower-case letters represent each treatment time, indicating significant differences between the different types of water for the same treatment time. (P≤0.05, n = 3) (Numeric values in Appendix B)

4.3.2 Inoculation tests for baby spinach leaves

Although due to *major force*, *L. monocytogenes* inactivation trials on baby spinach leaves were dismissed, sample settings and inoculum size were optimized, as described hereafter. The predominant size of baby spinach leaves in a commercial bag of baby spinach leaves was determined (Figure 35). The leaves were sorted into small, intermediate and big size categories, with the intermediate leaves being the predominant size. Subsequently, each intermediate-size leaf was weighed and several 5 g batches were prepared (Table 23) in order to determine the number of leaves per batch, so that the sample area for surface inoculation with *L. monocytogenes* was about the same in each batch (Figure 35).

Figure 35. Baby spinach leaves sorted into 3 groups based on their size; small (lower row), intermediate (two middle rows) and big (upper row)

Table 23. Weight and number of intermediate-size leaves in 3 different 5 g batches.

	Batch 1	**Batch 2**	**Batch 3**
Sample nr.	Weight (g)	Weight (g)	Weight (g)
1	0.53	0.66	0.63
2	0.52	0.54	0.39
3	0.51	0.52	0.75
4	0.60	0.78	0.60
5	0.51	0.62	0.86
6	0.90	0.48	0.44
7	0.78	0.59	0.74
8	0.71	0.86	0.70
Total:	5.06	5.05	5.11
Average of total weight + SD:			5.07 ± 0.03

To achieve a total weight of approximately 5 g in each batch, 8 intermediate-sized leaves were needed (Table 23). The average weight of the three batches being 5.07 ± 0.03 g, while the average weight of each leaf was 0.63 ± 0.14 g. Additionally to getting similar weight, the surface of each leaf was also taken in consideration when sorting leaves into batches. This was to get equally large surface area to inoculate, in order to achieve approximately the same initial concentration of *L. monocytogenes*. Figure 36 demonstrates the surface area of the three batches corresponding to the weight listed in Table 23.

Figure 36. Three batches of baby spinach leaves with similar weight (5 g) and surface area

Furthermore, the inoculation procedure to achieve an initial concentration of *L. monocytogenes* of 10^7 cfu/g onto the baby spinach leaves was optimized. As mentioned in section 4.3.1, such a high inoculum size is not representative of the contamination levels in ready-to-eat fresh produce, but typically established in challenge tests to quantify bacterial log-reductions within the detection limit of the analytical enumeration technique (viable plate counting). From literature, several causes of fresh produce contaminated levels with *L. monocytogenes* has been documented. An assessment of lettuce in restaurants and at home determined a concentration of 0.15 and 1.05 log cfu/g, respectively [124]. Also, research on market vegetables showed *L. monocytogenes* contamination in 3.1% of the samples, where five salad samples had contamination levels of between 1.0×10^1 and 2.6×10^2 cfu/g [178]. The contamination of *L. monocytogenes* in fresh produce and ready-to-eat foods are a major concern for the food industry today. Food that are kept for a long period of time at low temperature poses a risk as *L. monocytogenes* can grow under refrigerated conditions and the microbiological limit throughout the shelf-life is 100 cfu/g for the food to be regarded as safe for consumption [179]. Ready-to-eat food that support the growth of *L. monocytogenes* are those that have a high pH (<5), high water activity (≥0.92) and have a long shelf-life (≥10 days), RTE meat and poultry, fresh produce and dairy products fall under this category [180]. In Table 24 the final concentration of *L. monocytogenes* on three 5 g batches of baby spinach leaves is listed, where the surface of each leaf (8 leaves per batch) was inoculated with 100 µL of either a direct 1:10 dilution (v/v) or 2:3 dilution direct or where the stationary phase cells were recovered before dilution (v/v) of the bacterial suspension in the stationary phase of growth (10^9 cfu/mL). The final concentration of *L. monocytogenes* on the batches inoculated with the 1:10 dilution was $2.71 \times 10^6 \pm 1.86 \times 10^5$ cfu/g, while $6.35 \times 10^6 \pm 6.35 \times 10^6$ cfu/g was achieved on the samples

inoculated with the 2:3 dilution, listed in Table 24. The variability in the final concentration of *L. monocytogenes*, especially for the 2:3 dilution, could be attributed to the variability in the sample size/weight, which further lead to variability in surface inoculation for each batch. Furthermore, the variability in cell recovery during stomaching, as well as the innate variability in the dilutions and viable plating methods could have an effect on the final concentration. Interestingly, for the batches inoculated with the 2:3 dilution after centrifugation of the stationary phase cells, viable counts were not detected on the lowest dilution plated (1:1000), which means that the final concentration on the baby spinach leaves was lower than 10^5 cfu/mL. This lower concentration of *L. monocytogenes* cells when the inoculum is centrifuged before the dilution step can be attributed to the loss of cells when removing the supernatant from the pellet.

Table 24. Concentration of L. monocytogenes achieved in three 5 g batches of baby spinach leaves using a dilution 1:10 and 2:3 (with/out centrifugation),

	Dilution		
Batch	1:10	2:3	2:3 (centrifuged)
B1	2.86×10^6	8.08×10^6	$< 10^5$
B2	2.76×10^6	4.72×10^6	$< 10^5$
B3	2.50×10^6	6.26×10^6	$< 10^5$
Average	2.71×10^6	6.35×10^6	
SD	1.86×10^5	1.68×10^6	

4.4 Effect of PAW for decontamination of seaweed

4.4.1 Seaweeds washed with tap water and EDTA

The purpose of these trials was to assess the efficacy of different preservation strategies on the microbial levels on *L. hyperborea*, namely 0.1 M EDTA (disodium salt dihydrate), PAW and tap water (TW) at 4℃, alone and in combination with ultrasonic (US) treatment (68/170 kHz, 1000 W) for different exposure times (5-60 min range). The seaweed samples were harvested at Frøya (Norway) on 20th January 2020 (batch #1) and 12th February 2020 (batch #2), transported overnight to Nofima in seawater under refrigerated conditions, and treated immediately after reception. Noticeable variability between batch #1 and batch #2 with regards to surface epiphytic biofouling is illustrated in Figure 38 which may be attributed to differences in harvesting deployment and the time elapsed between batches (3 weeks), both affecting local weather and thus, extrinsic macroalgal conditions (e.g. temperature) and microbial proliferation [181]. Bacterial numbers from 10^1 to 10^8 /cm^2 are reported in literature, often with a higher number in warmer waters, additionally does cell density vary for different macroalgae species

[146, 182, 183]. Specifically for *L. hyperbolea,* Bengtsson et al. (2010) [183] findings show that the biofilm density was highly affected by the season and resulted in the lowest density of 8.3 x 10^2 cells cm^{-2} in March, whilst non growing kelp in July to February had a density of approximately 1.0 x 10^7 cells cm^{-2}. Moreover, the differences after visual inspection were also reflected on the total bacterial concentration on untreated samples (Figure 37 - Figure 40), with average values of ≈10^4 and ≈10^5 cfu/g for batch #1 and #2, respectively. It is noteworthy that lactic acid bacteria and aerobic/anaerobic spores were not detected on untreated samples. Figure 37 shows the total bacterial concentration on untreated samples (batch #1), right after reception (day 0) and after 1, 2 and 3 days of storage at 4 °C. There is no significant difference in bacterial concentration after 1, 2 or 3 days, however, from considering the microbial stability at least during 72 hours after reception, it is assumed that the 48-hour refrigerated transport did not affect significantly the bacterial load in the samples.

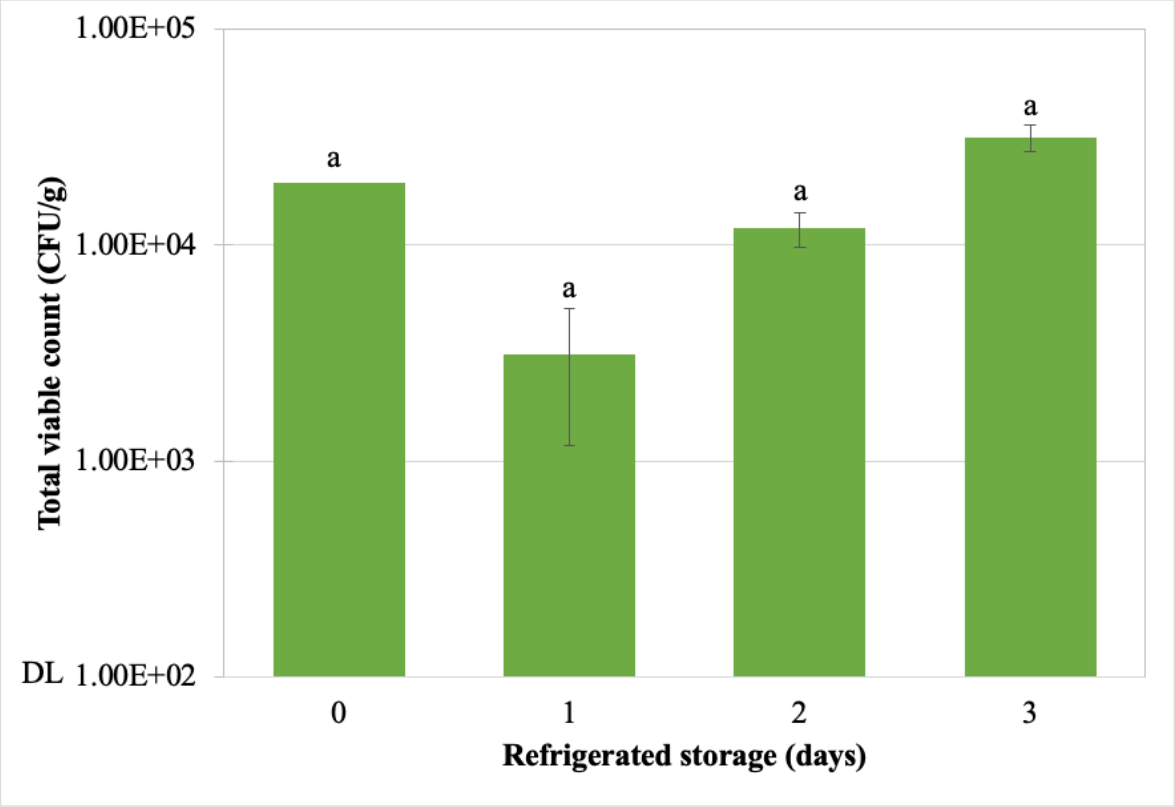

Figure 37. Total bacterial concentration of untreated (UT) seaweeds (batch #1) on the day of reception (24 hours after harvesting) and after 1, 2 and 3 days of storage at 4 ℃. Statistical analysis was performed and the lower case letters represent the significant difference between the total viable count and the storage days with a significant level set at 95% (n=2, P≤0.05) (Numeric values in Appendix C)

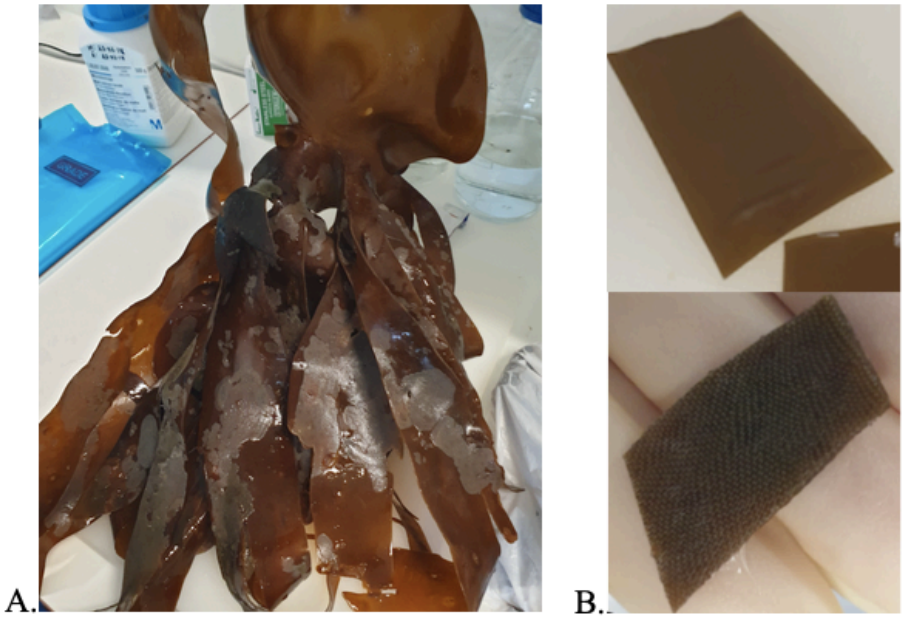

Figure 38. A) Seaweed Batch #2 B) Surface of seaweed from batch #1 (top) and seaweed from batch #2 (bottom)

Figure 39 displays the total viable counts (average and standard deviation, n=2) on seaweed samples (batch #1) treated with TW (5, 15, 30 & 60 min) and EDTA (30 & 60 min) at 4℃, alone and in combination with US (30 & 60 min) at 68/170 kHz and 1000 W. While the 5 and 15 min treatments with TW resulted in about 1 log reduction as compared to untreated samples, no detectable bacterial levels on samples treated with TW or EDTA, alone or in combination with US treatment (> 2 log reductions; detection limit 10^2 cfu/g) were obtained for longer treatment times (30 & 60 min). It would be interesting to further assess the effect of TW/US, EDTA and EDTA/US on microbial levels for shorter treatment times, as well as the impact on seaweed quality attributes (e.g. texture, color).

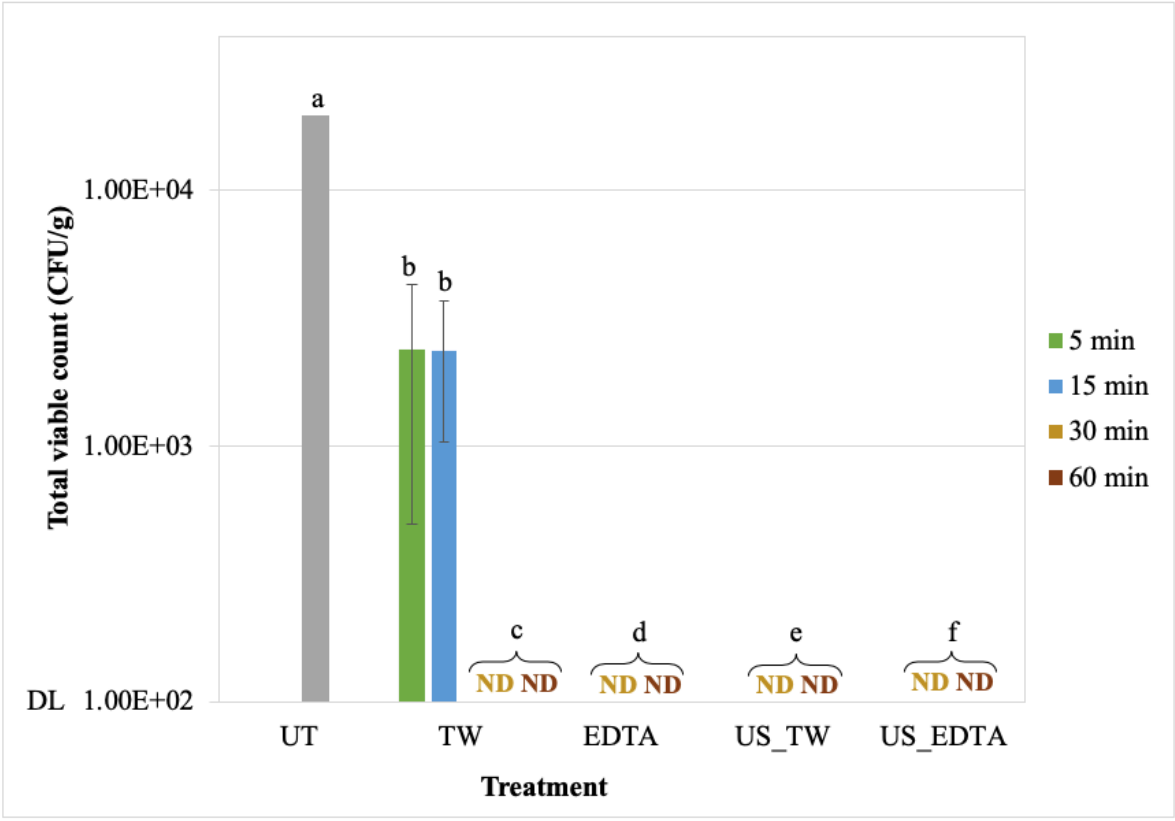

Figure 39. Effect of different preservation strategies on macroalgal samples: TW (5, 15, 30 & 60 min) and EDTA (30 & 60 min) alone or in combination with US (30 & 60 min) at 68/170 kHz and 1000 W. Statistical analysis was performed and the lower case letters represent the significant difference between the total viable count and the treatment times with a significant level set at 95% (n=2, P≤0.05) (Numeric values in Appendix C)

4.4.2 Seaweeds washed with tap water and PAW

As above mentioned, the surface of macroalgal biomass from batch #2 was severely affected by epiphytic biofouling, which resulted in a significant increase in bacterial levels and innate biological variability of individual samples, both influencing preservation efficacy. Moreover, bacteria associated/entrapped in biofilm structures typically present higher resistance to disinfection strategies than planktonic state cells [173]. Since severe biofouling reduces the value of macroalgal harvests (not fit for human consumption), management biofouling strategies include shortening the harvest season, relocating harvest sites/farms or alternatively redirecting the algal biomass towards low-value markets, all with a significant socioeconomic impact on the sector [184-186]. Thus, the decontamination potential of PAW (L-10 and L-30) and TW at 4 °C alone or in combination with US at 68/170 kHz was assessed for 30 min (realistic on-board processing time) on batch #2 samples and the results (average and standard deviation, n=2) are presented in Figure 40. Seaweed treated with the PAW L-10 resulted in approximately one log reduction, whilst the synergistic effect of L-10 and US resulted in a

significantly higher reduction of 2 log. On the other hand, the seaweed treated with the PAW L-30 showed no difference in the bacterial concentration in compared to the untreated samples, suggesting that this sample might have had a higher initial bacterial concentration, perhaps covered in more seasonal epiphytic biofouling. The average bacterial concentration of the L-30 together with US treatment did result in approximately a 1.7 log reduction. Nevertheless, there was statistically no significant difference between L-30 with or without additional US treatment, possibly because the standard deviation of the L-30 + US was larger than the value itself. The tap water treatment of seaweed resulted in the approximately a 4 log reduction, which was a higher average log reduction than the tap water combined with US, which was approximately 0.9 log. Again, this could be due to a higher initial concentration of bacteria and a higher coverage of season epiphytic biofouling, nevertheless, there was no significant difference between the Tap water with or without US treatment. Additionally, with regards to the different water media, used for treatment neither US nor no US resulted in a significant difference. Currently, to the authors knowledge there is very little in the literature specifically about using PAW for decontamination of macroalgae. However, Nisol et al. (2018) [149] reported great effectiveness in reducing viable cells of harmful green algae (*Scenedesmus*) when treated with PAW generated with HC discharge in Ar/O_2. Additionally, Puligundla, Kim & Mok (2015) [150] and Kim, Puliggundla & Mok (2015) [151] both conducted studies on dried laver, with low pressure ait plasma and atmospheric pressure corona discharge plasma jet, respectively, and reported over 1-log and 2 log (99%) reduction in viable cell count of aerobic bacteria was observed over a 20 min period, respectively. Other methods that has potential to be effective for decontamination of seaweed is e.g. targeted microbial ensilage additives for seaweed storage or dewatering methods to increase dry matter content [187, 188].

Finally, based on the L-10 and L-30 treatments, it indicates that the synergistic effect of US combined with PAW possibly has a positive effect in increasing the log reduction of bacterial concentration. US has been proven an effective green decontamination method, especially combined with other decontamination methods [189], thus the synergistic effect of the methods together could have great potential. Nevertheless, with the uncertainties in regard to initial bacterial concentration, the amount of seasonal epiphytic biofouling covering the macroalgae and the small number of samples analyzed, more research with additional samples and over several season would be interesting to get a more definite conclusion.

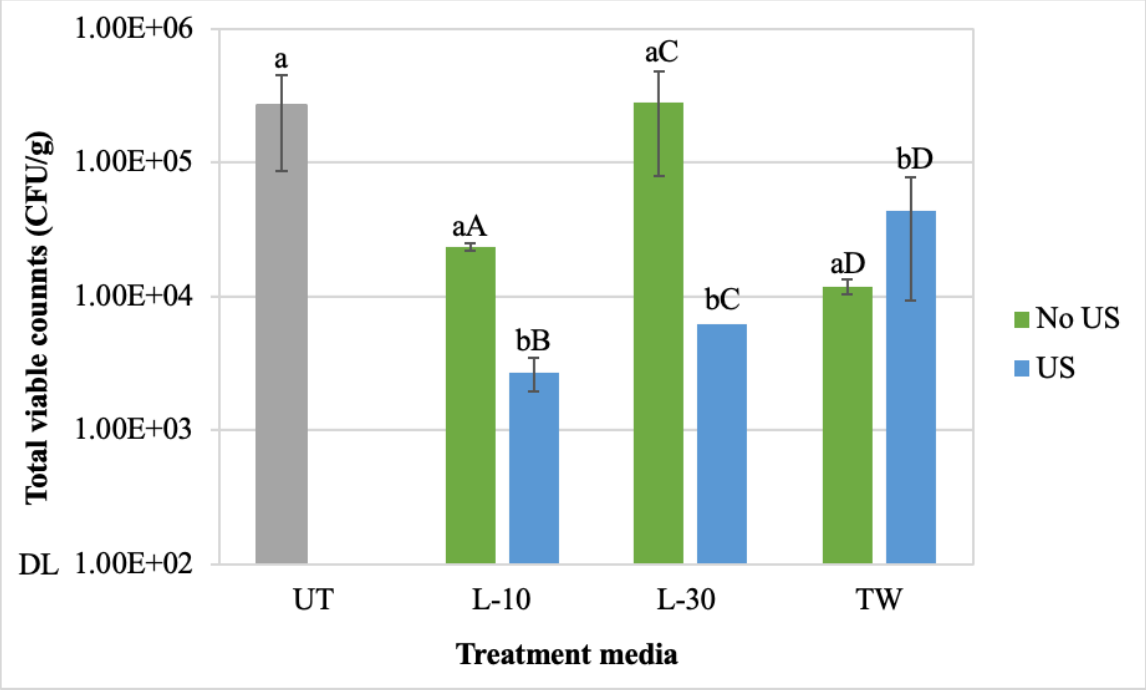

Figure 40. Effect of different preservation strategies on macroalgal samples: TW and PAW (L-10 and L-30) at 4 ℃ for 30 min, alone or in combination with US at 68/170 kHz and 1000 W. Statistical analysis was performed and the lower case letters represent the significant difference between the different treatment media either combined with US or not, whereas the upper-case letters represent significant difference for each treatment with a significant level set at 95% (n=2, P≤0.05). The L-30 treatment combined with US resulted in such large standard deviation (larger than the value itself) that it is not included on the logarithmic graph (negative values not allowed) (Numeric values in Appendix C)

4.5 Effect of PAW as a fertilizer for tomato plants

Different trials were conducted to assess the potential of PAW as a fertilizing agent on tomato plants. The purpose of those trials was to (1) assess the effect of PAW generated under different operating conditions (plasma power and activation time) on plant growth; (2) to evaluate the isolated effect of RONS (nitrogen compounds and hydrogen peroxide) on plant growth and (3) to unravel a potential synergistic effect of PAW combined with a multi-nutrient solution on plant growth. Table 16 in section 3.2.4 an overview of the conditions of PAW used for the different tomato trials.

4.5.1 Effect of PAW generation conditions (plasma power and activation time) on tomato plant growth

As described in section 3.2.4, the purpose of this trial was to compare the growth of tomato plants (*Solanum lycopersicum* cultivar Heinz) sown in vermiculite substrate and watered at different time intervals (after 8, 14, 21 and 28 days of incubation) with tap water (TW; control)

and PAW generated under the conditions of plasma power and activation time characterized in section 4.1 (L-10, L-30, H-10 and H-30), with no addition of multi-nutrient solution. Figure 41 represents the length of the plants (average and standard deviation, n=5) during 28 days of incubation with a regime of 16 h light followed by 8 h dark. Statistically significant differences were not found in the length of the plants watered with PAW, independently of the generation conditions. However, already at day 8, a significant increase in stem length was noticed for the PAW treated samples compared to the plants watered with tap water (control).

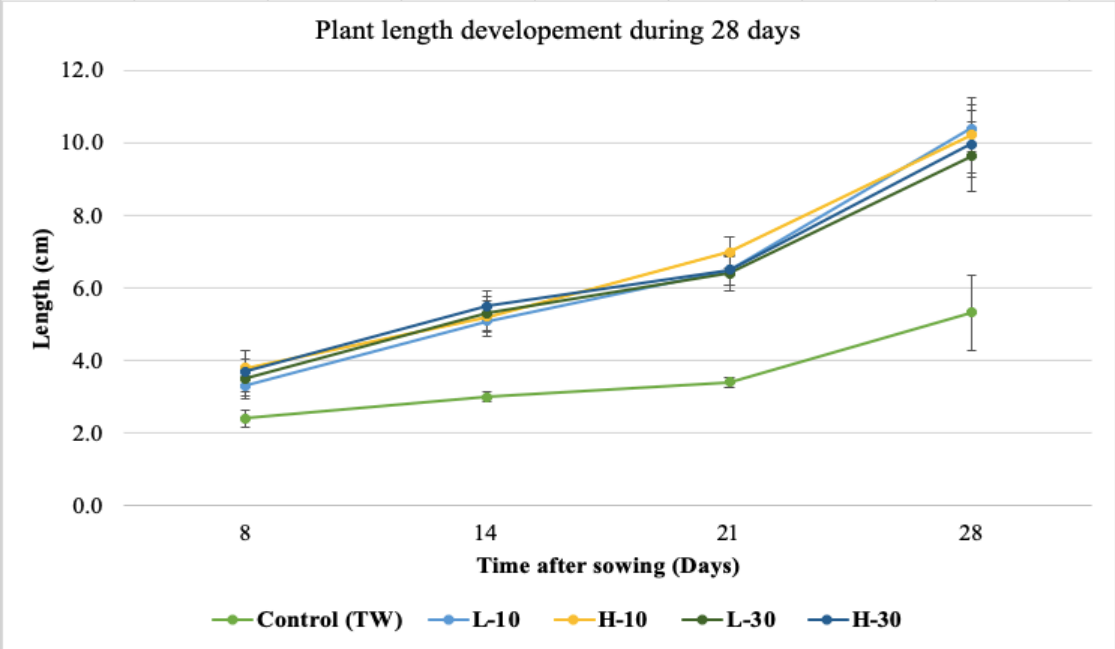

Figure 41. Length (cm) of tomato plants watered with PAW (L-10; H-10; L-30; H-20) and tap water (TW) once per week for 28 days incubation. Statistical analysis was performed for the length of the different plants comparing the effect of different PAW every week with a significance level of 95 %, (n=5, P≤0.05)

Figure 42 shows the development of the tomato plants after 8, 14, 21 and 28 days of incubation. The difference between PAW treated plants and control plants (TW) can be appreciated at first glance at day 14 after sowing, as the height of the PAW-treated plants was higher and the leave surface larger, with all of the plants showing a light green color. However, on day 21 the PAW plants exhibited a darker green color that can be observed even more vividly on day 28. After the 28 days the average length and standard deviation for the control plants, L-10, H-10, L-30 and H-30 was 5.32 ± 1.03, 10.4 ± 0.65, 10.22 ± 1.03, 9.64 ± 0.96 and 9.98 ± 0.94 cm, respectively.

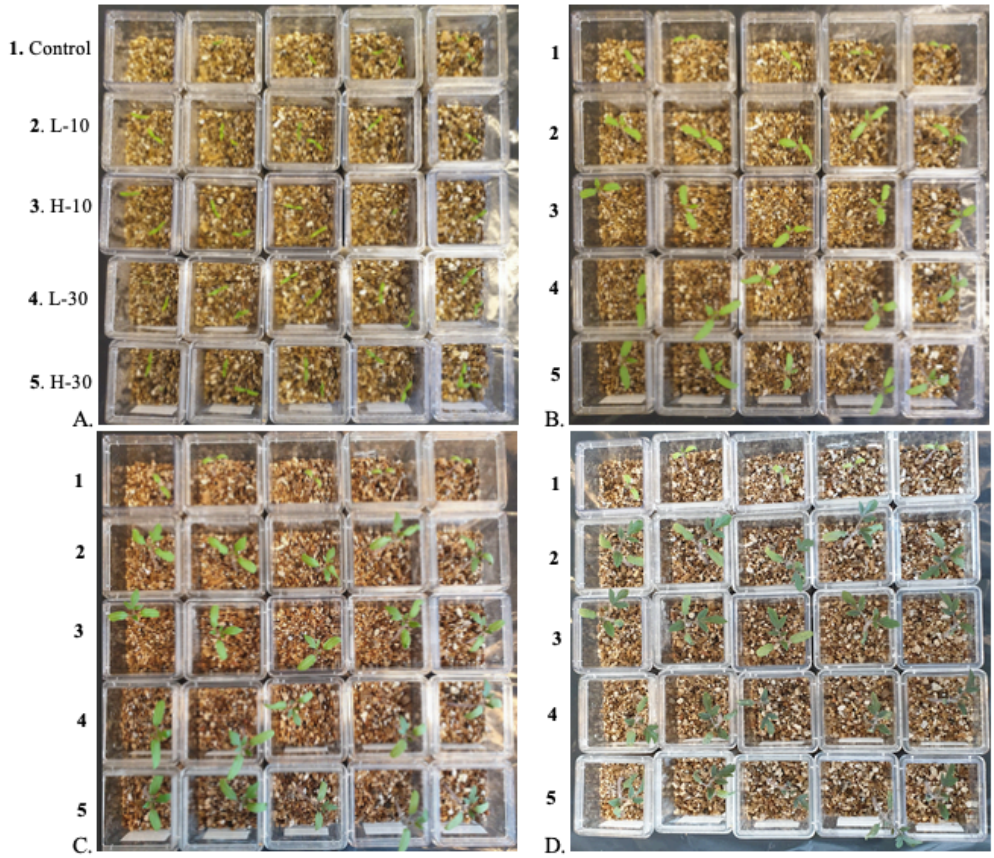

Figure 42. The development and growth of tomato plants (n=5) watered with tap water (1. Control) and PAW (2. L-10; 3. H-10; 4. L-30; 5. H-30) once per week during a 28-day incubation period: A) 8 days; B) 14 days; C) 21 days and D) 28 days after sowing

Furthermore, Figure 43 represents (average and standard deviation, n=5) of the individual and cumulative (A) length of root and stem and (B) weight of root and stem + leaves right after harvesting the tomato plants (day 28) treated with PAW and TW. For the plants watered with the four types of PAW there was no significant difference in the length of stem nor root, whilst a significant increase was observed in the stem length between plants treated with PAW compared to TW, the root length, however, was not significantly affected by the watering media. Interestingly, both the root weight and the weight of the stem + leaves were significantly higher between plants watered with PAW compared to TW, although as with the plant length there was no significant effect of using PAW with different operating conditions on the weight. Similarly, Adhikari et al. (2019) [159] showed a significant difference in plant growth (length shoot) for tomato seedlings when irrigated with PAW, activated for 15 and 30 min with a plasma jet using air as the feed gas, as compared to tap water, despite no significant differences being observed in the root length. Nevertheless, when the tomato seedlings was irrigated with PAW activated for 60 min there was no significant difference in shoot length compared to tap water, thus indicating that the 15 and 30 min activation times did not induce oxidative damage,

however, the longer activation time of 60 min, produced excessive RONS, initiating RONS stress and toxicity. In addition, Sivachandiran and Khacef (2017) [160] investigated the synergistic effect of treating both seeds and water with plasma on tomato and sweet pepper, using a DBD system. When seeds (tomato and sweet pepper) were exposed to 10 min plasma and watered with PAW (activated for 15 min) for the first 9 days, followed by tap water for 51 days, the stem length increased about 60% compared to control sample.

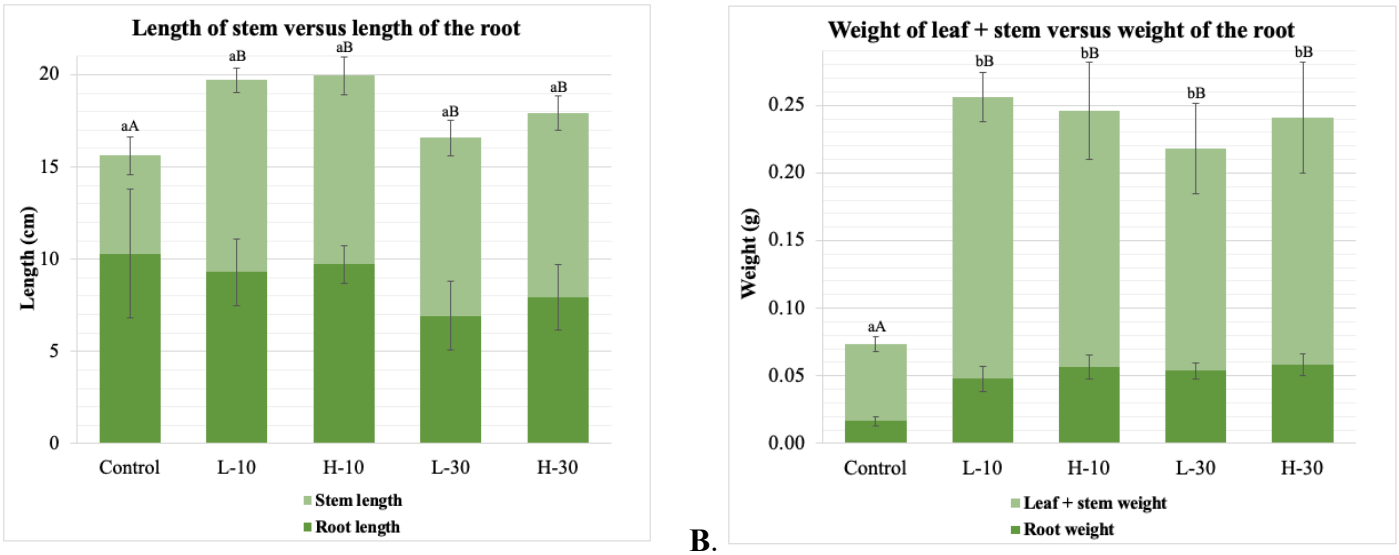

Figure 43. The individual and cumulative A) root and stem length; and B) root and stem + leaves weight after plant harvest for plants watered with the four different types of PAW (L-10, H-10, L-30 and H-30) and control (TW) on day 28. Different upper-case letters represent a significant difference in the length and weight of the stem + leaves between TW and the four PAWs treated samples in A and B, respectively. Whereas, the lower-case letters represent a significant difference in the length and weight of the root in A and B, respectively (n=5, $P \leq 0.05$) (Numeric value in Appendix D)

From Figure 44 it can be observed that the root system of plants watered with PAW L-10, and in general with the different PAWs, developed a thicker root system with more root hairs, whereas longer and thinner roots were observed in plants watered with tap water. Shorter roots with more root hairs observed for the plants irrigated with PAW could mean a larger surface area leading to better water and nutrient uptake [190]. On the other hand, the many root hairs may also indicate nutrient deficiency, such as phosphorus, where the plant adapt foreign strategies to find new sources of nutrient [190, 191]. Furthermore, Adhikari et al. (2019) [159] suggested that the higher oxygen content of PAW resulted in improved nutritional uptake capacity of the roots, supporting the theory of a better water uptake for the PAW plants in present work. Additionally, the long, thin roots of the control plants could indicate nutritional deficiency, such as nitrogen [190]. An increase in the RONS concentration has been reported to trigger expression of defense genes, i.e. H_2O_2 and NO mutually regulate plant hormones

synthesis by inducing concentration of salicylic acid and Jasmonic acid genes, which both regulate plant vegetative growth, seed germination, nutrition uptake and water relations [192, 193]. Indeed, several studies with cold plasma have reported an increase in the plant ability for water uptake [76, 139]. Additionally, Garbin et al. (2008) [194] suggested an important role of NO_3^- in root branching for *Araucaria angustifolia* when conducting a study supplementing NO_3^- or NH_4^+ as the nitrogen source, which resulted in a more advanced root system for the plants receiving NO_3^-.

A.  B. 

Figure 44. Tomato plants watered with TW (A) and PAW L-10 (B) after harvesting on day 28. The L-10 represent the plants watered with different types of PAW, as they all looked similar (H-10, L-30 and H-10 are added in Appendix D)

A distinct purple color was observed on the underside or abaxial surface of the leaves for both TW and PAW treated plants after 28 incubation days (Figure 44), which has been attributed to nutrient deficiency and in particular to the lack of phosphorus or nitrogen, known to cause a purple/red coloring [152]. Additionally, the adaxial surface of the plant leaves treated with PAW exhibited a darker green color as compared to the control samples, which is also a known symptom for phosphorus deficiency [152]. In the present study, the concentration of nitrates and nitrites in the PAW ranged from 1.24 to 5.52 mM and 3.6 to 37,4 µM, respectively, which could for the plants watered with PAW, suggest phosphorus deficiency as main reason for the purplish discoloration. In present work, the phosphorus concentration in PAW was not determined, however, Judée et al. (2018) [31] reported concentration of phosphate, hydrogen phosphate, dihydrogen phosphate and phosphoric acid in PAW (after 30 min activation time on tap water using a DBD system) to be 140 ± 59 pM, 7.71 ± 2.14 µM, 2.56 ± 1.08 µM and

7.55 ± 4.29 μM, respectively. However, even if PAW in present work had similar concentrations, it is low to rule out phosphorus deficiency. When a plant suffers from phosphorus deficiency the purplish color in the leaves is caused by the accumulation of sugar that further favors the synthesis of anthocyanins [195, 196]. The accumulation of sugar is due to low level of phosphorus influences the balance between the synthesis and catabolism of carbon metabolites [197]. This together with the green color of chlorophyll may be the reason for the dark green color in PAW treated samples. Nevertheless, Garbin et al. (2008) [194] conducted an experiment supplying 4 mM NO_3^- as the only nitrogen source (together with other essential minerals) for *A. angustifolia* and still reported signs of N deficiency in the plants. Furthermore, N deficiency led to lighter and more yellowish leaves, as N is a vital component in chlorophyll, responsible for the green color of plants. Thus, the lighter green color of the control plants could be an indication of N deficiency [198]. In addition, Islam et al. (2019) [199] reported a significantly higher chlorophyll concentration for rapeseed (*Brassica Napus*) exposed to PAW (generated 10 min with an arc discharge, using Ar or O_2 as feed gas and deionized water) for 30 min compared to control plants.

Moreover, the pH has a great effect on the anthocyanin accumulation, where a low pH has resulted in a higher anthocyanin content. Suzuki, M. (1995) [200] reported that both cell number in the cell suspension and anthocyanin content increased with a low pH, the biggest to smallest increase being at pH 4.5, 5.5 and 7, respectively. As discussed in section 4.1.2, PAW has a significantly lower pH than tap water, 2.5 ± 0.04 – 3.9 ± 0.04 and 8.0 ± 0.07, respectively, thus indicating that the pH could also play a role in plant growth enhancement and the purplish coloring of the plants. Indeed, the pH of the soil influences plant nutrient absorption, transport and distribution, which could lead to nutritional imbalance and further effect the plant growth and development [201]. Nevertheless, too low pH makes the soil acidic which further can be toxic to the plants and the optimal pH for most plant is between 5 and 7 [202]. The pH in PAW are lower than 5 for all conditions, indicating that this could potentially also lead to a stress response for the plant.

Since the vermiculite substrate does not hold much nutritional value on its own [203], the nutrients sources supporting plant growth in the present study rely mostly on either the TW or the PAW. Norwegian tap water does contain small amount of NO_3^- (nitrogen source) and PO_4^{3-} (phosphorus source), according to the geological survey of Norway the median concentration of NO_3^- was 0.68 mg/L, whereas for PO_4^{3-} 94 % of samples had concentration below the

detection limit (0.2 mg/L) [204]. Although nitrogen is available for the plants treated with PAW, other essential nutrients for plant physiology, growth and development are absent, which causes a severe nutritional imbalance that could further lead to a stress response in the plants [152]. Moreover, stress in plants can lead to anthocyanin accumulation, as this is one of the defense mechanisms in plants, the darker color of PAW treated samples indicating a nutritional imbalance and thus, a stress reaction. Nevertheless, watering with PAW did indeed result in growth enhancement, as compared to the control in TW, thus making it interesting to further investigate the effect of PAW on plants sown in vermiculite and watered with a multi-nutrient solution besides the PAW / tap water (section 4.4.3), or even on plants sown in soil, which naturally contains many of the essential minerals [205].

4.5.2 Experiment to check the concentration of Nitrogen in PAW and its effect on the plants

The purpose of this trial was to determine the effect of nitrogen levels in PAW on plant growth, as compared to a nitrogen solution with both NH_4^+ and NO_3^- as the nitrogen source for the plant (50 μM NH_4NO_3). PAW L-30 (4.5 mM NO_3^-, 23.0 μM NO_2^-, 21.0 μM and pH: 2.7 ± 0.04) was selected as a compromise between the results presented in section 4.4.1 (no significant differences between different PAWs on plant growth) and sustainable generation conditions (low mode, 25 W). In literature, most nitrogen solution used in trials have a nitrate concentration ranging from 6 – 15 mM, additionally including a small concentration of NH_4^+ (0.5 – 5 mM) [164, 206, 207]. Moreover, the effect of a higher concentration of hydrogen peroxide on plant growth, with regards to PAW L-30 and in general the different PAWs characterized in section 4.1.2, was assessed by applying PAW_IB (5.0 mM NO_3^-, 1.0 μM NO_2^-, 4.2 mM and pH: 2.4 ± 0.006) as watering media. Figure 45 shows the evolution of plant growth (average and standard deviation, n=3) during the 37 days of incubation with a regime of 16 h light followed by 8 h dark, watered 10, 16, 23, 30 after they were sown. Overall, no significant differences in the length of the stem were found between PAW L-30, PAW_IB and NH_4NO_3 after the 37 days, although from Figure 45 the average of the plants treated with PAW_IB are somewhat shorter than the plants watered with PAW L-30 or NH_4NO_3. Moreover, already after 16 days of incubation the plants watered with PAW L-30 and PAW_IB was significantly longer than the control plants, whereas 23 days of incubation were needed for the NH_4NO_3 watered plants to show a statistically significant higher average than the controls (TW).

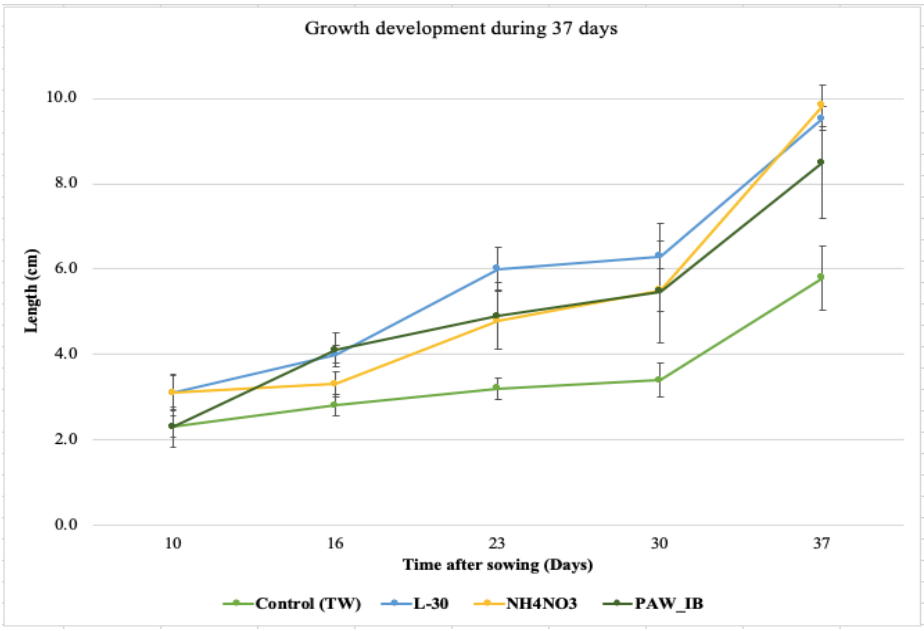

Figure 45. Plant length development of L-30, Nitrogen solution, PAW_IB and control for 37 days. Statistical analysis was performed for the length of the different plants comparing the effect of different PAW every week with a significance level of 95 %, (n=5, P≤0.05)

The development of the tomato plants during the 37 days of incubation is illustrated in Figure 46. It was decided to harvest the plants after 37 days due the plants becoming very weak and showing severe response to stress without further nutrition. On a first glance, the plants watered with PAW L-30 seemed to grow faster than the plants treated with the NH_4NO_3 solution, also exhibiting more developed leaves. It can also be noted that from day 16 on the leaves of PAW L-10 treated plants turned into dark green color and started to shrink, while the plants watered with the NH_4NO_3 solution did not show such strong stress reaction, they as well did start to look darker, yet the leaves were still growing. The PAW_IB treated plants showed similar development as the L-30 treated plants (Pictures not included). In section 4.4.1 the potential of nitrogen and phosphorus deficiency as one of the reasons behind the coloring of the plants was discussed, in addition to an imbalance in nutritional value that could lead to a stress reaction in the plant, which further could lead to the accumulation of anthocyanin. The concentration of nitrate/nitrite is higher in PAW (4.5 mM/23 µM and 5.0 mM/1 µM for L-30 and PAW_IB, respectively) than in the $NH_4NO_3^-$ solution (50 µM), indicating that perhaps a higher concentration of only nitrogen led to a stronger stress response. Additionally, the results show that the L-30 and PAW_IB treated plants grew faster the first week, suggesting that the higher concentration of nitrate increased the stem length after germination, but after a while the high concentration led to the stress response, whereas the lower concentration of nitrate in $NH_4NO_3^-$ led to a slower yet steady increase in stem length and did not show the same strong stress

response. Furthermore, in literature, studies have reported that for most species the combination of NO_3^- and NH_4^+ as a nitrogen source will increase plant growth and yield [208, 209], thus the addition of NH_4^+ in the plants treated with $NH_4NO_3^-$ could potentially be part of the reason to why these plants have a lighter green color compared to plants treated with the different PAWs, as well as having less shrinkage of the leaves.

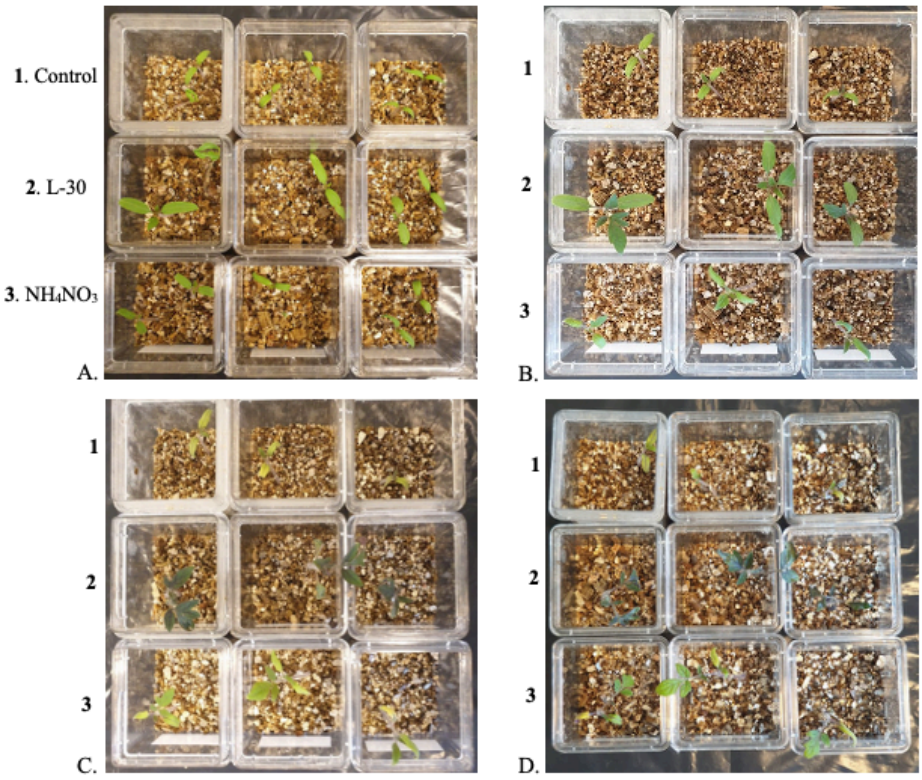

Figure 46. Development of plants watered with tap water (control), PAW (L-30) and a nitrogen solution ($NH_4NO_3^-$) once every week for 37 days to assess the effect the nitrate concentration in PAW compared to a nitrogen solution with a concentration of 50 µL, A) taken 10 days after sowing B) 16 days after sowing C) 23 days after sowing and D) 30 days after sowing (n=3)

In Figure 47 the results (average and standard deviation, n=3) after plant harvesting (day 37) are presented, in terms of the individual and cumulative (A) length of root and stem and (B) weight of root and stem + leaves. With regards to the length of the stem, there is indeed a significant higher length of the plants treated with the two PAWs and NH_4NO_3 compared to the control plants, whilst there were no significant differences found in the length of the root. Although plants treated with PAW_IB can be observed from Figure 47 A, to on average, have a shorter root length. In Figure 46 it is clear to see after 16 days that the L-30 planted was longer and had more developed leaves. On the other hand, a significantly higher root weight was

observed in PAW_IB watered plants as compared to the controls, with no statistically significant differences between control and NH_4NO_3/PAW L-10 treated plants. Likewise, as discussed in section 4.2.2, the higher root weight can be attributed to a thicker and highly branched root system, which further could be a response to the plant having a better water uptake, the NO_3^- as the nitrogen source or phosphorus deficiency. Additionally, as mentioned in section 4.4.2, Adhikari et al. (2019) [159] suggested that the higher oxygen content of PAW resulted in improved nutritional uptake capacity of the roots. PAW_IB had a higher hydrogen peroxide concentration suggesting that this could be a reason for thicker and more highly branched root system. Moreover, hydrogen peroxide plays a versatile roles in physiological and biochemical processes in the plant as well as in its resistance to stress and has proven effective for plant growth enhancement, better fruit growth and to increase germination percentage of seeds [210-213]. For instance, Orabi et al. (2018) [214] reported that canola plants sprayed with 2 mM with 4 days intervals for 61 days increased the dry matter of shoots and roots from 6.21 g in control plants to 7.37 g for hydrogen peroxide treated ones and 1.91 g in control plants to 2.59 g in hydrogen peroxide treated plants, respectively. Additionally, Habib et al. (2020) [215] reported that NO together with H_2O_2 improved the photosynthetic pigments of wheat plants, in addition they increased the accumulation of the amino acid proline, glycine betaine and total soluble protein which is important in the osmotic adjustment and could lead to better water uptake. In present work, the higher concentration of hydrogen peroxide present in PAW_IB (4.5 mM) did not give an increase in stem length compared to the plants treated with L-30 (23 μM) or the $NH_4NO_3^-$ solution (1 μM), nevertheless, to get a more thorough indication of the effect H_2O_2 has on the physiological and biochemical processes happening in the plant, measurements would need to be conducted of chemicals inside the plant, e.g. anthocyanin levels, total soluble protein or proline levels. Moreover, with regards to the weight of the stem + leaves, no significant differences were found between any of the conditions assayed. Although there was no statistical significant differnt, from Figure 47 B it is clear to see that the average weight of the control plants are lower than the plants for the other three conditions.

A.

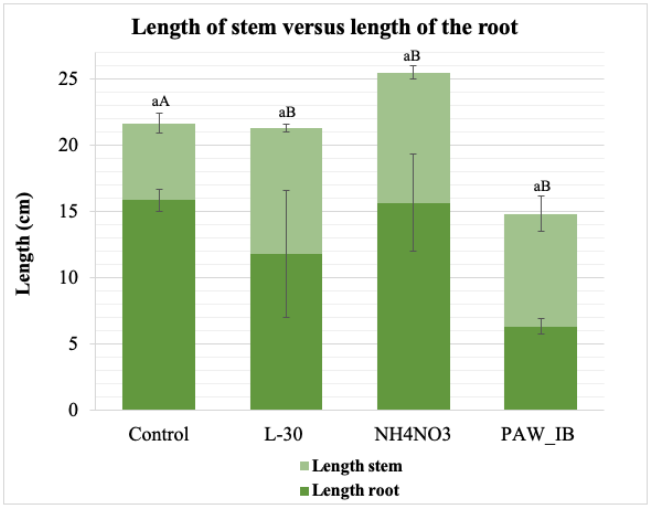

B.

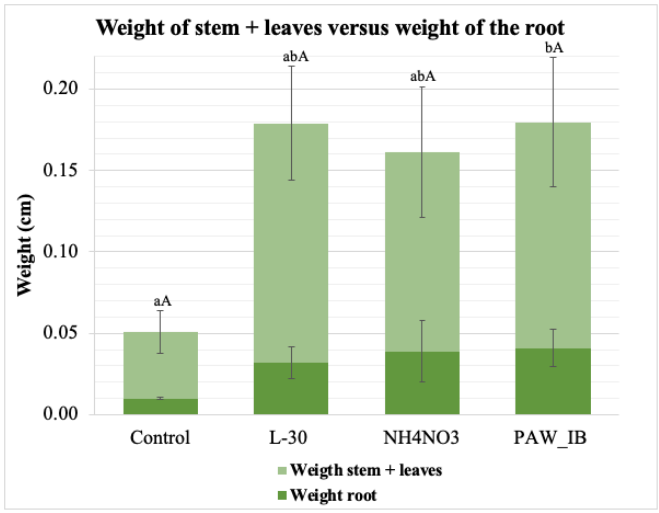

Figure 47. The individual and cumulative A) root and stem length; and B) root and stem + leaves weight after plant harvest on day 37. Different upper-case letters represent a significant difference in the length and weight of the stem + leaves between the control (TW), PAW treated samples (L-30 and PAW_IB) and NH_4NO_3 treated plants in A and B, respectively. Whereas, the lower-case letters represent a significant difference in the length and weight of the root in A and B, respectively (n=5, $P \leq 0.05$) (Numeric values in Appendix D)

In Figure 48 the plants treated with tap water, PAW L-30, NH_4NO_3 and PAW_IB after harvesting are shown. Similarly, to the observations in section 4.4.1, the control plants had long thin roots, while the plants treated with PAW_IB presented shorter but thicker roots. All of the plants have a purple color on the underside of the leaves, although the color is more distinct and darker for the plants treated with PAW_IB or L-30. Additionally, the green color of the leaves was also lighter for control plants as compared to the PAW treated ones, including the NH_4NO_3 solution presented lighter green color than the PAW plants. Interestingly, the NH_4NO_3 solution was applied in a concentration of 50 µM, which is significantly lower than the concentration of nitrates and nitrites in PAW. The higher concentration of nitrate might have caused a stronger and faster imbalance in the plants which further cause a stronger stress reaction and a higher accumulation of anthocyanin. Additionally, as mentioned in section 4.4.1, the pH also has an important role in regard to color, growth and uptake of nutrition [200, 202]. The pH of PAW_IB and L-30 are 2.4 ± 0.006 and 2.5 ± 0.05, respectively, whilst NH_4NO_3 dissolved in water give rise to a slightly acidic solution (>7) [216], it is not nearly as acidic as the PAW. Hence, the low pH could attribute to the darker color of the plant treated with PAW as well.

A.  B. 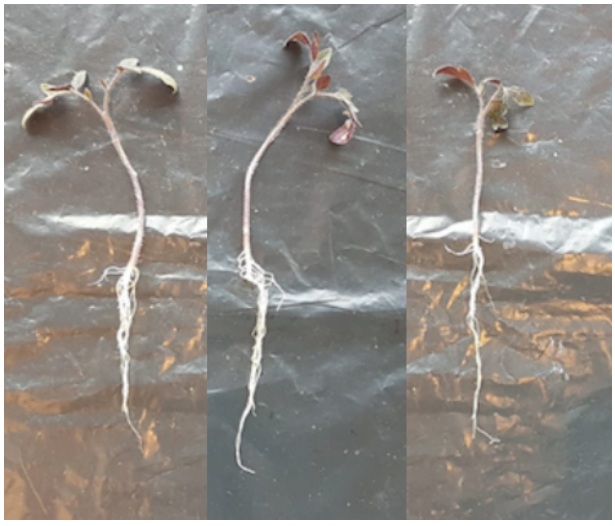

Figure 48. Harvesting of (A) the nitrogen solution, the PAW L-30, the control plants and (B) the PAW_IB plants on day 37

Finally, both plants treated with PAW and the plants treated with NH_4NO_3 had a significantly longer stem and more developed leaves than the control plants treated with water. The PAW_IB treated plants had additionally a statistically heavier stem and leaves. From Figure 47 it can be observed that even though the weight of the root of plants watered with PAW_IB was not significantly higher than the control plants, the average roots was shorter, which could be attributed to the thick and highly branched root system. As already discussed, this could indicate a better water uptake and sturdier root system for the plants, nevertheless, to conclude the specific effect of a higher hydrogen peroxide concentration on the plants, more research is required. Moreover, the effect of the NH_4NO_3 solution compared to the PAW L-30 resulted in plants that exhibited less signs of stress. Whether this can be attributed to the effect of NH_4^+ and NO_3^- being together as the nitrogen source, the higher pH or the lower concentration of NO_3^- would need to be research separately to truly determine.

4.5.3 Trial with PAW and control with nutritional solution

In previous sections, it was concluded that PAW indeed plays a significant role in tomato plant growth with regards to control plants. To further investigate the synergistic effect of PAW and other essential nutrients, tomato plants were watered with a 1/10 Hoagland solution combined with either PAW or tap water as described in section 3.2.4. Due to the failure/maintenance of the large plasma system first and then, *major force* measures (restricted access to the laboratory), spare PAW stored at 4 °C (HS-5 for 2 weeks and then HS-30) was used in this trial. However, since significant differences in plant growth were not found in section 4.4.1 for

PAWs generated at different operating conditions (plasma power and activation time), it is assumed that this variation in the PAW source did have a negligible effect.

The development of the stem length (average and standard deviation, n=5) during 39 days of incubation under a similar light regime to that described in previous sections is presented in Figure 43. Already 10 days after sowing, plants watered with PAW showed a significantly longer stem than that in control plants. For the 29 remaining days of incubation, the difference between PAW treated and control plants became even more evident, with the final average length for the PAW and TW treated plants being 23.8 ± 1.8 and 18.9 ± 0.74 cm, respectively. From Figure 36 in section 4.4.1 the difference between TW (control plants) and PAW (average of the four PAWs) was 4.8 cm, whilst in this trial the difference was 4.9 cm, thus the enhancement of plant length is approximately the same magnitude when the there are some nutrition present, nevertheless, this trial had a 10 days longer incubation time. Further research to determine the long-time effect of irrigation with PAW would be interesting as the gap between TW plants and PAW plant increased each week after day 25 (Figure 47). In Figure 50 the overall plant development is shown after 10, 17, 25 and 32 days of incubation. The PAW treated plants presented a more developed branched structure and larger leaves than the control plants, while still exhibiting a light and vibrant green color. Comparing these to the plants watered with PAW in Figure 42 from section 4.4.1, which could be seen to have a dark purplish color, in addition to starting to shrink in on themselves, the small amount of extra nutrition seem to have kept the plants green and looking healthier. Indicating that as discussed in section 4.4.1 and 4.4.2, nutritional deficiency could very well be a big reason for the stress response shown in the plants.

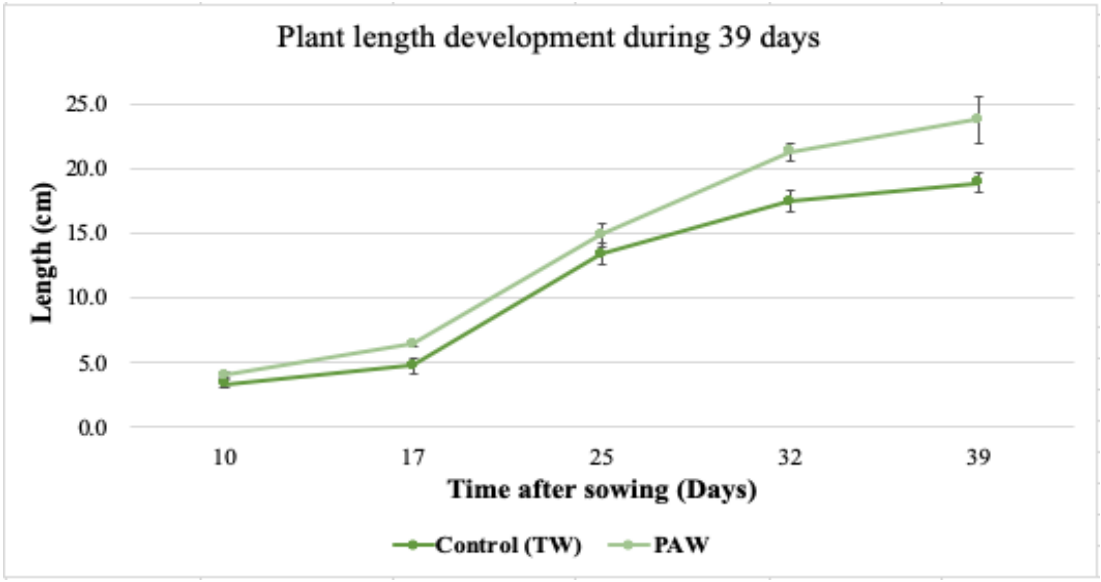

Figure 49. Stem length (cm) of tomato plants watered with 1/10 Hoagland solution combined with either PAW or tap water (control) for 39 days incubation period (average and SD, n=5). Statistical analysis was performed for the length of the different plants comparing the effect of different PAW every week with a significance level of 95 %, (n=5, P≤0.05)

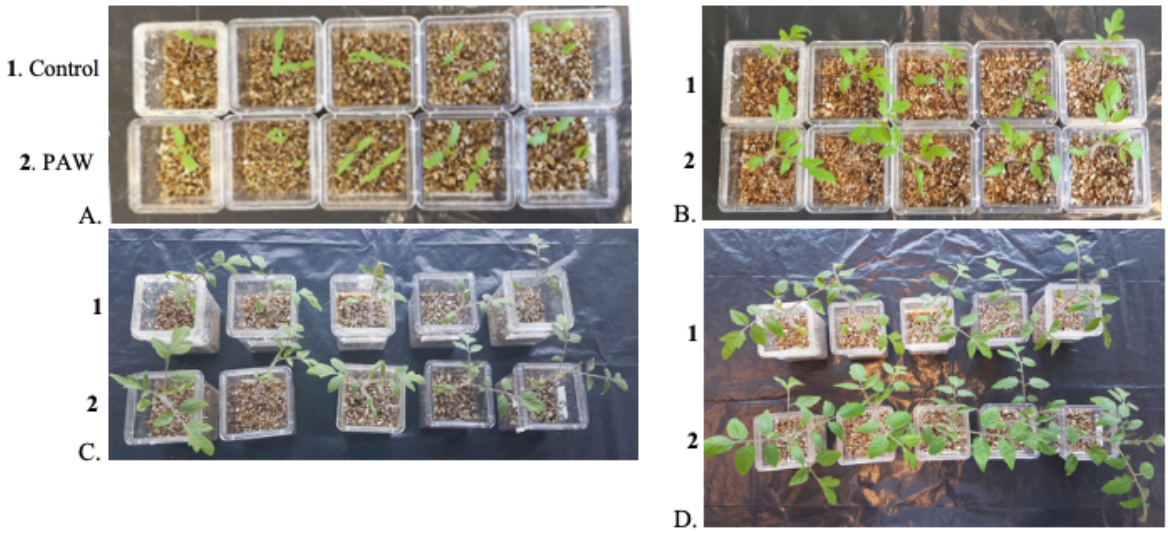

Figure 50. Development of plants watered with 1/10 Hoagland solution combined with tap water (control) or PAW (PAW), A) taken 10 days after sowing B) 17 days after sowing C) 25 days after sowing and D) 32 days after sowing (n=5)

Figure 51 show the individual and cumulative (A) root and stem length and (B) root and stem + leaves weight after harvesting of the plants (day 39) treated with PAW or tap water in combination with the Hoagland solution. Similarly, to the observations in section 4.4.1, no significant differences were found in the root length for the conditions assayed, although plants treated with PAW exhibited a significantly longer stem. With regards to the weight, statistically, the PAW treated plants was heavier for both stem + leaves and the root. It should be noted that

this trial with the Hoagland solution was intended for the fortification of the vermiculite substrate, which lacks essential nutrients for plant growth. However, in soil-grown plants, where the soil has a good nutritional value itself [205], enhanced plant growth can be expected when watering with only PAW. For instance, Sivachandiran and Khacef (2017) [160] conducted a study for enhanced growth long term on tomato and sweet pepper plants planted in soil after 10 min seed activation of CP and left to grow for 61 days while irrigated with PAW the first 9 days. The study resulted in the most effective growth enhancement when combining CP and PAW treatment and showed that different species react differently to the treatment, thus optimal treatment timing and operating conditions would need to be determined for each specie.

A.

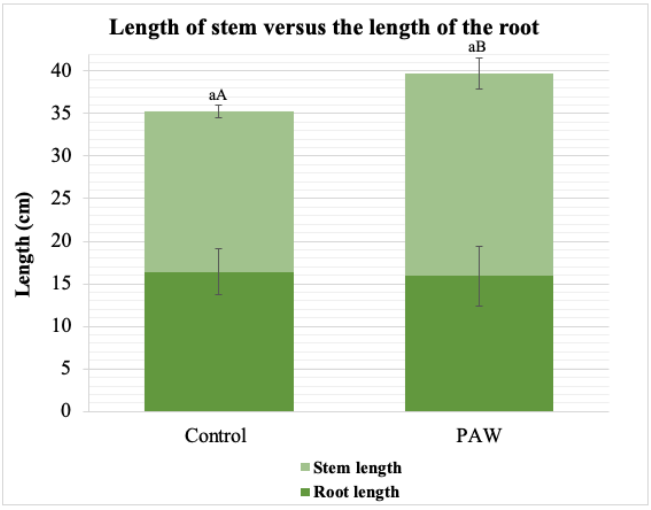

B.

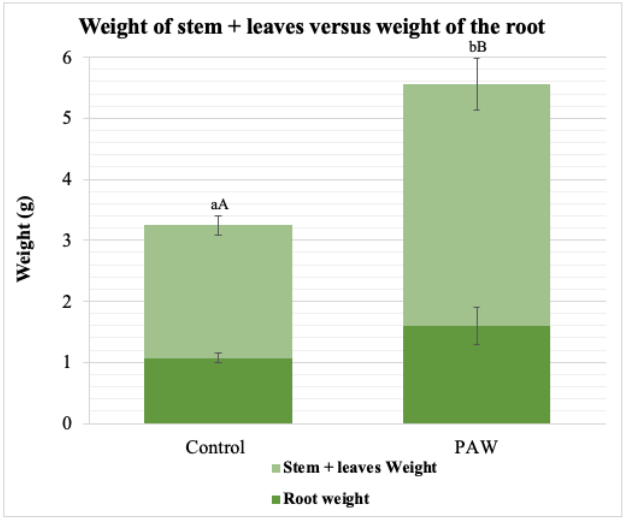

Figure 51. The individual and cumulative A) root and stem length; and B) root and stem + leaves weight after plant harvest on day 39. Different upper-case letters represent a significant difference in the length and weight of the stem + leaves between the plants treated with 1/10 Hoagland solution in combination with TW or PAW in A and B, respectively. Whereas, the lower-case letters represent a significant difference in the length and weight of the root in A and B, respectively (n=5, $P \leq 0.05$) (Numeric values in Appendix D)

In Figure 52 the tomato plants harvested after the 39 days incubation period are shown. As also observed in Figure 44, the plants watered with PAW in combination with the Hoagland solution presented a highly branched structure with more and larger leaves than the control plants, although no noticeable differences were observed in the color of the plant leaves A complex and relatively short root system was present in both control and PAW treated plants, as compared to the observations in previous sections where the tomato plants were lacking essential nutrients. Roots are an important plant organ, as they absorb water and nutrient that are transported throughout the rest of the plant, additionally, they give mechanical support to the plant and supply hormones that affect many physiological and biochemical processed [217-219]. Thus, the highly branched stem and larger leaves for the PAW treated plants indicates

more nutrition is available for the roots to take up, which would be expected as there is a higher concentration of nitrate in PAW that not only works as a nitrogen source for the plant, but also as a singling molecule to regulate gene expression and plant growth and development [220].

A. 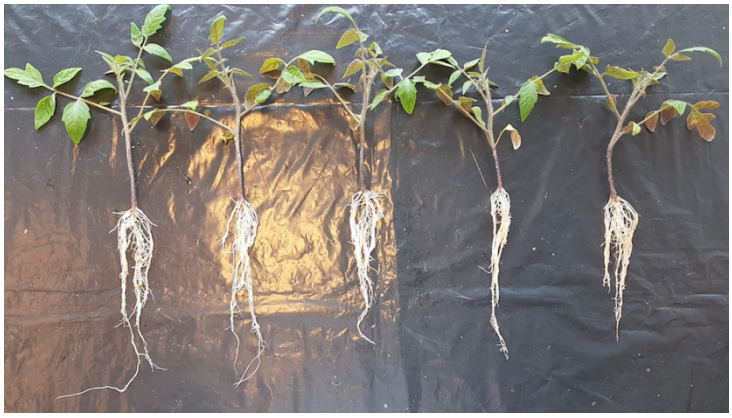 B. 

Figure 52. Plants watered with the 1/10 Hoagland solution in combination with (A) tap water and (B) PAW after a growth period of 39 days

Finally, taking in consideration the results presented in all three trials in section 4.5, it can be concluded that PAW enhances the growth of tomato plants. However, further research is needed towards industrial implementation, both on a much larger sample size and on different plant species and growing substrates (e.g. soil, hydroponics), as research studies have reported variability with regards to these factors [160, 221, 222].

5. Conclusions

In the present study, a remarkable dependency between PAW composition and CP operating parameters (activation time and plasma power) has been demonstrated. Although, a significant drop in pH and significantly higher ORP and RONS levels were observed towards both increasing activation time and plasma power, the most pronounced effect in PAW composition, including carbonic compounds, was attributed to the activation time, regardless of the plasma power. Furthermore, PAW stored for four weeks at different temperatures relevant for industrial settings (i.e. 10, 4 and -20 °C) remained stable with regards to pH, ORP, nitrate and carbonic compounds concentrations, whilst nitrite and hydrogen peroxide concentrations were negligible or not detectable after 24 h. PAW storability for at least four weeks, independently of the storage temperature, will streamline supply-chain logistics and confer a more flexible operational margin to food industry players .

The present work has demonstrated the antilisterial activity of PAW in planktonic cells, with the highest bacterial reduction (≈5 log CFU/g) achieved after just 5 min exposure to the PAW generated under the most severe operating conditions (HS-30), and thus exhibiting the lowest pH and highest ORP and RONS levels. Although, a synergistic effect with US treatment was observed for certain PAW conditions (L-10), the individual HS-30 treatment was nonetheless the most effective. Furthermore, results from this study suggest the promising potential of PAW as an alternative preservation strategy on wild harvested macroalgal biomass. Although longer treatment times (30 and 60 min) improved PAW preservation efficacy, the synergistic effect of US and PAW L-10 showed great potential with relatively high bacterial log reductions (≈2 log) and much shorter treatment time (5 min). Thus, the potential of PAW to extended product shelf-life and reduce food waste generation was demonstrated. PAW can contribute to the possibility of implementing the use of macroalgae more into food product, which is an alternative source to the terrestrial biomass and can further contribute to meet the demand for a higher food supply in a growing population. Additionally, macroalgae is the largest unexploited biomass today, entailing a number of environmental and societal benefits compared to terrestrial crops, such as being a highly renewable source, has a high nutritional value (rich in minerals and protein) and can accumulate a variety of phytochemical constituents (potential in the prevention/treatment of health diseases).

In the present work, irrigation of tomato plants with PAW, independently of the PAW generation conditions, resulted in significantly more developed plants as compared to those treated with tap water. Moreover, potential nutritional deficiencies in PAW were compensated with a nutrient-rich solution, similar to the conditions present in soil or hydroponics, this combination resulting in a synergistic effect on plant growth and yield, which demonstrates the potential of PAW as a sustainable alternative to mineral nitrogen fertilizer. Thus, PAW will contribute to minimize the environmental impact caused by mineral fertilizer, and the increase in crop yield for plants irrigated with PAW will contribute to the global food supply meeting the demand of a growing and urbanization population, that according to FAO will be 60% bigger in 2050.

6. Future work

Moving towards the implementation of PAW at industrial scale as a sustainable technology for food and agricultural applications further research is needed towards e.g cost-effective PAW generation systems meeting industrial demands and accurate prediction of PAW composition and storability as a function of e.g. operating variables and the water source. The present work has demonstrated the antilisterial activity of PAW in cell suspensions and the potential as a preservation method for macroalgae, and further work could investigate PAW decontamination efficacy on fresh produce (e.g. baby spinach leaves), including nutritional sensory (e.g. color and texture) and toxicological (e.g. remaining levels of RONS in the product) assessments. Including, assessing the potential for biofilm removal in food contact surface and materials, currently being a common contamination source in industrial setting. Furthermore, investigate the efficacy of artificial cocktails containing RONS (i.e. NO_2^-, NO_3^- and H_2O_2) at similar pH as PAW to unravel the mechanisms of actions. Additionally, a storage trial at relevant conditions for industrial settings would be necessary to determine the potential for shelf-life extension and the nutritional sensory properties during storage.

With regards to agricultural applications, further activities could explore the effect of PAW on plants in soil (contains essential minerals) for a longer period of time. As mentioned in the discussion the purple coloring of tomato plants watered with PAW could be a result of stress-related anthocyanin accumulation, which could be characterized in further studies. It has been reported that different plant species react differently to PAW, further work could be to investigate the fertilizing potential of PAW with regard to different species. Finally, the techno-economic and upscaling feasibility of PAW technology should be determined for all the applications in food and agriculture.

References

[1] U. Nations, "World Population Prospect 2019: Highlights ", Department of Economic and Social Affairs, Population Division (2019), 2019.

[2] F.A.O, "2018 Revision of World Urbanization Prospects," Food and Agriculture Organization of the United Nations, 2018. [Online]. Available: un.org/development/desa/publications/2018-revision-of-world-urbanization-prospects.html

[3] FAO, *Second global plan of action for plant genetic resources for food and agriculture*. Rome, Italy 2012.

[4] F.A.O, "The state of Food and Agriculture 2019: Moving Forward on Food Loss and Waste Reduction," in "The state of the world," Rome, 978-92-5-131789-1, 2019.

[5] N. F. S. Authorities, "2018 Annual Report," 2019.

[6] RASFF, "2017 Annual report ", Health and Food Safety 2019.

[7] B. Scheibehenne, L. Miesler, and P. M. Todd, "Fast and frugal food choices: Uncovering individual decision heuristics," *Fast and frugal food choices: Uncovering individual decision heuristics,* vol. 49, pp. 578-589, 2007.

[8] A. Steptoe, T. M. Pollard, and J. Wardle, "Development of a Measure of the Motives Underlying the Selection of Food: the Food Choice Questionnaire," *Appetite,* vol. 25, no. 3, pp. 267-284, 1995, doi: 10.1006/appe.1995.0061.

[9] "Ready-to-eat foods; microbial concerns and control measures," vol. 34, ed. Portland: Ringgold Inc, 2010.

[10] "COMISSION REGULATION (EC) No 2073/2005 of 15 November 2005 on microbiological criteria for foodstuffs," *Official Journal of the European Union,* 2005. [Online]. Available: eur-lex.europa.eu/legal-content/EN/TXT/PDF/?uri=CELEX:32005R2073&from=EN.

[11] Deloitte, "Annual Report 2012/2013," 2013.

[12] A. Lem, T. Bjørndal, and A. Lappo, "Economic analysis of supply and demand for food up to 2030. Special focus on fish and fishery products," in *Economic analysis of supply and demand for food up to 2030. Special focus on fish and fishery products*, ed. Rome (Italy): Rome (Italy): FAO, 2014, p. graphs.

[13] R. Huang, D. de Vries, and H. Chen, "Strategies to enhance fresh produce decontamination using combined treatments of ultraviolet, washing and disinfectants," *International Journal of Food Microbiology,* vol. 283, pp. 37-44, 2018, doi: 10.1016/j.ijfoodmicro.2018.06.014.

[14] A. Rajwar, P. Srivastava, and M. Sahgal, "Microbiology of Fresh Produce: Route of Contamination, Detection Methods, and Remedy," *Critical Reviews in Food Science and Nutrition,* vol. 56, no. 14, pp. 2383-2390, 2016, doi: 10.1080/10408398.2013.841119.

[15] F.-G. Chizoba Ekezie, D.-W. Sun, and J.-H. Cheng, "A review on recent advances in cold plasma technology for the food industry: Current applications and future trends," *Trends in Food Science & Technology,* vol. 69, pp. 46-58, 2017, doi: 10.1016/j.tifs.2017.08.007.

[16] G. Pardo and J. Zufía, "Life cycle assessment of food-preservation technologies," *Journal of Cleaner Production,* vol. 28, no. C, pp. 198-207, 2012, doi: 10.1016/j.jclepro.2011.10.016.

[17] C. Tobler, V. H. M. Visschers, and M. Siegrist, "Eating green. Consumers' willingness to adopt ecological food consumption behaviors," *Appetite,* vol. 57, no. 3, pp. 674-682, 2011, doi: 10.1016/j.appet.2011.08.010.
[18] M. van Birgelen, J. Semeijn, and M. Keicher, "Packaging and Proenvironmental Consumption Behavior: Investigating Purchase and Disposal Decisions for Beverages," *Environment and Behavior,* vol. 41, no. 1, pp. 125-146, 2009, doi: 10.1177/0013916507311140.
[19] L. Probst, L. Frideres, B. Pedersen, and F. Amato, "Food processing technologies " *Sustainable, Safe and Nutritious Food,* vol. Case study 53, 2015.
[20] M. Stoica, L. Mihalcea, D. Borda, and P. Alexe, "Non-thermal novel food processing technologies. An overview," *Journal of Agroalimentary Processes and Technologies,* vol. 19, pp. 212-217, 2013.
[21] H. C. Langelaan, F. Pereira da Silva, U. Thoden Van Velzen, J. Broeze, A. M. Master, and M. Vollebregt, "Technology options for feeding 10 billion people: Options for sustainable food processing " *Science and Technology Ptions Assessment,* 2013, doi: 10.2861/43440.
[22] M. A. Augustin *et al.*, "Role of food processing in food and nutrition security," *Trends in Food Science & Technology,* vol. 56, pp. 115-125, 2016, doi: 10.1016/j.tifs.2016.08.005.
[23] H. De Vries, A. Matser, and A. O. Prodinra, "NovelQ: Novel processing methods for the production and distribution of high-quality and safe foods : Final publishable report," ed, 2011.
[24] E. Georget *et al.*, "Inactivation of microorganisms by high isostatic pressure processing in complex matrices: A review," *Innovative Food Science and Emerging Technologies,* vol. 27, pp. 1-14, 2015, doi: 10.1016/j.ifset.2014.10.015.
[25] M. Gänzle, Y. Liu, and M. Gänzle, "Mechanisms of pressure-mediated cell death and injury in Escherichia coli: from fundamentals to food applications," *Frontiers in microbiology,* vol. 6, pp. 599-599, 2015, doi: 10.3389/fmicb.2015.00599.
[26] H. J. Rowan, V. P. Valdramidis, and V. M. Gómez-López, "A review of quantitative methods to describe efficacy of pulsed light generated inactivation data that embraces the occurrence of viable but non culturable state microorganisms," *Trends in Food Science & Technology,* vol. 44, no. 1, pp. 79-92, 2015, doi: 10.1016/j.tifs.2015.03.006.
[27] G. Monica, F. Lydia, and N. Daniele, "Application of Ultrasound in Food Science and Technology: A Perspective," *Foods,* vol. 7, no. 10, p. 164, 2018, doi: 10.3390/foods7100164.
[28] D. M. Sango, D. Abela, A. McElhatton, and V. P. Valdramidis, "Assisted ultrasound applications for the production of safe foods," *Journal of Applied Microbiology,* vol. 116, no. 5, pp. 1067-1083, 2014, doi: 10.1111/jam.12468.
[29] N. Misra, B. Tiwari, K. Raghavarao, and P. Cullen, "Nonthermal Plasma Inactivation of Food-Borne Pathogens," *Food Engineering Reviews,* vol. 3, no. 3, pp. 159-170, 2011, doi: 10.1007/s12393-011-9041-9.
[30] P. J. Cullen *et al.*, "Translation of plasma technology from the lab to the food industry," *Plasma Processes and Polymers,* vol. 15, no. 2, pp. n/a-n/a, 2018, doi: 10.1002/ppap.201700085.
[31] F. Judée, S. Simon, C. Bailly, and T. Dufour, "Plasma-activation of tap water using DBD for agonomy applications: Idenfication and quantification of long lifetime chemical

species and production/consumption mechanisms " *Water research,* vol. 133, 2018, doi: 10.1016/j.watres.2017.12.035.
[32] J. Jiang *et al.*, "Effect of cold plasma treatment on seed germination and growth of wheat," *Plasma Science and Technology,* vol. 16, no. 1, pp. 54-58, 2014, doi: 10.1088/1009-0630/16/1/12.
[33] M. Henselová, Ľ. Slováková, M. Martinka, and A. Zahoranová, "Growth, anatomy and enzyme activity changes in maize roots induced by treatment of seeds with low-temperature plasma," *Botany, Zoology and Cellular and Molecular Biology,* vol. 67, no. 3, pp. 490-497, 2012, doi: 10.2478/s11756-012-0046-5.
[34] B. Surowsky, A. Fischer, O. Schlueter, and D. Knorr, "Cold plasma effects on enzyme activity in a model food system," *Innovative Food Science and Emerging Technologies,* vol. 19, p. 146, 2013.
[35] M. Yin, "Stimulating effects of seed treatment by magnetized plasma on tomato growth and yield," *Plasma Science and Technology,* vol. 7, no. 6, pp. 3143-3147, 2005, doi: 10.1088/1009-0630/7/6/017.
[36] B. Peethambaran *et al.*, "Nonthermal Plasma Reduces Water Consumption While Accelerating Arabidopsis thaliana Growth and Fecundity," *Plasma Medicine,* vol. 5, no. 2-4, pp. 87-98, 2015, doi: 10.1615/PlasmaMed.2016015723.
[37] S. La Barre and S. S. Bates, *Blue biotechnology: production and use of marine molecules*. 2018.
[38] R. Thirumdas, C. Sarangapani, and U. Annapure, "Cold Plasma: A novel Non-Thermal Technology for Food Processing," *Food Biophysics,* vol. 10, no. 1, pp. 1-11, 2015, doi: 10.1007/s11483-014-9382-z.
[39] A. Peratt, "Plasma and the universe: large scale dynamics, filamentation, and radiation," *An International Journal of Astronomy, Astrophysics and Space Science,* vol. 227, no. 1-2, pp. 97-107, 1995, doi: 10.1007/BF00678070.
[40] D. P. Richard, "Plasmas everywhere," *Nature,* vol. 343, no. 6253, p. 21, 1990, doi: 10.1038/343021a0.
[41] R. Ranjan, P. Krishnamraju, T. Shankar, and S. Gowd, "Nonthermal plasma in dentistry: An update.(Review Article)," *Journal of International Society of Preventive and Community Dentistry,* vol. 7, no. 3, p. 71, 2017, doi: 10.4103/jispcd.JISPCD_29_17.
[42] V. Nehra, A. JKumar, and H. K. Dwivedi, "Atmospheric Non-Thermal Plasma Sources," *International Journal of Engineering,* vol. 2, no. 1, 2008.
[43] M. Risa Vaka *et al.*, "Towards the Next-Generation Disinfectant: Composition, Storability and Preservation Potential of Plasma Activated Water on Baby Spinach Leaves," *Foods (Basel, Switzerland),* vol. 8, no. 12, 2019, doi: 10.3390/foods8120692.
[44] H. Conrads and M. Schmidt, "Plasma generation and plasma sources," *Plasma Sources Science and Technology,* vol. 9, no. 4, pp. 441-454, 2000/10/31 2000, doi: 10.1088/0963-0252/9/4/301.
[45] K. Vaideki, *5 - Plasma technology for antimicrobial textiles*. Elsevier Ltd, 2016, pp. 73-86.
[46] B. Marcandalli and C. Riccardi, *11 - Plasma treatments of fibres and textiles*. Elsevier Ltd, 2007, pp. 282-300.
[47] "Plasma, the fourth state of matter," *Plasma physics*. [Online]. Available: grinp.com/plasma/physics.html

[48] P. K. Chu and X. Lu, *Low Temperature Plasma Technology*, 1 ed. (Methods and Applications). 2013.
[49] B. Jiang *et al.*, "Review on electrical discharge plasma technology for wastewater remediation," *Chemical Engineering Journal,* vol. 236, p. 21, 2014, doi: https://doi.org/10.1016/j.cej.2013.09.090.
[50] A. Bogaerts, E. Neyts, R. Gijbels, and J. v. d. Mullen, "Gas discharge plasmas and their applications," *Spectrochimica Acta* Part B, p. 50, 2002, doi: http://dx.doi.org/10.1016/S0584-8547(01)00406-2.
[51] "Opinion on the use of plasma processes for tratment of foods," Germany 2012.
[52] R. Mandal, A. Singh, and A. P. Singh, "Recent developments in cold plasma decontamination technology in the food industry," *Trends in Food Science & Technology* vol. 80, p. 20, 2018, doi: https://doi.org/10.1016/j.tifs.2018.07.014.
[53] C. Cardinaud, "Fluorine-based plasmas: Main features and application in micro-and nanotechnology and in surface treatment," *Comptes rendus - Chimie,* vol. 21, no. 8, pp. 723-739, 2018, doi: 10.1016/j.crci.2018.01.009.
[54] "Plasma physics." lasers.llnl.gov/science/understanding-the-universe/plasma-physics (accessed 2020).
[55] V. Scholtz, J. pazlarova, H. Souskova, J. Khun, and J. Julak, "Nonthermal plasma - A tool for decontamination and disinfection," *Biotechnology Advances* Research review paper vol. 33, no. 6, 2, p. 12, 2015, doi: 10.1016/j.biotechadv.2015.01.002.
[56] J. Guo, K. Huang, and J. Wang, "Bactericidal effect of various non-thermal plasma agents and the influence of experimental conditions in microbial inactivation: A review," *Food Control,* vol. 50, pp. 482-490, 2015, doi: 10.1016/j.foodcont.2014.09.037.
[57] S. Patil *et al.*, "Influence of high voltage atmospheric cold plasma process parameters and role of relative humidity on inactivation of Bacillus atrophaeus spores inside a sealed package," *Journal of Hospital Infection,* vol. 88, no. 3, pp. 162-169, 2014, doi: 10.1016/j.jhin.2014.08.009.
[58] R. Thirumdas *et al.*, "Plasma activated water (PAW): Chemistry: physico-chemical properties, applications in food and agriculture," *Trends in Food Science & Technology,* vol. 77, p. 10, 2018, doi: 10.1016/j.tifs.2018.05.007.
[59] "Plasma activated water " vitalfluid.nl/plasma-activated-water (accessed.
[60] , "Elementary Chemical and Physical Phenomena in Electrical Discharge Plasma in Gas–Liquid Environments and in Liquids." Weinheim, Germany: Weinheim, Germany: Wiley-VCH Verlag GmbH & Co. KGaA, 2012, pp. 185-241.
[61] G. Kamgang-Youbi *et al.*, "Microbial inactivation using plasma-activated water obtained by gliding electric discharges," *Letters in Applied Microbiology,* vol. 48, no. 1, pp. 13-18, 2009, doi: 10.1111/j.1472-765X.2008.02476.x.
[62] M. Naitali, G. Kamgang-Youbi, J.-M. Herry, M.-N. Bellon-Fontaine, and J.-L. Brisset, "Combined Effects of Long-Living Chemical Species during Microbial Inactivation Using Atmospheric Plasma-Treated Water," *Applied and Environmental Microbiology,* vol. 76, no. 22, p. 7662, 2010, doi: 10.1128/AEM.01615-10.
[63] R. Ma, G. Wang, T. Ying, K. Wang, J. Zhang, and J. Fang, "Non-Thermal Plasma-Activated Water Inactivation of Food-Borne Pathogen on Fresh Produce," *Journal of Hazardous Materials,* vol. 300, pp. 643-651, 2015, doi: doi.org/10.1016/j.jhazmat.2015.07.061.

[64] G. Haghighat, A. Sohrabi, P. M. Shaibani, C. W. Van Neste, S. Naicker, and T. Thundat, "The role of chloride ions in plasma-activated water treatment processes," *Environ. Sci.: Water Res. Technol.,* vol. 3, no. 1, pp. 156-168, 2017, doi: 10.1039/c6ew00308g.

[65] N. Puač *et al.*, "Activity of catalase enzyme in Paulownia tomentosa seeds during the process of germination after treatments with low pressure plasma and plasma activated water," *Plasma Processes and Polymers,* vol. 15, no. 2, pp. n/a-n/a, 2018, doi: 10.1002/ppap.201700082.

[66] R. Ma *et al.*, "Effect of Non-Thermal Plasma-Activated Water on Fruit Decay and Quality in Postharvest Chinese Bayberries," *An International Journal,* vol. 9, no. 11, pp. 1825-1834, 2016, doi: 10.1007/s11947-016-1761-7.

[67] I. Naumova, A. Maksimov, and A. Khlyustova, "Stimulation of the germinability of seeds and germ growth under treatment with plasma-activated water," *Surface Engineering and Applied Electrochemistry,* vol. 47, no. 3, pp. 263-265, 2011, doi: 10.3103/S1068375511030136.

[68] D. P. Park *et al.*, "Reactive nitrogen species produced in water by non-equilibrium plasma increase plant growth rate and nutritional yield," *Reactive nitrogen species produced in water by non-equilibrium plasma increase plant growth rate and nutritional yield,* vol. 13S1, pp. S19-S29, 2013.

[69] N. Shainsky *et al.*, "Retraction: Plasma Acid: Water Treated by Dielectric Barrier Discharge," *Plasma Processes and Polymers,* vol. 9, no. 6, pp. n/a-n/a, 2012, doi: 10.1002/ppap.201100084.

[70] J. Shen *et al.*, "Bactericidal Effects against S. aureus and Physicochemical Properties of Plasma Activated Water stored at different temperatures," *Sci Rep,* vol. 6, no. 1, pp. 28505-28505, 2016, doi: 10.1038/srep28505.

[71] Q. Zhang *et al.*, "Sterilization Efficiency of a Novel Electrochemical Disinfectant against Staphylococcus aureus," *Environmental Science & Technology,* vol. 50, no. 6, pp. 3184-3192, 2016, doi: 10.1021/acs.est.5b05108.

[72] R. Zhou *et al.*, "Plasma-activated water: generation, origin of reactive species and biological applications," *Journal of Physics D: Applied Physics,* vol. 53, 2020, doi: 10.1088/1361-6463/ab81cf.

[73] T.-P. Chen, J. Liang, and T.-L. Su, "Plasma-activated water: antibacterial activity and artifacts?," *Environmental Science and Pollution Research,* vol. 25, no. 27, pp. 26699-26706, 2018, doi: 10.1007/s11356-017-9169-0.

[74] U. K. Ercan, J. Smith, H.-F. Ji, A. D. Brooks, S. G. Joshi, and U. K. Ercan, "Chemical Changes in Nonthermal Plasma-Treated N-Acetylcysteine (NAC) Solution and Their Contribution to Bacterial Inactivation," *Scientific reports,* vol. 6, no. 1, pp. 20365-20365, 2016, doi: 10.1038/srep20365.

[75] R. Zhou *et al.*, "Microplasma Bubbles: Reactive Vehicles for Biofilm Dispersal," *ACS applied materials & interfaces,* vol. 11, no. 23, p. 20660, 2019, doi: 10.1021/acsami.9b03961.

[76] L. Li *et al.*, "Effects of cold plasma treatment on seed germination and seedling growth of soybean," *Scientific Reports,* vol. 4, no. 1, 2014, doi: 10.1038/srep05859.

[77] G. Fridman *et al.*, "Applied Plasma Medicine," *Plasma Processes and Polymers,* vol. 5, no. 6, pp. 503-533, 2008, doi: 10.1002/ppap.200700154.

[78] K. Oehmigen *et al.*, "The Role of Acidification for Antimicrobial Activity of Atmospheric Pressure Plasma in Liquids," *Plasma Processes and Polymers,* vol. 7, no. 3-4, pp. 250-257, 2010, doi: 10.1002/ppap.200900077.

[79] P. Lukes, E. Dolezalova, I. Sisrova, and M. Clupek, "Aqueous-phase chemistry and bactericidal effects from an air discharge plasma in contact with water: evidence for the formation of peroxynitrite through a pseudo-second-order post-discharge reaction of h 2 o 2 and hno 2," *Plasma Sources Science and Technology,* vol. 23, no. 1, p. 015019, 2014, doi: 10.1088/0963-0252/23/1/015019.

[80] S. Jung *et al.*, "The use of atmospheric pressure plasma-treated water as a source of nitrite for emulsion-type sausage," *Meat Science,* vol. 108, pp. 132-137, 2015, doi: 10.1016/j.meatsci.2015.06.009.

[81] Y. Xu, Y. Tian, R. Ma, Q. Liu, and J. Zhang, "Effect of plasma activated water on the postharvest quality of button mushrooms, Agaricus bisporus," *Food Chemistry* vol. 197, pp. 436-444, 2016, doi: 10.1016/j.foodchem.2015.10.144.

[82] Y. Tian *et al.*, "Assessment of the Physicochemical Properties and Biological Effects of Water Activated by Non-thermal Plasma Above and Beneath the Water Surface," *Plasma Processes and Polymers,* vol. 12, no. 5, pp. 439-449, 2015, doi: 10.1002/ppap.201400082.

[83] S. Jung, J. Lee, Y. Lim, W. Choe, H. I. Yong, and C. Jo, "Direct infusion of nitrite into meat batter by atmospheric pressure plasma treatment," *Innovative Food Science and Emerging Technologies,* vol. 39, pp. 113-118, 2017, doi: 10.1016/j.ifset.2016.11.010.

[84] S. Ikawa, K. Kitano, and S. Hamaguchi, "Effects of pH on Bacterial Inactivation in Aqueous Solutions due to Low-Temperature Atmospheric Pressure Plasma Application," *Plasma Processes and Polymers,* vol. 7, no. 1, pp. 33-42, 2010, doi: 10.1002/ppap.200900090.

[85] M. J. Traylor *et al.*, "Long-term antibacterial efficacy of air plasma-activated water," *Journal of Physics D: Applied Physics,* vol. 44, no. 47, p. 472001, 2011, doi: 10.1088/0022-3727/44/47/472001.

[86] Z. Machala, B. Tarabova, K. Hensel, E. Spetlikova, L. Sikurova, and P. Lukes, "Formation of ROS and RNS in Water Electro- S prayed through Transient Spark Discharge in Air and their Bactericidal Effects," *Plasma Processes and Polymers,* vol. 10, no. 7, pp. 649-659, 2013, doi: 10.1002/ppap.201200113.

[87] R. Niquet, D. Boehm, U. Schnabel, P. Cullen, P. Bourke, and J. Ehlbeck, "Characterising the impact of post-treatment storage on chemistry and antimicrobial properties of plasma treated water derived from microwave and DBD sources," *Plasma Processes and Polymers,* vol. 15, no. 3, pp. n/a-n/a, 2018, doi: 10.1002/ppap.201700127.

[88] E. Feizollahi, N. N. Misra, M. S. Roopesh, and E. Feizollahi, "Factors influencing the antimicrobial efficacy of Dielectric Barrier Discharge (DBD) Atmospheric Cold Plasma (ACP) in food processing applications," *Critical reviews in food science and nutrition,* vol. ahead-of-print, no. ahead-of-print, pp. 1-24, 2020, doi: 10.1080/10408398.2020.1743967.

[89] B. R, G. R.G, S. K.-Y, B. D., and L. B.R, "Bacteria Inactivation Using Low Power Pulsed Gliding Arc Discharges with Water Spray," *Macromolecular Journals* vol. 7, p. 9, 2010, doi: 10.1002/ppap.200900183.

[90] X. Zhang *et al.*, "Quantification of plasma produced OH radical density for water sterilization," *Plasma Processes and Polymers,* vol. 15, no. 6, pp. n/a-n/a, 2018, doi: 10.1002/ppap.201700241.

[91] IVAR. "Vannkvalitet." https://www.ivar.no/vannkvalitet/ (accessed 06.04, 2020).

[92] "pH and alkalinity," in "Volunteer Estuary Monitoring Manual," United states, 2006. [Online]. Available: epa.gov/owow/estuaries/monitor/
[93] T. G. Klämpfl *et al.*, "Cold Atmospheric Air Plasma Sterilization against Spores and Other Microorganisms of Clinical Interest," *Applied and Environmental Microbiology,* vol. 78, no. 15, p. 5077, 2012, doi: 10.1128/AEM.00583-12.
[94] D. Wang, D. Zhao, K. Feng, X. Zhang, D. Liu, and S. Yang, "The cold and atmospheric-pressure air surface barrier discharge plasma for large-area sterilization applications," *Applied Physics Letters,* vol. 98, no. 16, 2011, doi: 10.1063/1.3582923.
[95] T. Maisch *et al.*, "Contact-Free Inactivation of Candida albicans Biofilms by Cold Atmospheric Air Plasma," *Applied and Environmental Microbiology,* vol. 78, no. 12, p. 4242, 2012, doi: 10.1128/AEM.07235-11.
[96] N. N. Misra and C. Jo, "Applications of Cold Plasma Technology for Microbiological Safet in Meat Industry " *Trends in Food Science & Technology,* vol. 64, pp. 74-86, 2017, doi: 10.1016/j.tifs.2017.04.005.
[97] X. Deng, J. Shi, and M. G. Kong, "Physical Mechanisms of Inactivation of Bacillus subtilis Spores Using Cold Atmospheric Plasmas," *IEEE Transaction on Plasma Science,* vol. 34, pp. 1310-1316, 2006, doi: doi:10.1109/tps.2006.877739
[98] N. N. Misra, S. K. Pankaj, A. Segat, and K. Ishikawa, "Cold plasma interactions with enzymes in foods and model systems," *Trends in Food Science & Technology,* vol. 55, pp. 39-47, 2016, doi: 10.1016/j.tifs.2016.07.001.
[99] H. I. Yong *et al.*, "Evaluation of pathogen inactivation on sliced cheese induced by encapsulated atmospheric pressure dielectric barrier discharge plasma," *Food Microbiology,* vol. 46, pp. 46-50, 2015, doi: 10.1016/j.fm.2014.07.010.
[100] O. Lunov *et al.*, "The interplay between biological and physical scenarios of bacterial death induced by non-thermal plasma," *Biomaterials,* vol. 82, pp. 71-83, 2016, doi: 10.1016/j.biomaterials.2015.12.027.
[101] Y. Liang *et al.*, "Rapid Inactivation of Biological Species in the Air using Atmospheric Pressure Nonthermal Plasma," *Environmental Science & Technology,* vol. 46, no. 6, pp. 3360-3368, 2012, doi: 10.1021/es203770q.
[102] A. Patange, D. Boehm, D. Ziuzina, P. J. Cullen, B. Gilmore, and P. Bourke, "High voltage atmospheric cold air plasma control of bacterial biofilms on fresh produce," *International Journal of Food Microbiology,* vol. 293, pp. 137-145, 2019, doi: 10.1016/j.ijfoodmicro.2019.01.005.
[103] Z. Wan, S. K. Pankaj, C. Mosher, and K. M. Keener, "Effect of high voltage atmospheric cold plasma on inactivation of Listeria innocua on Queso Fresco cheese, cheese model and tryptic soy agar," *LWT,* vol. 102, pp. 268-275, 2019, doi: 10.1016/j.lwt.2018.11.096.
[104] S. C. Min *et al.*, "Inactivation of Escherichia coli O157:H7 and Aerobic Microorganisms in Romaine Lettuce Packaged in a Commercial Polyethylene Terephthalate Container Using Atmospheric Cold Plasma.(Research Paper)(Report)," *Journal of Food Protection,* vol. 80, no. 1, p. 35, 2017, doi: 10.4315/0362-028X.JFP-16-148.
[105] A. Bauer *et al.*, "The effects of atmospheric pressure cold plasma treatment on microbiological, physical-chemical and sensory characteristics of vacuum packaged beef loin," *Meat Science,* vol. 128, pp. 77-87, 2017, doi: 10.1016/j.meatsci.2017.02.003.

[106] K. A. Lis *et al.*, "Inactivation of Salmonella Typhimurium and Listeria monocytogenes on ham with nonthermal atmospheric pressure plasma.(Research Article)(Report)," *PLoS ONE,* vol. 13, no. 5, p. e0197773, 2018, doi: 10.1371/journal.pone.0197773.
[107] E. a. Noriega, G. Shama, A. Laca, M. D?az, and M. G. Kong, "Cold atmospheric gas plasma disinfection of chicken meat and chicken skin contaminated with Listeria innocua," *Food Microbiology,* vol. 28, no. 7, pp. 1293-1300, 2011, doi: 10.1016/j.fm.2011.05.007.
[108] A. Fernández, E. Noriega, and A. Thompson, "Inactivation of Salmonella enterica serovar Typhimurium on fresh produce by cold atmospheric gas plasma technology," *Food Microbiology* vol. 33, pp. 24-29, 2013, doi: 10.1016/j.fm.2012.08.007.
[109] N. T. Quyen, T. Traikool, R. Nitisoravut, and T. Onjun, "Improvement of water quality using dielectric barrier discharge plasma," vol. 860, ed, 2017, p. 012031.
[110] C. Liu, C. Chen, A. Jiang, X. Sun, Q. Guan, and W. Hu, "Effects of plasma-activated water on microbial growth and storage quality of fresh-cut apple," *Innovative Food Science and Emerging Technologies,* vol. 59, 2020, doi: 10.1016/j.ifset.2019.102256.
[111] E. S. Inguglia, M. Oliveira, C. M. Burgess, J. P. Kerry, and B. K. Tiwari, "Plasma-activated water as an alternative nitrite source for the curing of beef jerky: Influence on quality and inactivation of Listeria innocua," *Innovative Food Science and Emerging Technologies,* vol. 59, 2020, doi: 10.1016/j.ifset.2019.102276.
[112] Q. Xiang, X. Liu, S. Liu, Y. Ma, C. Xu, and Y. Bai, "Effect of plasma-activated water on microbial quality and physicochemical characteristics of mung bean sprouts," *Innovative Food Science and Emerging Technologies,* vol. 52, pp. 49-56, 2019, doi: 10.1016/j.ifset.2018.11.012.
[113] H. I. Yong *et al.*, "An innovative curing process with plasma-treated water for production of loin ham and for its quality and safety," *Plasma Processes and Polymers,* vol. 15, no. 2, pp. n/a-n/a, 2018, doi: 10.1002/ppap.201700050.
[114] F. WHO, "Microbiological Hazards in Fresh Leafy Vegetables and Herbs: Meeting report," in "Microbiological Risk Assesment Series No. 14 " World Health Organization Rome, Italy, 2008.
[115] M. J. Sousa Gallagher and P. V. Mahajan, *22 - The stability and shelf life of fruit and vegetables*. Elsevier Ltd, 2011, pp. 641-656.
[116] M. Ufuk Kasım and R. Kasım, "Yellowing of fresh-cut spinach (Spinacia oleracea L.) leaves delayed by UV-B applications," *Information Processing in Agriculture,* vol. 4, no. 3, pp. 214-219, 2017, doi: 10.1016/j.inpa.2017.05.006.
[117] M. Glowacz, L. M. Mogren, J. P. H. Reade, A. H. Cobb, and J. M. Monaghan, "Can hot water treatments enhance or maintain postharvest quality of spinach leaves?," *Postharvest Biology and Technology,* vol. 81, pp. 23-28, 2013, doi: 10.1016/j.postharvbio.2013.02.004.
[118] Y. Pachepsky, D. Shelton, J. McLain, J. Patel, and R. Mandrell, "Irrigation Waters as a Source of Pathogenic Microorganisms in Produce," *Advances in Agronomy,* vol. 113, pp. 73-138, 2011, doi: 10.1016/B978-0-12-386473-4.00007-5.
[119] B. Swaminathan and P. Gerner-Smidt, "The epidemiology of human listeriosis," *Microbes and Infection,* vol. 9, no. 10, pp. 1236-1243, 2007, doi: 10.1016/j.micinf.2007.05.011.
[120] L. K. Gaul, N. H. Farag, T. Shim, M. A. Kingsley, B. J. Silk, and E. Hyytia-Trees, "Hospital-acquired listeriosis outbreak caused by contaminated diced celery--Texas,

2010," *Clinical infectious diseases : an official publication of the Infectious Diseases Society of America,* vol. 56, no. 1, p. 20, 2013, doi: 10.1093/cid/cis817.
[121] P. Jeyaletchumi *et al.*, "Assessment of Listeria monocytogenes in salad vegetables through kitchen simulation study," *Journal of Tropical Agriculture and Food Science,* vol. 40, pp. 55-62, 2012.
[122] J. Ponniah *et al.*, "Listeria monocytogenes in raw salad vegetables sold at retail level in Malaysia," *Food Control,* vol. 21, no. 5, pp. 774-778, 2010, doi: 10.1016/j.foodcont.2009.09.008.
[123] R. L. Thunberg, T. T. Tran, R. W. Bennett, R. N. Matthews, N. Belay, and R. L. Thunberg, "Microbial evaluation of selected fresh produce obtained at retail markets," *Journal of food protection,* vol. 65, no. 4, pp. 677-682, 2002, doi: 10.4315/0362-028X-65.4.677.
[124] T. Ding *et al.*, "Risk assessment for Listeria monocytogenes on lettuce from farm to table in Korea," *Food Control,* vol. 30, no. 1, pp. 190-199, 2013, doi: 10.1016/j.foodcont.2012.07.014.
[125] D. Althaus, E. Hofer, S. Corti, A. Julmi, R. Stephan, and D. Althaus, "Bacteriological survey of ready-to-eat lettuce, fresh-cut fruit, and sprouts collected from the Swiss market," *Journal of food protection,* vol. 75, no. 7, pp. 1338-1341, 2012, doi: 10.4315/0362-028X.JFP-12-022.
[126] G. A. Francis and D. O'Beirne, "Isolation and pulsed-field gel electrophoresis typing of Listeria monocytogenes from modified atmosphere packaged fresh-cut vegetables collected in Ireland," *Journal of food protection,* vol. 69, no. 10, p. 2524, 2006, doi: 10.4315/0362-028X-69.10.2524.
[127] S. Ruiz-Cruz, E. Acedo-Félix, M. Díaz-Cinco, M. A. Islas-Osuna, and G. A. González-Aguilar, "Efficacy of sanitizers in reducing Escherichia coli O157:H7, Salmonella spp. and Listeria monocytogenes populations on fresh-cut carrots," *Food Control,* vol. 18, no. 11, pp. 1383-1390, 2007, doi: 10.1016/j.foodcont.2006.09.008.
[128] K. V. Sy, M. B. Murray, M. D. Harrison, L. R. Beuchat, and K. V. Sy, "Evaluation of gaseous chlorine dioxide as a sanitizer for killing Salmonella, Escherichia coli O157:H7, Listeria monocytogenes, and yeasts and molds on fresh and fresh-cut produce," *Journal of food protection,* vol. 68, no. 6, pp. 1176-1187, 2005, doi: 10.4315/0362-028X-68.6.1176.
[129] A. Kamat, N. Ghadge, M. Ramamurthy, and M. Alur, "Effect of low-dose irradiation on shelf life and microbiological safety of sliced carrot," *Journal of the Science of Food and Agriculture,* vol. 85, no. 13, pp. 2213-2219, 2005, doi: 10.1002/jsfa.2231.
[130] R. J. Meldrum, C. L. Little, S. Sagoo, V. Mithani, J. McLauchlin, and E. de Pinna, "Assessment of the microbiological safety of salad vegetables and sauces from kebab take-away restaurants in the United Kingdom," *Assessment of the microbiological safety of salad vegetables and sauces from kebab take-away restaurants in the United Kingdom,* vol. 26, pp. 573-577, 2009.
[131] J. Hossein, P. Mohammadjavad, Y. L. Chung, and F. W. Won, "Prevalence of Listeria species and Listeria monocytogenes serotypes in ready mayonnaise salads and salad vegetables in Iran," *African Journal of Microbiology Research,* vol. 7, no. 19, pp. 1903-1906, 2013, doi: 10.5897/AJMR2013.5658.
[132] E. Scallan *et al.*, "Foodborne illness acquired in the United States--major pathogens.(RESEARCH)," *Emerging Infectious Diseases,* vol. 17, no. 1, p. 7, 2011, doi: 10.3201/eid1701.P11101.

[133] S. M. H. Easa, "Microorganisms found in fast and traditional fast foods," *Microorganisms found in fast and traditional fast foods,* no. 2, pp. 226-243, 2011.
[134] L. Skalina and V. Nikolajeva, "Growth potential of Listeria monocytogenes strains in mixed ready-to-eat salads," *International Journal of Food Microbiology,* vol. 144, no. 2, pp. 317-321, 2010, doi: 10.1016/j.ijfoodmicro.2010.10.001.
[135] Y. Pan, J. H. Cheng, and D. W. Sun, "Cold Plasma-Mediated Treatments for Shelf Life Extension of Fresh Produce: A Review of Recent Research Developments," *Comprehensive Reviews in Food Science and Food Safety,* vol. 18, no. 5, pp. 1312-1326, 2019, doi: 10.1111/1541-4337.12474.
[136] S. Srey, S. Y. Park, I. K. Jahid, and S.-D. Ha, "Reduction effect of the selected chemical and physical treatments to reduce L. monocytogenes biofilms formed on lettuce and cabbage," *Food Research International,* vol. 62, pp. 484-491, 2014, doi: 10.1016/j.foodres.2014.03.067.
[137] H. Lee, J. E. Kim, M.-S. Chung, and S. C. Min, "Cold plasma treatment for the microbiological safety of cabbage, lettuce, and dried figs," *Food Microbiology,* vol. 51, pp. 74-80, 2015, doi: 10.1016/j.fm.2015.05.004.
[138] N. Matan, K. Puangjinda, S. Phothisuwan, and M. Nisoa, "Combined antibacterial activity of green tea extract with atmospheric radio-frequency plasma against pathogens on fresh-cut dragon fruit," *Food Control,* vol. 50, pp. 291-296, 2015, doi: 10.1016/j.foodcont.2014.09.005.
[139] C. Lo Porto *et al.*, "Plasma activated water and airborne ultrasound treatments for enhanced germination and growth of soybean," *Innovative Food Science and Emerging Technologies,* vol. 49, pp. 13-19, 2018, doi: 10.1016/j.ifset.2018.07.013.
[140] FAO, "Contributing to food security and nutrition for all," *The State of World Fisheris and Aquaculture 2016,* 2016.
[141] P. Stévant, C. Rebours, and A. Chapman, "Seaweed aquaculture in Norway: recent industrial developments and future perspectives," *Aquaculture International,* vol. 25, no. 4, pp. 1373-1390, 2017, doi: 10.1007/s10499-017-0120-7.
[142] S. Holdt and S. Kraan, "Bioactive compounds in seaweed: functional food applications and legislation," *Journal of Applied Phycology,* vol. 23, no. 3, pp. 543-597, 2011, doi: 10.1007/s10811-010-9632-5.
[143] L. O'Sullivan *et al.*, "Prebiotics from Marine Macroalgae for Human and Animal Health Applications," *Marine Drugs,* vol. 8, no. 7, pp. 2038-2064, 2010, doi: 10.3390/md8072038.
[144] T. S. Zaporozhets *et al.*, "The prebiotic potential of polysaccharides and extracts of seaweeds," *Russian Journal of Marine Biology,* vol. 40, no. 1, pp. 1-9, 2014, doi: 10.1134/S1063074014010106.
[145] F. Maghin, "Biological Functions and Health Promoting Effects of Brown Seaweeds in Swine Nutrition," *Journal of Dairy, Veterinary & Animal Research,* vol. 1, no. 1, 2014, doi: 10.15406/jdvar.2014.01.00005.
[146] D. Arne *et al.*, "Potential risks posed by macroalgae for application as feed and food - a Norwegian perspective," ed: National Institute of Nutrition and Seafood research, 2016.
[147] A. B. Ellingsen, "Vibrio parahaemolyticus, V. cholera and V. vulnificus in Norway, with special attention to V. parahaemolyticus.," PhD, Norwegian School of Veterinary Science, 2008.

[148] P. Stévant *et al.*, "Effects of drying on the nutrient content and physico-chemical and sensory characteristics of the edible kelp Saccharina latissima," *Journal of Applied Phycology,* vol. 30, no. 4, pp. 2587-2599, 2018, doi: 10.1007/s10811-018-1451-0.
[149] B. Nisol, S. Watson, Y. Leblanc, S. Moradinejad, M. R. Wertheimer, and A. Zamyadi, "Cold plasma oxidation of harmful algae and associated metabolite BMAA toxin in aqueous suspension," *Plasma Processes and Polymers,* vol. 16, no. 2, p. n/a, 2019, doi: 10.1002/ppap.201800137.
[150] P. Puligundla, J.-W. Kim, and C. Mok, "Effect of low-pressure air plasma on the microbial load and physicochemical characteristics of dried laver," *LWT - Food Science and Technology,* vol. 63, no. 2, pp. 966-971, 2015, doi: 10.1016/j.lwt.2015.04.010.
[151] J.-W. Kim, P. Puligundla, and C. Mok, "Microbial decontamination of dried laver using corona discharge plasma jet (CDPJ)," *Journal of Food Engineering,* vol. 161, pp. 24-32, 2015, doi: 10.1016/j.jfoodeng.2015.03.034.
[152] L. Taiz, E. Zeiger, I. Møller, and A. Murphy, "Mineral nutrition," in *Plant physiology and development* Sunderland Ed. Massachusetts: Sinauer Associates, Inc, 2015, ch. 5, pp. 119-142.
[153] E. Jan Willem, A. S. Mark, G. James, K. Zbigniew, and W. Wilfried, "How a century of ammonia synthesis changed the world," *Nature Geoscience,* vol. 1, no. 10, p. 636, 2008, doi: 10.1038/ngeo325.
[154] C. Meyer, U. Lea, F. Provan, W. Kaiser, and C. Lillo, "Is nitrate reductase a major player in the plant NO (nitric oxide) game?," *Official Journal of the International Society of Photosynthesis Research,* vol. 83, no. 2, pp. 181-189, 2005, doi: 10.1007/s11120-004-3548-3.
[155] R. Basosi, D. Spinelli, A. Fieroo, and S. Jez, "Mineral Nitrogen Fertilizer: Environmental Impact of Production and Use," Italy, 2014, pp. 3-43.
[156] A. Lindsay *et al.*, "Fertilization of Radishes, Tomatoes, and Marigolds Using a Large-Volume Atmospheric Glow Discharge," *Plasma Chemistry and Plasma Processing,* vol. 34, no. 6, pp. 1271-1290, 2014, doi: 10.1007/s11090-014-9573-x.
[157] M. Ito, J. S. Oh, T. Ohta, M. Shiratani, and M. Hori, "Current status and future prospects of agricultural applications using atmospheric-pressure plasma technologies," *Plasma Processes and Polymers,* vol. 15, no. 2, pp. n/a-n/a, 2018, doi: 10.1002/ppap.201700073.
[158] K. Takaki *et al.*, "Improvements in plant growth rate using underwater discharge," *Journal of Physics: Conference Series,* vol. 418, no. 1, p. 012140, 2013, doi: 10.1088/1742-6596/418/1/012140.
[159] B. Adhikari, M. Adhikari, B. Ghimire, G. Park, E. H. Choi, and B. Adhikari, "Cold Atmospheric Plasma-Activated Water Irrigation Induces Defense Hormone and Gene expression in Tomato seedlings," *Scientific reports,* vol. 9, no. 1, pp. 16080-16080, 2019, doi: 10.1038/s41598-019-52646-z.
[160] L. Sivachandiran and A. Khacef, "Enhanced seed germination and plant growth by atmospheric pressure cold air plasma: combined effect of seed and water treatment," *RSC Adv.,* vol. 7, no. 4, pp. 1822-1832, 2017, doi: 10.1039/c6ra24762h.
[161] G. Eisenberg, "Colorimetric Determination of Hydrogen Peroxide," *Industrial & Engineering Chemistry Analytical Edition,* vol. 15, no. 5, pp. 327-328, 1943, doi: 10.1021/i560117a011.

[162] C. Gay and J. M. Gebicki, "A Critical Evaluation of the Effect of Sorbitol on the Ferric–Xylenol Orange Hydroperoxide Assay," *Analytical Biochemistry,* vol. 284, no. 2, pp. 217-220, 2000, doi: 10.1006/abio.2000.4696.
[163] "Regulations," *Official Journal of the European Union* 2011. [Online]. Available: https://webgate.ec.europa.eu/foods_system/main/?event=document.view&identifier=2581&documentCrossTable=legislation&documentType=legislation&documentTypeIdentifier=-1.
[164] D. R. Hoagland and D. J. Arnon, "The water culture method for growing plants without soil," *Circular, California Agriculture Experiment station,* vol. 347, p. 32, 1950.
[165] C.-M. Lin *et al.*, "The Optimization of Plasma-Activated Water Treatments to Inactivate Salmonella Enteritidis (ATCC 13076) on Shell Eggs," *Foods (Basel, Switzerland),* vol. 8, no. 10, 2019, doi: 10.3390/foods8100520.
[166] T. Abuzairi, S. Ramadhanty, D. F. Puspohadiningrum, A. Ratnasari, N. R. Poespawati, and R. W. Purnamaningsih, "Investigation on physicochemical properties of plasma-activated water for the application of medical device sterilization," vol. 1933, ed, 2018.
[167] T. V. Suslow, "Oxidation-Reduction Potential (ORP) for Water Disinfection Monitoring, Control, and Documentation," vol. 8149. [Online]. Available: https://www.water-research.net/pdf/orpdisinfection.pdf
[168] B. R. Locke and K.-Y. Shih, "Review of the methods to form hydrogen peroxide in electrical discharge plasma with liquid water," *Plasma Sources Science and Technology,* vol. 20, no. 3, p. 034006, 2011, doi: 10.1088/0963-0252/20/3/034006.
[169] M. S. Rayson, J. C. Mackie, E. M. Kennedy, and B. Z. Dlugogorski, "Accurate Rate Constants for Decomposition of Aqueous Nitrous Acid," *Inorganic Chemistry,* vol. 51, no. 4, pp. 2178-2185, 2012, doi: 10.1021/ic202081z.
[170] D. Thomas and J. Vanderschuren, "Modeling of NO x Absorption into Nitric Acid Solutions Containing Hydrogen Peroxide," *Industrial & Engineering Chemistry Research,* vol. 36, no. 8, pp. 3315-3322, 1997, doi: 10.1021/ie960436g.
[171] "Comprehensive Reviews Food Science and food Safety," *Journal of Food Science,* vol. 2, pp. 46 - 50, 2003.
[172] K. H. Baek *et al.*, "Antimicrobial effects and mechanism of plasma activated fine droplets produced from arc discharge plasma on planktonic listeria monocytogenes and escherichia coli o157:h7," *Journal of Physics D: Applied Physics,* vol. 53, no. 12, p. 124002, 2020, doi: 10.1088/1361-6463/ab634d.
[173] C. Smet, M. Govaert, A. Kyrylenko, M. Easdani, J. L. Walsh, and J. F. Van Impe, "Inactivation of Single Strains of and Typhimurium Planktonic Cells Biofilms With Plasma Activated Liquids," *Frontiers in microbiology,* vol. 10, no. JULY, p. 1539, 2019, doi: 10.3389/fmicb.2019.01539.
[174] F. Chemat, E. H. Zill, and M. K. Khan, "Applications of ultrasound in food technology: Processing, preservation and extraction," *Ultrasonics - Sonochemistry,* vol. 18, no. 4, pp. 813-835, 2011, doi: 10.1016/j.ultsonch.2010.11.023.
[175] M. Cameron, L. McMaster, and T. Britz, "Impact of ultrasound on dairy spoilage microbes and milk components," *Dairy Science & Technology,* vol. 89, no. 1, pp. 83-98, 2009, doi: 10.1051/dst/2008037.
[176] T. J. Mason, E. Joyce, S. S. Phull, and J. P. Lorimer, "Potential uses of ultrasound in the biological decontamination of water," *Ultrasonics - Sonochemistry,* vol. 10, no. 6, pp. 319-323, 2003, doi: 10.1016/S1350-4177(03)00102-0.

[177] T. Royintarat, E. H. Choi, D. Boonyawan, P. Seesuriyachan, W. Wattanutchariya, and T. Royintarat, "Chemical-free and synergistic interaction of ultrasound combined with plasma-activated water (PAW) to enhance microbial inactivation in chicken meat and skin," *Scientific reports,* vol. 10, no. 1, pp. 1559-1559, 2020, doi: 10.1038/s41598-020-58199-w.
[178] A. S. Sant'Ana, M. C. Igarashi, M. Landgraf, M. T. Destro, and B. D. G. M. Franco, "Prevalence, populations and pheno- and genotypic characteristics of Listeria monocytogenes isolated from ready-to-eat vegetables marketed in São Paulo, Brazil," *International Journal of Food Microbiology,* vol. 155, no. 1-2, pp. 1-9, 2012, doi: 10.1016/j.ijfoodmicro.2011.12.036.
[179] S. Wang and R. H. Orsi, *Chapter 11 - Listeria*, Fourth Edition ed. Elsevier Inc, 2013, pp. 199-216.
[180] J. M. Jay, M. J. Loessner, and D. A. Golden, "Foodborne Listeriosis," in *Modern Food Microbiology* D. R. Heldmann Ed.: Springer Science + Buisness Media, Inc. , 2005, ch. 25, pp. 591-618.
[181] C. Rolin, R. Inkster, J. Laing, and L. McEvoy, "Regrowth and biofouling in two species of cultivated kelp in the Shetland Islands, UK," *Journal of Applied Phycology,* vol. 29, no. 5, pp. 2351-2361, 2017/10/01 2017, doi: 10.1007/s10811-017-1092-8.
[182] M. Wahl *et al.*, "Ecology of antifouling resistance in the bladder wrack Fucus vesiculosus : patterns of microfouling and antimicrobial protection," *Marine Ecology Progress Series,* vol. 411, pp. 33-48, 2010.
[183] M. M. Bengtsson, K. Sjøtun, and L. Øvreås, "Seasonal dynamics of bacterial biofilms on the kelp Laminaria hyperborea," 2010.
[184] C. Park and E. Hwang, "Seasonality of epiphytic development of the hydroid Obelia geniculata on cultivated Saccharina japonica (Laminariaceae, Phaeophyta) in Korea," *Journal of Applied Phycology,* vol. 24, no. 3, pp. 433-439, 2012, doi: 10.1007/s10811-011-9755-3.
[185] C. Peteiro and Ó. Freire, "Epiphytism on Blades of the Edible Kelps Undaria pinnatifida and Saccharina latissima Farmed under Different Abiotic Conditions," *Journal of the World Aquaculture Society,* vol. 44, no. 5, pp. 706-715, 2013, doi: 10.1111/jwas.12065.
[186] H. Førde *et al.*, "Development of bryozoan fouling on cultivated kelp (Saccharina latissima) in Norway," *Journal of Applied Phycology,* vol. 28, no. 2, pp. 1225-1234, 2016, doi: 10.1007/s10811-015-0606-5.
[187] E. Malmhäll-Bah, "Targeted microbial ensilage additives for Laminaria digitata and Saccharina latissima," Masters degree, Department of Biology and Biological Engineering, Chalmers University of Technology Gothenburg, Sweden, 2017.
[188] J. A. Gallagher, L. B. Turner, J. M. M. Adams, P. W. Dyer, and M. K. Theodorou, "Dewatering treatments to increase dry matter content of the brown seaweed, kelp (Laminaria digitata ((Hudson) JV Lamouroux))," *Bioresource Technology,* vol. 224, no. C, pp. 662-669, 2017, doi: 10.1016/j.biortech.2016.11.091.
[189] F. Turantaş, G. B. Kılıç, and B. Kılıç, "Ultrasound in the meat industry: General applications and decontamination efficiency," *International Journal of Food Microbiology,* vol. 198, pp. 59-69, 2015, doi: 10.1016/j.ijfoodmicro.2014.12.026.
[190] R. F. H. Giehl and N. von Wirén, "Root nutrient foraging," (in eng), *Plant physiology,* vol. 166, no. 2, pp. 509-517, 2014, doi: 10.1104/pp.114.245225.

[191] Z. Shahzad and A. Amtmann, "Food for thought: how nutrients regulate root system architecture," *Current Opinion in Plant Biology,* vol. 39, pp. 80-87, 2017, doi: 10.1016/j.pbi.2017.06.008.
[192] M. Černý, H. Habánová, M. Berka, M. Luklová, B. Brzobohatý, and M. Černý, "Hydrogen Peroxide: Its Role in Plant Biology and Crosstalk with Signalling Networks," *International journal of molecular sciences,* vol. 19, no. 9, 2018, doi: 10.3390/ijms19092812.
[193] M. C. Palmieri *et al.*, "Nitric oxide-responsive genes and promoters in Arabidopsis thaliana: a bioinformatics approach," *Journal of experimental botany,* vol. 59, no. 2, pp. 177-186, 2008, doi: 10.1093/jxb/erm345.
[194] M. L. Garbin and L. R. Dillenburg, "Effects of different nitrogen sources on growth, chlorophyll concentration, nitrate reductase activity and carbon and nitrogen distribution in Araucaria angustifolia," *Brazilian Journal of Plant Physiology,* vol. 20, no. 4, pp. 295-303, 2008, doi: 10.1590/S1677-04202008000400005.
[195] Y. Zheng, L. Tian, H. Liu, Q. Pan, J. Zhan, and W. Huang, "Sugars induce anthocyanin accumulation and flavanone 3-hydroxylase expression in grape berries," *An International Journal on Plant Growth and Development,* vol. 58, no. 3, pp. 251-260, 2009, doi: 10.1007/s10725-009-9373-0.
[196] A. Carstensen *et al.*, "The Impacts of Phosphorus Deficiency on the Photosynthetic Electron Transport Chain," *Plant Physiology,* vol. 177, no. 1, pp. 271-284, 2018, doi: 10.1104/pp.17.01624.
[197] G. J. F. Smolders, J. Van Der Meij, M. C. M. Van Loosdrecht, and J. J. Heijnen, "Model of the anaerobic metabolism of the biological phosphorus removal process: Stoichiometry and pH influence," *Biotechnology and Bioengineering,* vol. 43, no. 6, pp. 461-470, 1994, doi: 10.1002/bit.260430605.
[198] L. Ding *et al.*, "Effects of nitrogen deficiency on photosynthetic traits of maize hybrids released in different years," (in eng), *Ann Bot,* vol. 96, no. 5, pp. 925-930, 2005, doi: 10.1093/aob/mci244.
[199] S. Islam *et al.*, "Effects of LPDBD Plasma and Plasma Activated Water on Germination and Growth in Rapeseed (Brassica napus)," *Pflanzenschutz - Verbraucherschutz - Umweltschutz,* vol. 71, no. 3, pp. 175-185, 2019, doi: 10.1007/s10343-019-00463-9.
[200] M. Suzuki, "Enhancement of Anthocyanin Accumulation by High Osmotic Stress and Low pH in Grape Cells (Vitis hybrids)," *Journal of Plant Physiology,* vol. 147, no. 1, pp. 152-155, 1995, doi: 10.1016/S0176-1617(11)81428-8.
[201] Y. Jiang, Y. Li, Q. Zeng, J. Wei, and H. Yu, "The effect of soil in pH on plant growth, leaf chlorophyll fluorescence and mineral element concent of two blueberries. ," *Acta Hortic,* vol. 1180, pp. 269-276, 2017, doi: 10.17660/actahortic.2017.1180.36
[202] R. Gentili, R. Ambrosini, C. Montagnani, S. Caronni, and S. Citterio, "Effect of Soil pH on the Growth, Reproductive Investment and Pollen Allergenicity of Ambrosia artemisiifolia L," (in eng), *Front Plant Sci,* vol. 9, pp. 1335-1335, 2018, doi: 10.3389/fpls.2018.01335.
[203] R. van den Driessche, R. van den Driessche, Ed. *Mineral Nutrition of Conifer Seedlings*. Canada: CRC Press, Inc, 1991.
[204] A. Seither, P. E. Eide, T. Berg, and B. Frengstad, "The inorganic drinking water quality of some groundwaterworks and regulated wells in Norway," NGU, Trondheim, Norway, 2012.073, 2012.

[205] B. Singh and D. G. Schulze, "Soil Minerals and Plant Nutrition," *Nature education Knowledge,* vol. 6, no. 1, 2015.
[206] C. Martínez-Andújar, M. E. Ghanem, A. Albacete, and F. Pérez-Alfocea, "Response to nitrate/ammonium nutrition of tomato (Solanum lycopersicum L.) plants overexpressing a prokaryotic NH4+-dependent asparagine synthetase," *Journal of Plant Physiology,* vol. 170, no. 7, pp. 676-687, 2013, doi: 10.1016/j.jplph.2012.12.011.
[207] P. Flores, M. Carvajal, A. Cerdá, and V. Martínez, "SALINITY AND AMMONIUM/NITRATE INTERACTIONS ON TOMATO PLANT DEVELOPMENT, NUTRITION, AND METABOLITES," *Journal of Plant Nutrition,* vol. 24, no. 10, pp. 1561-1573, 2001, doi: 10.1081/PLN-100106021.
[208] M. Ghanem *et al.*, "Nitrogen Form Alters Hormonal Balance in Salt-treated Tomato (Solanum lycopersicum L.)," *Journal of Plant Growth Regulation,* vol. 30, no. 2, pp. 144-157, 2011, doi: 10.1007/s00344-010-9178-4.
[209] D. Britto, A. Glass, and H. Kronzucker, "Cytosolic concentrations and transmembrane fluxes of NH4+/NH3. An evaluation of recent proposals," *Plant Physiology,* vol. 125, no. 2, pp. 523-6, 2001, doi: 10.1104/pp.125.2.523.
[210] G. Barba-Espin *et al.*, "Interaction between hydrogen peroxide and plant hormones during germination and the early growth of pea seedlings," *Plant, Cell & Environment,* vol. 33, no. 6, pp. 981-994, 2010, doi: 10.1111/j.1365-3040.2010.02120.x.
[211] M. M. Khandaker, A. N. Boyce, and N. Osman, "The influence of hydrogen peroxide on the growth, development and quality of wax apple (Syzygium samarangense, [Blume] Merrill & L.M. Perry var. jambu madu) fruits," *Plant Physiology and Biochemistry,* vol. 53, pp. 101-110, 2012, doi: 10.1016/j.plaphy.2012.01.016.
[212] M. M. Khandaker, S. Z. Ismail, N. Mat, and A. N. Boyce, "Effects of Hydrogen Peroxide on Growth, Development and Quality of Fruits: A Review," *Journal of Agronomy,* vol. 14, no. 4, pp. 331-336, 2015, doi: 10.3923/ja.2015.331.336.
[213] L. J. Quan, B. Zhang, W. W. Shi, and H. Y. Li, "Hydrogen Peroxide in Plants: a Versatile Molecule of the Reactive Oxygen Species Network," *Journal of Integrative Plant Biology,* vol. 50, no. 1, pp. 2-18, 2008, doi: 10.1111/j.1744-7909.2007.00599.x.
[214] S. Orabi, M. Moursy, S.-N. Zaki, and F. Sharara, "Influence of hydrogen peroxide on growth, yield and biochemical constituents of canola plants grown under different irrigation intervals," *Current science,* vol. 07, pp. 407-418, 08/20 2018.
[215] N. Habib *et al.*, "Use of Nitric Oxide and Hydrogen Peroxide for Better Yield of Wheat (L.) under Water Deficit Conditions: Growth, Osmoregulation, and Antioxidative Defense Mechanism," *Plants (Basel, Switzerland),* vol. 9, no. 2, 2020, doi: 10.3390/plants9020285.
[216] WesCEF, "Safety Data Sheet: Ammonium Nitrate," 2017. [Online]. Available: csbp.com.au/docs/default-source/msds---products/ammonia-ammonium-nitrate-products/msds_ammonium-nitrate.pdf?sfvrsn=4cc56c0d_31
[217] U. M. Sainju, B. P. Singh, and W. F. Whitehead, "Tillage, Cover Crops, and Nitrogen Fertilization Effects on Cotton and Sorghum Root Biomass, Carbon, and Nitrogen," *Agronomy Journal,* vol. 97, no. 5, pp. 1279-1290, 2005, doi: 10.2134/agronj2004.0213.
[218] N. Fageria and A. Moreira, "The Role of Mineral Nutrition on Root Growth of Crop Plants," *Advances in Agronomy,* vol. 110, pp. 251-331, 2011, doi: 10.1016/B978-0-12-385531-2.00004-9.

[219] R. W. Zobel, "Rhizogenetics (root genetics) of vegetable crops," *Rhizogenetics (root genetics) of vegetable crops,* no. 4, pp. 956-959, 1986.
[220] L. Zhao, F. Liu, N. M. Crawford, Y. Wang, and L. Zhao, "Molecular Regulation of Nitrate Responses in Plants," *International journal of molecular sciences,* vol. 19, no. 7, 2018, doi: 10.3390/ijms19072039.
[221] M. Shafi and O. Binta, "Plasma activated water: the next generation eco-friendly stimulant for enhancing plant seed germination, vigor and increased enzyme activity, a study on black gram (Vigna mungo L.)," *Plasma Chemistry and Plasma Processing,* vol. 40, no. 1, pp. 119-143, 2020, doi: 10.1007/s11090-019-10028-3.
[222] B. Liu, B. Honnorat, H. Yang, J. Arancibia, L. Rajjou, and A. Rousseau, "Non-thermal dbd plasma array on seed germination of different plant species," *Journal of Physics D: Applied Physics,* vol. 52, no. 2, p. 025401, 2019, doi: 10.1088/1361-6463/aae771.

Appendix

A. Composition of PAW

The values used when making the graphs that demonstrates the trends in concentration for the reactive species, directly after treatment and for storage are listed in Table 25 - 33

Table 25. The exact ORP value directly after treatment and for four weeks storage

		Oxidation reduction potential (mV)					
		0 D	1 D	7 D	14 D	21 D	28 D
H-30	4 ºC	284.1±11.5	280.1±2.1	278.6±2.3	277.4±1.7	283.7±7.5	275.7±3.6
	10 ºC	284.1±11.5	277.9±1.0	276.9±2.0	276.3±0.8	280.9±5.7	275.7±1.2
	- 20 ºC	284.1±11.5	275.4±2.5	277.4±2.2	276.8±2.6	280.2±5.4	275.9≈3.2
L-30	4 ºC	267.3±2.5	269.4±1.4	267.6±2.9	270.8±1.2	273.0±5.4	267.1±2.3
	10 ºC	267.3±2.5	267.5±2.9	268.5±0.9	266.7±2.3	272.3±4.6	266.6±0.9
	- 20 ºC	267.3±2.5	265.2±0.6	267.5±2.9	268.0±2.3	270.0±4.1	265.3±2.1
H-10	4 ºC	231.7±3.8	234.4±8.4	236.1±6.2	238.5±5.9	235.0±3.7	237.6±3.1
	10 ºC	231.7±3.8	232.6±10.4	234.1~2.7	238.7±3.3	253.3±2.7	237.5±2.9
	- 20 ºC	231.7±3.8	231.6±12.8	234.9±5.2	239.0±4.4	235.4±2.9	236.7±2.9
L-10	4 ºC	200.2±19	202.5±26	205.6±13	207.7±14	203.0±9	205.3±11
	10 ºC	200.2±19	201.9±27	207.1±8	208.4±9	203.2±11	204.6±13
	- 20 ºC	200.2±19	204.1±25	207.2±12	207.9±16	202.5±13	203.8±15

Table 26. The exact pH value directly after treatment and for four weeks storage

		pH					
		0 D	1 D	7 D	14 D	21 D	28 D
H-30	4 ºC	2.51 ± 0.5	2.47 ± 0.03	2.47±0.04	2.51±0.03	2.46±0.06	2.52±0.05
	10 ºC	2.51 ± 0.5	2.49 ± 0.01	2.51±0.03	2.51±0.02	2.47±0.06	2.52±0.02
	- 20 ºC	2.51 ± 0.5	2.54 ± 0.05	2.51±0.05	2.52±0.04	2.49±0.05	2.53±0.06
L-30	4 ºC	2.68 ± 0.02	2.64 ± 0.03	2.68±0.04	2.62±0.03	2.63±0.04	2.67±0.05
	10 ºC	2.68 ± 0.02	2.67 ± 0.04	2.68±0.02	2.70±0.04	2.63±0.04	2.69±0.01
	- 20 ºC	2.68 ± 0.02	2.70 ± 0.0	2.68±0.07	2.67±0.05	2.69±0.04	2.70±0.03
H-10	4 ºC	3.27 ± 0.06	3.27 ± 0.20	3.23±0.10	3.20±0.12	3.22±0.07	3.19±0.06
	10 ºC	3.27 ± 0.06	3.27 ± 0.19	3.26±0.04	3.18±0.06	3.23±0.06	3.19±0.05
	- 20 ºC	3.27 ± 0.06	3.29 ± 0.23	4.24±0.09	3.21±0.13	3.22±0.07	3.20±0.06
L-10	4 ºC	3.90 ± 0.26	3.78 ± 0.40	3.75±0.22	3.72±0.24	3.78±0.17	3.75±0.18
	10 ºC	3.90 ± 0.26	3.81 ± 0.46	3.75±0.14	3.71±0.16	3.78±0.19	3.76±0.21
	- 20 ºC	3.90 ± 0.26	3.80 ± 0.40	3.74±0.19	3.71±0.25	3.77±0.20	3.77±0.25

Table 27. The exact concentration of nitrate directly after treatment and for four weeks storage

Nitrite (mg/L)							
		0 D	1 D	7 D	14 D	21 D	28 D
H-30	4 ºC	1.57 ± 0.12	0.23 ± 0.09	0.51 ± 0.34	0.59 ± 0.36	0.36 ± 0.08	0.44 ± 0.20
	10 ºC	1.57 ± 0.12	0.19 ± 0.04	0.45 ± 0.32	0.45± 0.24	0.28 ± 0.09	0.30 ± 0.13
	- 20 ºC	1.57 ± 0.12	ND	ND	ND	ND	ND
L-30	4 ºC	1.0 ± 0.06	ND	ND	ND	ND	ND
	10 ºC	1.0 ± 0.06	ND	ND	ND	ND	ND
	- 20 ºC	1.0 ± 0.06	ND	ND	ND	ND	ND
H-10	4 ºC	0.41 ± 0.07	ND	ND	ND	ND	ND
	10 ºC	0.41 ± 0.07	ND	ND	ND	ND	ND
	- 20 ºC	0.41 ± 0.07	ND	ND	ND	ND	ND
L-10	4 ºC	0.15 ± 0.10	ND	ND	ND	ND	ND
	10 ºC	0.15 ± 0.10	ND	ND	ND	ND	ND
	- 20 ºC	0.15 ± 0.10	ND	ND	ND	ND	ND

Table 28. The exact concentration of nitrate directly after treatment and during four weeks storage

Nitrate (mg/L)							
		0 D	1 D	7 D	14 D	21 D	28 D
H-30	4 ºC	342.5 ± 13.5	336 ± 16.2	336.5 ± 22.4	340.1 ± 23.0	342.6 ± 23.1	346. 0 ± 23.7
	10 ºC	342.5 ± 13.5	340.8 ± 11.3	339.3 ± 34.8	339.5 ± 24.3	338.6 ± 29.2	341.6 ± 27.1
	- 20 ºC	342.5 ± 13.5	306.0 ± 23.1	324.5 ± 33.6	334.0 ± 24.2	324.4 ± 20.6	332.7 ± 23.7
L-30	4 ºC	278.3 ± 19.8	252.7 ± 14.1	261.1 ± 13.6	258.1 ± 5.2	258.6 ± 6.9	256.4 ± 3.0
	10 ºC	278.3 ± 19.8	248.4 ± 16.6	258.8 ± 4.23	261 ± 2.4	254.4 ± 4.6	256.0 ± 3.0
	- 20 ºC	278.3 ± 19.8	245.7 ± 12.1	434.8 ± 11	260.1 ± 6.1	241.1 ± 13.4	230.2 ± 18.1
H-10	4 ºC	109.2 ± 6.0	103.7 ± 16.9	112.6 ± 4.9	115.5 ± 8.6	114.1 ± 7.3	111.2 ± 1.9
	10 ºC	109.2 ± 6.0	105.2 ± 17.2	110.6 ± 6.6	113.7 ± 8.0	111.7 ± 8.8	98.0 ± 21.5
	- 20 ºC	109.2 ± 6.0	100.7 ± 20.6	111.8 ± 4.7	114.0 ± 9.1	110.6 ± 8.8	1066.2 ± 5.9
L-10	4 ºC	76.9 ± 7.7	70.6 ± 15.1	82.6 ± 11.6	79.3 ± 3.2	79.8 ± 3.6	75.9 ± 6.9
	10 ºC	76.9 ± 7.7	69.9 ± 15.4	83.5 ± 11.8	78.9 ± 5.6	80.4 ± 3.1	79.6 ± 5.5
	- 20 ºC	76.9 ± 7.7	69.6 ± 14	80.1 ± 12.4	79.8 ± 7.6	77.1 ± 2.9	74.5 ± 7.0

Table 29. The exact concentration of hydronium ion directly after treatment and for four weeks storage

		H_3O^+ (mM)					
		0 D	1 D	7 D	14 D	21 D	28 D
H-30	4 ºC	3.08±0.36	3.39±0.20	3.37±0.3	3.12±0.22	3.49±0.47	3.06±0.32
	10 ºC	3.08±0.36	3.21±0.09	3.07±0.22	3.09±0.12	3.44±0.48	3.04±0.11
	- 20 ºC	3.08±0.36	2.87±0.32	3.13±0.37	3.03±0.31	3.23±0.38	2.99±0.37
L-30	4 ºC	2.09±0.08	2.29±0.14	2.11±0.21	2.42±0.16	2.33±0.19	2.13±0.22
	10 ºC	2.09±0.08	2.16±0.18	2.09±0.82	2.02±0.17	2.35±0.19	2.06±0.05
	- 20 ºC	2.09±0.08	2±0	2.09±0.33	2.13±0.23	2.05±0.17	2.01±0.12
H-10	4 ºC	0.54±0.07	0.57±0.23	0.59±0.13	0.65±0.16	0.61±0.09	0.65±0.08
	10 ºC	0.54±0.07	0.57±0.22	0.55±0.04	0.66±0.08	0.60±0.07	0.65±0.07
	- 20 ºC	0.54±0.07	0.56±0.24	0.58±0.12	0.64±0.18	0.60±0.09	0.63±0.08
L-10	4 ºC	0.14±0.07	0.21±0.17	0.19±0.09	0.21±0.10	0.17±0.06	0.19±0.07
	10 ºC	0.14±0.07	0.21±0.16	0.19±0.05	0.20±0.07	0.18±0.06	0.19±0.08
	- 20 ºC	0.14±0.07	0.21±0.17	0.19±0.07	0.22±0.10	0.18±0.07	0.19±0.09

Table 30. The exact concentration of hydroxide ion directly after treatment and for four weeks storage

		OH^- (pM)					
		0 D	1 D	7 D	14 D	21 D	28 D
H-30	4 ºC	0.059 ± 0.012	0.066 ± 0.10	0.078 ± 0.0069	0.079 ± 0.0044	0.057 ± 0.029	0.087 ± 0.013
	10 ºC	0.059 ± 0.012	0.078 ± 0.0006	0.081 ± 0.0074	0.080 ± 0.0044	0.067 ± 0.023	0.085 ± 0.0036
	- 20 ºC	0.059 ± 0.012	0.086 ± 0.0067	0.082 ± 0.0073	0.082 ± 0.0076	0.066 ± 0.023	0.086 ± 0.011
L-30	4 ºC	0.10 ± 0.004	0.11 ± 0.004	0.12 ± 0.011	0.10 ± 0.007	0.085 ± 0.036	0.12 ± 0.010
	10 ºC	0.10 ± 0.004	0.12 ± 0.012	0.12 ± 0.004	0.13 ± 0.011	0.091 ± 0.030	0.13 ± 0.006
	- 20 ºC	0.10 ± 0.004	0.13 ± 0.01	0.12 ± 0.016	0.12 ± 0.010	0.098 ± 0.034	0.13 ± 0.006
H-10	4 ºC	0.65 ± 0.078	0.40 ± 0.073	0.45 ± 0.09	0.39 ± 0.11	0.46 ± 0.07	0.40 ± 0.054
	10 ºC	0.65 ± 0.078	0.50 ± 0.22	0.46 ± 0.04	0.39 ± 0.08	0.46 ± 0.06	0.40 ± 0.047
	- 20 ºC	0.65 ± 0.078	0.53 ± 0.29	0.44 ± 0.09	0.42 ± 0.14	0.44 ± 0.03	0.42 ± 0.053
L-10	4 ºC	3.59 ± 2.39	2.02 ± 1.73	1.59 ± 0.99	1.46 ± 0.87	1.82 ± 0.77	1.55 ± 0.72
	10 ºC	3.59 ± 2.39	2.4 ± 2.39	1.48 ± 0.61	1.35 ± 0.56	1.74 ± 0.84	1.61 ± 0.89
	- 20 ºC	3.59 ± 2.39	2.04 ± 1.79	1.45 ± 0.77	1.45 ± 0.92	1.78 ± 0.92	1.75 ± 1.14

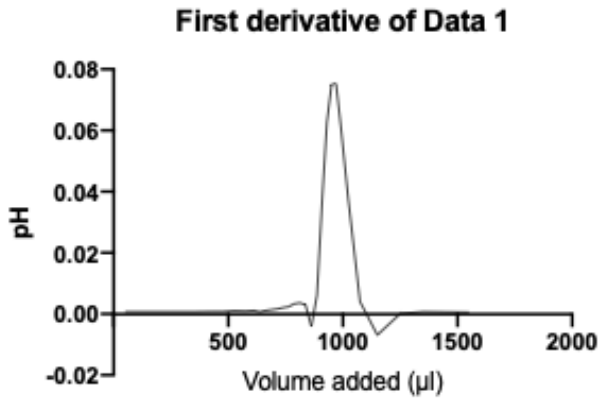

A.

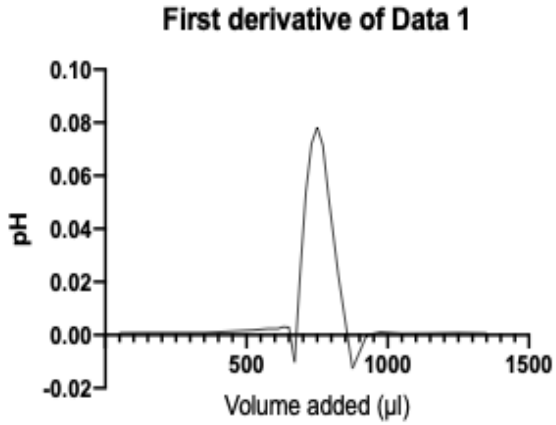

B.

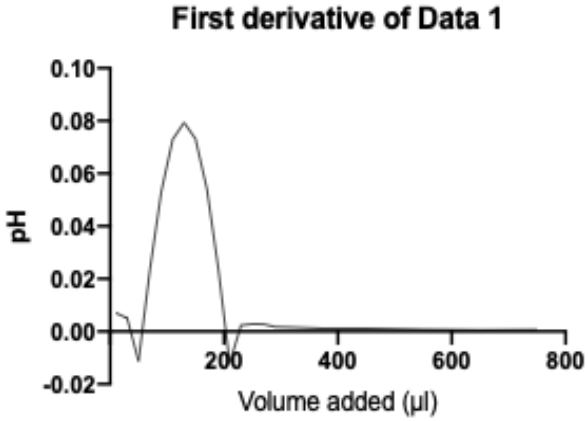

C.

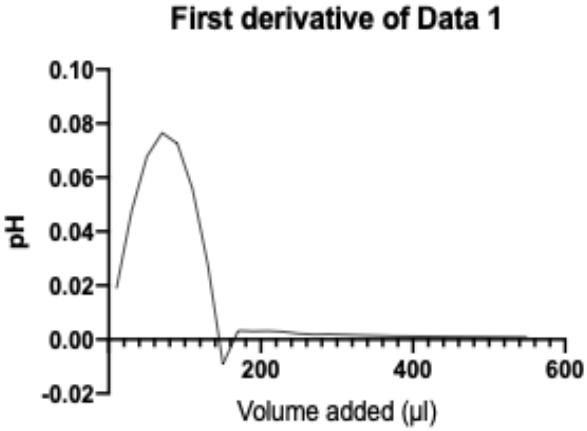

D.

*Figure 53. The first derivative graphs for **A)** H-30 **B)** L-30 **C)** H-10 **D)** L-10*

Table 31. The exact concentration of carbonic compounds directly after treatment and for four weeks storage

Total concentration of carbonic compounds (mM)						
		0 D	1 D	7 D	14 D	28 D
H-30	4 ºC	1.39 ± 0.26	1.16 ±– 0.21	1.28 ± 0.34	1.50 ± 0.12	1.46 ± 0.02
	10 ºC	1.39 ± 0.26	1.45 ± 0.13	1.54 ± 0.34	1.59 ± 0.26	1.47 ± 0.30
	- 20 ºC	1.39 ± 0.26	1.31 ± 0.22	1.34 ± 0.47	1.34 ± 0.22	1.38 ± 0.21
L-30	4 ºC	1.26 ± 0.48	0.76 ± 0.22	1.14 ± 0.21	0.80 ± 0.29	1.05 ± 0.13
	10 ºC	1.26 ± 0.48	0.89 ± 0.02	1.15 ± 0.14	1.23 ± 0.19	1.13 ± 0.06
	- 20 ºC	1.26 ± 0.48	1.02 ± 0.23	1.09 ± 0.26	1.15 ± 0.30	0.94 ± 0.30
H-10	4 ºC	0.31 ± 0.15	0.15 ± 0.13	0.19 ± 0.09	0.12 ± 0.04	0.13 ± 0.07
	10 ºC	0.31 ± 0.15	0.18 ± 0.14	0.30 ± 0.06	0.12 ± 0.03	0.13 ± 0.05
	- 20 ºC	0.31 ± 0.15	0.21 ± 0.13	0.24 ± 0.06	0.11 ± 0.08	0.15 ± 0.04
L-10	4 ºC	0.13 ± 0.02	0.10 ± 0.04	0.09 ± 0.05	0.01 ± 0.05	0.06 ± 0.06
	10 ºC	0.13 ± 0.02	0.09 ± 0.02	0.10 ± 0.07	0.05 ± 0.06	0.06 ± 0.04
	- 20 ºC	0.13 ± 0.02	0.08 ± 0.03	0.02 ± 0.02	0.03 ± 0.07	0.03 ± 0.03

Table 32. The exact concentration of carbonic acid directly after treatment and for four weeks storage

		H_2CO_3 (μM)				
		0 D	1 D	7 D	14 D	28 D
H-30	4 ºC	693.3 ± 131.9	578.7 ± 103.1	639.4 ± 170.5	748.7 ± 58.2	730.8 ± 12.3
	10 ºC	693.3 ± 131.9	727.3 ± 62.9	772.2 ± 172.4	795.7 ± 129.1	736.0 ± 150.7
	- 20 ºC	693.3 ± 131.9	654.9 ± 108.3	669.4 ± 233.9	668.1 ± 108.8	688.5 ± 104.0
L-30	4 ºC	627.7 ± 239.5	378.1 ± 111.0	569.0 ± 103.2	397.9 ± 145.4	527.0 ± 64.7
	10 ºC	627.7 ± 239.5	445.4 ± 12.5	575.6 ± 71.9	617.1 ± 92.9	562.6 ± 28.0
	- 20 ºC	627.7 ± 239.5	510.6 ± 112.7	546.7 ± 129.2	576.7 ± 150.9	468.5 ± 147.8
H-10	4 ºC	152.7 ± 75.2	74.0 ± 65.6	94.6 ± 45.4	62.2 ± 22.2	64.6 ± 33.6
	10 ºC	152.7 ± 75.2	92.3 ± 72.1	151.7 ± 28.1	61.9 ± 15.7	65.1 ± 25.4
	- 20 ºC	152.7 ± 75.2	105.2 ± 62.6	118.6 ± 29.5	55.7 ± 39.0	76.9 ± 1
L-10	4 ºC	63.0 ± 10.6	51.8 ± 21.2	45.8 ± 26.2	15.8 ± 11.3	31.2 ± 28
	10 ºC	63.0 ± 10.6	43.4 ± 11.9	49.2 ± 33	36.2 ± 34.2	30.9 ± 19.0
	- 20 ºC	63.0 ± 10.6	39.8 ± 13.2	17.2 ± 2.3	37.2 ± 13.9	15.6 ± 13.9

Table 33. The exact concentration of bicarbonate directly after treatment and for four weeks storage

		HCO_3^- (nM)				
		0 D	1 D	7 D	14 D	28 D
H-30	4 ºC	96.7 ± 19.1	73.3 ± 16.5	80.7 ± 20.0	102.4 ± 4.2	102.9 ± 11.7
	10 ºC	96.7 ± 19.1	96.7 ± 9.1	106.6 ± 17.3	109.4 ± 13.9	103.2 ± 21.7
	- 20 ºC	96.7 ± 19.1	97.9 ± 19.2	91.2 ± 31.3	95.1 ± 21.6	99.8 ± 23
L-30	4 ºC	129.4 ± 54.5	71.0 ± 23	116.9 ± 31.0	71.4 ± 31.0	107.1 ± 23.1
	10 ºC	129.4 ± 54.5	88.4 ± 7.4	117.8 ± 18.0	132.3 ± 31.3	116.7 ± 7.7
	- 20 ºC	129.4 ± 54.5	109.2 ± 24.1	115.8 ± 40.8	118.2 ± 40.2	100.1 ± 35.5
H-10	4 ºC	120.7 ± 64.8	48.3 ± 30.4	72.2 ± 39.1	44.9 ± 25.8	42.1 ± 22.0
	10 ºC	120.7 ± 64.8	60.1 ± 37.7	117.7 ± 12.5	39.6 ± 5.5	41.8 ± 13.6
	- 20 ºC	120.7 ± 64.8	75.5 ± 24.5	93.3 ± 45	44.7 ± 41.1	53.6 ± 21.0
L-10	4 ºC	231.4 ± 126.1	135.5 ± 120.6	108.3 ± 51.5	56.7 ± 60.1	72.6 ± 50.5
	10 ºC	231.4 ± 126.1	181.4 ± 209.5	104.6 ± 60.3	76.7 ± 50.7	75.9 ± 40.1
	- 20 ºC	231.4 ± 126.1	133.7 ± 137.7	51.1 ± 29.2	95.1 ± 16.0	60.7 ± 80.7

B. Inactivation of *Listeria monocytogenes* in cell suspension

The numeric values for the graphs in section 4.2.

Table 34. Bacterial concentration of L. monocytogenes in cell suspension after treatment with TW, L-10, PAW_IB and H-30

	Treatment time (min)			
	0 (UT)	5	15	30
TW	$2.1 \times 10^7 \pm 1.1 \times 10^6$	$2.3 \times 10^6 \pm 3.7 \times 10^5$	$2.2 \times 10^6 \pm 3.0 \times 10^5$	$2.2 \times 10^6 \pm 6.6 \times 10^5$
L-10	$2.1 \times 10^7 \pm 1.1 \times 10^6$	$8.3 \times 10^5 \pm 2.1 \times 10^5$	$6.8 \times 10^5 \pm 2.0 \times 10^5$	$6.4 \times 10^5 \pm 1.1 \times 10^5$
PAW_IB	$2.1 \times 10^7 \pm 1.1 \times 10^6$	$2.4 \times 10^4 \pm 1.3 \times 10^4$	$1.5 \times 10^4 \pm 1.5 \times 10^3$	$1.3 \times 10^4 \pm 1.3 \times 10^3$
H-30	$2.1 \times 10^7 \pm 1.1 \times 10^6$	$1.4 \times 10^4 \pm 3.5 \times 10^3$	$3.1 \times 10^3 \pm 6.4 \times 10^2$	$2.5 \times 10^2 \pm 2.1 \times 10^2$

Table 35. Bacterial concentration of L. monocytogenes in cell suspension after treatment with TW, H-30 and HS-30*

	Treatment time (min)		
	0 (UT)	5	2.5 x2
TW	$2.1 \times 10^7 \pm 1.1 \times 10^6$	$2.3 \times 10^6 \pm 3.7 \times 10^5$	$2.4 \times 10^4 \pm 5.4 \times 10^3$
H-30*	$2.1 \times 10^7 \pm 1.1 \times 10^6$	$1.4 \times 10^4 \pm 3.5 \times 10^3$	$4.9 \times 10^3 \pm 70.7$
HS-30	$2.1 \times 10^7 \pm 1.1 \times 10^6$	ND	ND

Table 36. Bacterial concentration of L. monocytogenes in cell suspension after treatment with TW and H-30 with and without US treatment.*

	Frequency (US treatment)		
	0 (UT)	68	68/170
TW	2.1 x107 ± 2.1 x 106	28300.0 ± 4525.5	30000.0 ± 9828.8
H-30*	2.1 x107 ± 2.1 x 106	7650 ± 2474.9	7000 ± 1838.5

C. Decontamination of Macroalgae

The numeric values for the graphs in section 4.3.

Table 37. Bacterial concentration of macroalgae after treatment with TW, EDTA, US_TW and US_EDTA.

	Treatment times (5 min)				
	0 (UT)	5	15	30	60
TW	19500	2400 ± 1902	2370 ± 1326	ND	ND
EDTA	19500	ND	ND	ND	ND
US_TW	19500	ND	ND	ND	ND
US_EDTA	19500	ND	ND	ND	ND

Table 38. Bacterial concentration of Macroalgae after refrigerated storage for 0, 1, 2 and 3 days.

	Refrigerated storage (days)			
	0	1	2	3
UT	1.95E+04	3.14E+03 ± 1957.84766	1.20E+04 ±2232.07519	3.15E+04 ± 4467.5259

Table 39. Bacterial concentration of Macroalgae treated with PAW (L-10 and L-30) alone an combined effect with US treatment.

	Treatment	
	No US	US
UT	$2.7 \times 10^5 \pm 1.8 \times 10^5$	$2.7 \times 10^5 \pm 1.8 \times 10^5$
L-10	$2.3 \times 10^4 \pm 1.6 \times 10^3$	$2.7 \times 10^3 \pm 7.7 \times 10^2$
L-30	$2.8 \times 10^5 \pm 2.0 \times 10^5$	$6.2 \times 10^3 \pm 6.8 \times 10^3$
TW	$1.2 \times 10^4 \pm 1.5 \times 10^3$	$4.4 \times 10^4 \pm 3.5 \times 10^4$

D. PAW as a fertilizer

The numeric values for the graphs in section 4.4.

Table 40. Weight and length of PAW (different operating conditions) and control (TW)

	Root weight (g)	Leaf + stem weight (g)	Root length (cm)	Stem length (cm)
Control	0.016 ± 0.003	0.057 ± 0.006	10.30 ± 3.47	5.32 ± 1.03
L-10	0.048 ± 0.009	0.208 ± 0.019	9.30 ± 1.79	10.40 ± 0.65
H-10	0.057 ± 0.009	0.190 ± 0.036	9.72 ± 1.01	10.22 ± 1.03
L-30	0.054 ± 0.006	0.164 ± 0.033	6.94 ± 1.86	9.64 ± 0.96
H-30	0.058 ± 0.008	0.183 ± 0.041	7.92 ± 1.78	9.98 ± 0.94

A.  **B.** 

C. 

*Figure 54. Plants on the after harvests **A.** H-10 **B**. L-30 **C**. H-30*

Table 41. Weight and length of PAW (L-30/PAW_IB), NH_4NO_3 and control (TW) after harvest

	Root weight (g)	Leaf + stem weight (g)	Root length (cm)	Stem length (cm)
Control	0.010 ± 0.001	0.041 ± 0.013	15.87 ± 0.81	5.80 ± 0.75
L-30	0.032 ± 0.001	0.147 ± 0.035	11.80 ± 4.80	9.53 ± 0.29
NH_4NO_3	0.039 ± 0.001	0.122 ± 0.040	15.67 ± 3.68	9.83 ± 0.49
PAW_IB	0.041 ± 0.011	0.139 ± 0.040	6.33 ± 0.58	8.50 ± 1.32

Table 42. Weight and length of PAW and control (TW) (diluted with a multi nutritional solution) after harvest.

	Root weight (g)	Stem + leaves Weight (g)	Root length (cm)	Stem length (cm)
Control	1.07 ± 0.08	2.17 ± 0.16	16.40 ± 2.70	18.90 ± 0.74
PAW	1.60 ± 0.31	3.96 ± 0.42	15.90 ± 3.49	23.8 0± 1.79